THE UNIVERSITY
of EDINBURGH

Replication arrest and bypass at Tus/*ter* complexes in the terminus of the *Escherichia coli* chromosome

Anton Kurakov

Thesis presented for the degree of Doctor of Philosophy

Institute of Cell Biology

The University of Edinburgh

October 2019

Declaration

I hereby declare that this thesis was composed by me, and the research presented is my own, except where otherwise stated. This work has not been submitted for any other degree or professional qualification.

Anton Kurakov

Acknowledgements

I am extremely grateful to Prof. David Leach for offering me the opportunity to work on this research under his supervision. I would like to say personal thanks for being patient and always welcoming, for all the guidance and support provided throughout all four years. Finally, it was a great pleasure to discuss scientific matters and ideas.

I would also like to say personal thanks to the senior postdoc of the laboratory, Dr Elise Darmon. For all the time you spent helping me and correcting my mistakes and a very pleasant atmosphere in the lab all those years!

I am also grateful to everyone in my thesis committee for providing invaluable feedback and honing my presentation skills. And also for all the words of support and guidance.

A big thanks to everyone in the lab who shared late hours with me and spent time supporting me. It was more valuable than it may seem!

Finally, I want to express my gratitude to the Darwin Trust of Edinburgh for funding this research and giving me the opportunity to study at the world-class University of Edinburgh.

Lay summary

One of the most intriguing and seemingly simple questions in biology is how a single cell can become two cells. For a cell to divide, it must first copy all the information encoded in its chromosome to ensure that the new cell will be able to use it to survive and divide. The process of replication has to be accurate in order to preserve the encoded information intact and requires proper function of numerous proteins. The aim of this study is to understand the work of some of these proteins that help the cell finish replicating its chromosome. In particular, to understand how these proteins assist replication machinery to cease its work and stop in a certain area of the chromosome where accidental damage to DNA can be avoided. The data this study obtained provide better understanding how proteins interact with the replication machinery when it has to stop moving, and revealed a novel function of the protein, that assists replication machinery in avoiding dangerous consequences of breaking apart.

Abstract

Genome replication is frequently challenged by obstacles that can result from DNA damage, topological stress or tightly bound proteins. Replication fork stalling at DNA-bound proteins can lead to collapse of the fork and promote mutation and genomic instability, a hallmark of cancer cells. Interaction between replisomes and naturally occurring barriers can provide important information for understanding genome instability mechanisms.

The simplicity of the *Escherichia coli* chromosome replication is ideal for studies of complex interactions between replication forks and replication barriers. *E. coli* carries a single chromosome that encodes a single origin of bidirectional replication, *oriC*, and a region diametrically opposite to *oriC* where replication terminates. The terminus region encodes four 23 bp ter sites, *terA* and *terD* on right replichore and *terC* and *terB* on the left. A *ter* sequence bound by Tus protein acts as a polar (unidirectional) natural barrier to fork progression. The Tus/*ter* system allows replisomes to enter the terminus, but will arrest their progress into the opposite replichore, that is, towards *oriC*.

In this work two dimensional native-native gel electrophoresis was utilized to detect stalled replication forks at naturally occurring Tus/*ter* barriers in the *E. coli* chromosome terminus. The majority of arrested replication forks were found to accumulate at the first Tus/*ter* barrier on the left replichore, Tus/*terC*. Notably fewer arrested forks were detected at *terA*, *terB* and *terD*. The strength of ter sites was shown to be independent of the location in the terminus, whereas the sequence of ter sites was critical. The *terB* sequence forms the strongest terminator and restricts frequent replication fork bypass observed at *terC*. This correlates with the published data on the strength of nucleoprotein barriers formed by *ter* sequences observed *in vitro*. The presence of a strong terminator on each replichore helps the

Tus/*ter* system prevent unwanted replication to escape the terminus. In the situation where additional rounds of replication were initiated in the terminus in the absence of the RecG helicase, most of replication forks were able to bypass Tus/*terC* barrier and were arrested at Tus/*terB*.

Previous studies, in the Michel laboratory, revealed that the UvrD helicase can promote the bypass of a synthetically introduced Tus/*terB* replication fork barrier in the middle of the right replichore, but only as a consequence of RecA-mediated homologous recombination. The work presented in this thesis shows that, even in the absence of RecA-mediated homologous recombination, UvrD could promote the bypass of the naturally occurring Tus/*terC* (soft) barrier in the chromosome terminus. However, UvrD was unable to promote fork movement through stronger Tus/*terB* and Tus/*terA* barriers in the terminus. The *terC* and terB nucleotide sequences differ in three separate segments. I have shown that, one of the segments outside of the conserved region plays a critical role in the UvrD-dependent replication fork bypass of the Tus/*terC* barrier. My results suggest a distinct role of the UvrD helicase in the alleviation of replication fork stalling at the naturally occurring Tus/*terC* barrier in the chromosomal terminus.

Abbreviations

P^{32}	Phosphorus-32
2-D GE	native/native two-dimension gel electropohresis
ara	Arabinose
ATP	Adenosine triphosphate
bp	Base pair
Cm	Chloramphenicol
Cm^R	Chloramphenicol resistance cassette
dif	Deletion-induced filamentation
DNA	Deoxyribonucleic acid
dNTP	Deoxynucleotide triphosphate
DSB	Double-strand break
DSBR	Double-strand break repair
dsDNA	Double-stranded DNA
EDTA	Ethylenediaminetetraacetic acid
EtBr	Ethidium bromide
Glu	Glucose
HJ	Holliday junction
HR	Homologous recombination
Kb	Kilo base pair
Km	Kanamycin
Km^R	Kanamycin resistance cassette

KOPS	FtsK orienting polar sequences
L	Litre
LB	Luria broth
M	Molar
m	milli
Mb	Mega base pair
MFA	Marker frequency analysis
MCS	Multiple cloning site
n	Nano
OD_{600nm}	Optical density at 600 nanometers
ori	Origin
PBS	Phosphate buffered saline
PCR	Polymerase chain reaction
pH	Power of hydrogen
PMGR	Plasmid mediated gene replacement
Pol	Polymerase
RNA	Ribonucleic acid
SDS	Sodium dodecyl sulphate
SSB	Single-stranded binding protein
ssDNA	Single-stranded DNA
Suc	Sucrose
Suc^S	Sucrose sensitivity cassette
TAE	Tris acetate-EDTA

Tc	Tetracycline
Tc^R	Tetracycline resistance cassette
ter	replication terminator site
Tm	Melting temperature
Ts	Temperature-sensitive
tus	Termination utilisation substance
UV	Ultraviolet light
v/v	Volume per unit volume
w/v	Weight per unit volume
WGS	Whole genome sequencing
μ	Micro

CONTENTS

Table of figures

Table of tables

1 LITERATURE REVIEW

1.1 General Introduction

How a single cell can become two cells is one of the central questions in biology. For a cell to divide, its genome must first be duplicated, and all the genetic information necessary to survive and repeat the process passed to the newborn cell. General knowledge of DNA replication stems from studies of the replication complexes in model bacterial organisms, such as *Escherichia coli* and *Bacillus subtilis*, and also from bacteriophages, like T4 and T7 (Lee and Lee, 2003). The ability to rapidly and effectively create recombinant bacterial strains suitable for a particular test or an experiment permits scientists to investigate and understand many fundamental genetic and molecular mechanisms with relative ease. Information obtained from these relatively simple (in terms of biochemical processes) organisms provided a valuable basis for studying more complex DNA replication and maintenance systems in eukaryotes.

The ability to maintain genomic stability is essential for all organisms. Multiple complex and interrelated processes exist to allow complete and accurate replication and segregation of the chromosomes as well as extrachromosomal DNA. Because these processes require the proper function of all proteins involved, mutations that affect genomic stability can have lethal consequences. Especially in multicellular organisms, in which certain mechanisms ensure that cells with undesired genomic alterations no longer divide or, alternatively, die (Zhivotovsky and Kroemer, 2004). Genomic instability in humans underlies a number ofs genetic disorders and other diseases, including cancer (Aguilera and Gómez-González, 2008; López Castel, Cleary and Pearson, 2010; Shen, 2011). Accumulation of errors during replication is considered one of the major causes of mutations that lead to the development of cancer cells (Tomasetti, Li and Vogelstein, 2017). It is important to expand our knowledge

of DNA replication not only to uncover fundamental processes of life itself but also to learn how to prevent or utilise its imperfections.

Simple prokaryotic organisms, such as *E. coli*, are less susceptible to genomic instability due to the natural plasticity of their genomes (Esnault *et al.*, 2007; Vandecraen *et al.*, 2017). Yet, pathological DNA replication processes can cause delayed or incomplete chromosome replication and segregation and in some cases lead to the loss of viability of the cells (Mirkin and Mirkin, 2007; Helmrich *et al.*, 2013; Gupta, Yeeles and Marians, 2014). It was reported that the replication termination system in the *E. coli* chromosome has the potential to cause DNA damage or even loss of genetic information as a result of illegitimate recombination (Bierne, Ehrlich and Michel, 1991; Azeroglu *et al.*, 2016). The primary focus of this research is on expanding our understanding of molecular events at replication terminator sequences during replication using *E. coli* as a model organism.

1.2 Cell duplication and cell cycle in *E. coli*

Throughout the cell cycle of all living organisms, processes governing cell growth, chromosome duplication and cell division must be carefully coordinated. Eukaryotic cells have numerous checkpoints at each stage of the cell cycle to prevent the initiation of the next process until the previous one is completed (Harashima, Dissmeyer and Schnittger, 2013). The bacterial cell cycle, and, specifically, the cycle of *E. coli,* was initially proposed to be regulated by the accumulation of a critical cell mass, that would trigger DNA replication initiation (Donachie, 1993). Recently, this view was expanded to include three stages. The period of cell growth, B-period is followed by the genome replication phase, called C-period. Chromosome segregation and cell division is the last stage of the cell cycle and is known as D-period (Figure 1.1).

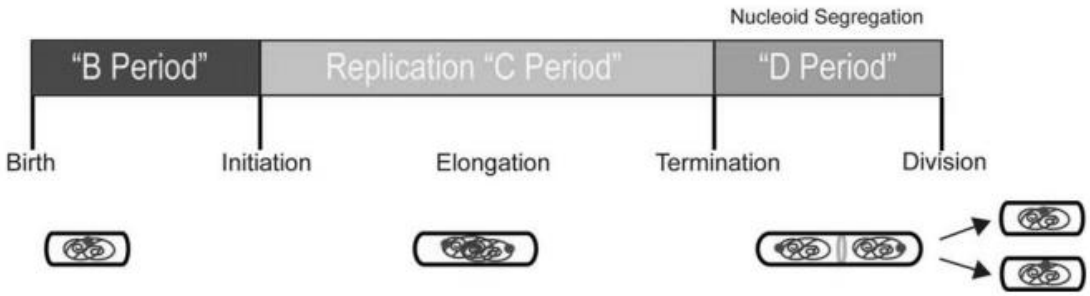

Figure 1.1

Schematic representation of the bacterial cell cycle. Three separate periods can normally be identified in slow-growing cells. Cell growth happens in B-period, but continues until the end of the cell cycle. Replication happens during C-period, and D-period represents cell division (adapted from Hausser and Levin, 2008 with modifications).

E. coli cells are able to adapt to a range of growth rates depending on the environmental conditions. The time between each cell division can be as short as 20 minutes. At the same time, to complete the replication of the chromosome cells need at least about 40 minutes (Ferullo *et al.*, 2009). To overcome the limit imposed by the C-period, cells can initiate the second round of replication before the first round is completed. Therefore, new cells generated after division will have already partially replicated chromosome and can carry, at a given time, up to 16 copies of the chromosome origin locus (Ferullo *et al.*, 2009). Cells initiate replication at the chromosome origin and continue to grow throughout each cell cycle. (Bates *et al.*, 2005). Studies of the effect of three growth rates (Td= 90, 125 and 300 minutes) on the timing of replication events (B, C, D periods) revealed that predominantly the D phase, between the end of bulk replication and cell division, accommodated differences in growth rates, suggesting that growth conditions affect septation and cell division but not DNA replication dynamics.

1.3 The *E. coli* chromosome and fundamental aspects of replication

The *E. coli* chromosome is a 4.6 Mbp long circular molecule more than 80% of which encodes over 4000 different proteins (Blattner, 1997). A single replication origin, *oriC*, located at ~85 min on the chromosome genetic map is responsible for the initiation of bidirectional replication. As in eukaryotes, bacterial replication is semi-conservative with each daughter cell receiving a new DNA double helix made of one parental and one newly synthesized strand. The process of DNA replication involves the coordinated activity of many proteins that collectively comprise a molecular machinery called the replisome. Two replisomes move across each half of the chromosome until they meet and fuse in the region diametrically opposite from *oriC*, called the terminus.

1.4 Replisome composition

Each replisome consists of a primosome, a multisubunit complex of helicase DnaB and primase DnaG, DNA polymerase III (Pol III) holoenzyme and accessory factors (Figure 1.2).

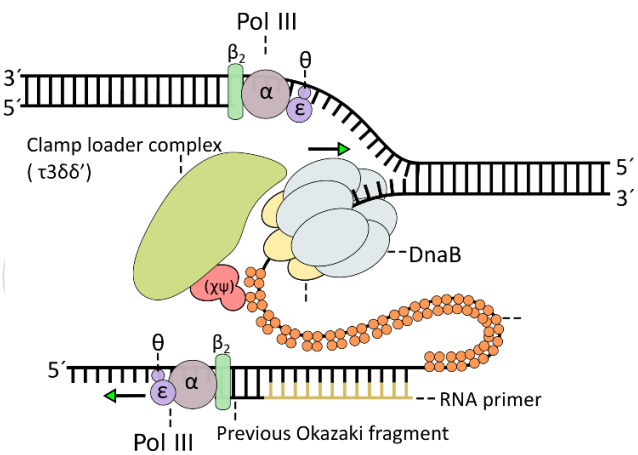

Figure 1.2. Schematic representation of the replisome structure in *E. coli*. χψ are components of the clamp loader complex. α, ε and θ together with the β_2 sliding clamp are parts of the polymerase III holoenzyme complexes.

The Pol III holoenzyme contains two (or three) Pol III core molecules two of which are securely attached to a DNA strand by two β clamps and a single clamp loader molecule that coordinates and maintains the multiprotein complex (Weigel *et al.*, 1999; McInerney *et al.*, 2007; Georgescu, Yao and O'Donnell, 2010; Dohrmann *et al.*, 2016).

Replicative helicase DnaB is a toroid molecule composed of six identical subunits of a ~52 kDa size. Its ATP-dependent translocase activity allows the helicase to traverse across dsDNA and in the 5' to 3' direction of ssDNA. At the replication fork it encircles the lagging strand and unwinds the DNA duplex of the parental strand in front of polymerases (LeBowitz and McMacken, 1986; Patel and Picha, 2000; Schaeffer, Headlam and Dixon, 2005). DnaB interaction with DnaG is important for the recurrent primer formation (Bárcena *et al.*, 2001). DnaG is a 64 kDa DNA-dependent RNA polymerase that requires SSB coated ssDNA or the presence of DnaB to synthesise an 8-12 nt RNA primer at 1 kb intervals preferentially at 5'-CTG sequence on the lagging strand (Frick and Richardson, 2001; Mitkova, Khopde and Biswas, 2003; Wing, Bailey and Steitz, 2008). DnaB also interacts with the τ subunit of the clamp loader protein complex, DnaX, which determines the rate of replisome movement by coordinating Pol III holoenzyme and DnaB dynamics (Kim *et al.*, 1996). Accessory helicase Rep was also shown to interact with DnaB providing a secondary helicase motor at the active replisome. Active recruitment of Rep to the replication fork ensures rapid removal of DNA-bound proteins ahead of the fork (Guy *et al.*, 2009; Atkinson, Gupta and McGlynn, 2010; Syeda *et al.*, 2019).

The single-stranded DNA binding protein (SSB) is a small 20 kDa molecule that has an affinity to ssDNA regions independently of the sequence (Meyer and Laine, 1990; Shereda *et al.*, 2008). SSB can quickly coat ssDNA produced in the wake of duplex DNA unwinding by

DnaB and protects it from nucleases and the formation of secondary structures such as hairpins of cruciforms (Kuznetsov *et al.*, 2006). The N-terminal domain of SSB allows four subunits to tetramerise with each directly interacting with ssDNA (Raghunathan *et al.*, 1997, 2000). Through its unstructured C-domain SSB interacts with multiple proteins, including RecJ, RecG, PriA, RecQ, ExoI and other DNA metabolism proteins to recruit them to specific regions on the DNA or stimulate their activity (Han, 2006; Shereda, Bernstein and Keck, 2007; Lu and Keck, 2008; Yu *et al.*, 2016).

DNA Polymerase III holoenzyme is a protein complex that consists of three subassemblies: the core (αεθ), the β_2 sliding clamp and the clamp loader (γ) (Schaeffer, Headlam and Dixon, 2005; McInerney *et al.*, 2007). The core is composed of the polymerizing catalytic subunit α, 3' to 5' exonuclease ε and the accessory unit θ involved in stimulating proofreading function of ε (Benkovic, Valentine and Salinas, 2001; El Houry Mignan *et al.*, 2011). Two to three core complexes are present in the replisome, but only 2 are active at any given time (Georgescu, Kurth and O'Donnell, 2011; Beattie and Reyes-Lamothe, 2015; Dohrmann *et al.*, 2016). The β_2 sliding clamp is formed by two identical monomers that form a circle around the DNA duplex and interacts with the subunit α of the core complex to facilitate continuous DNA polymerisation (Burnouf *et al.*, 2004; Lewis, Jergic and Dixon, 2016). The clamp loader complex γ consists of 6 subunits that interact with all components of the replication fork enhancing their stability and processivity (Kim *et al.*, 1996; McHenry, 2003; Witte, 2003; Anderson *et al.*, 2007; Lia, Michel and Allemand, 2011; Lewis, Jergic and Dixon, 2016).

1.5 Initiation of replication

Replication origin, *oriC*, is a 245 bp region that encodes multiple asymmetric 9 bp sites called DnaA boxes and three 13 bp repeats in the AT-rich region at one side of the origin, called DNA-unwinding element (DUE). Two types of DnaA boxes are present in the *oriC* region. High-affinity boxes are bound by DnaA proteins throughout most of the cell cycle. Low-affinity boxes can only be bound by the active form of DnaA protein, ATP-bound DnaA (Messer, 2002; Mott and Berger, 2007; Hansen and Atlung, 2018). During cell growth the concentration of DnaA-ATP molecules increases until a critical number accumulates that trigger chromosomal replication initiation (McGarry *et al.*, 2004; Fujimitsu, Senriuchi and Katayama, 2009). The DnaA-initiator association protein DiaA recruits DnaA-ATP multimers to the *oriC* region (Keyamura *et al.*, 2007; Ozaki and Katayama, 2009). This leads to increased occupancy of low-affinity DnaA boxes and locally distorts the DNA at the origin facilitating DNA duplex melting within the DUE (Leonard and Grimwade, 2004; Miller *et al.*, 2009). Exposed single-stranded DNA at the DUE region is quickly covered by single-stranded binding protein (SSB) permitting the assembly of DnaB helicase. DnaA molecules bound with low-affinity boxes interact with the pre-primosome complex $(DnaBC)_6$ facilitating the loading of two DnaB homohexamer molecules on each strand of the locally melted DNA (Konieczny, 2003; Leonard and Grimwade, 2004). DnaC dissociates from the $(DnaBC)_6$ complex after or during DnaB loading and causes the subsequent ATP-hydrolysis to activate the helicase activity of DnaB (Kurth and O'Donnell, 2009). By extending the replication bubble to about 65 nucleotides DnaB recruits DnaG primase that begins to synthesise short RNA primers. Two β sliding clamps and then DNA Polymerases III are loaded onto each primed template by the γ complex, forming complete replisomes that proceed to the

elongation stage of replication (Fang, Davey and O'Donnell, 1999; Pomerantz and O'Donnell, 2007; Nielsen and Løbner-Olesen, 2008).

1.6 Elongation phase of DNA replication

The elongation stage begins when two replisomes established at *oriC* move away from the origin. The speed of each replisome fluctuates due to the presence of various obstacles on the path and can reach approximately 750 bp s^{-1}(Pham *et al.*, 2013). The counter clockwise-moving replisome was shown to proceed at a slightly higher rate than the clockwise-moving one (Breier, Weier and Cozzarelli, 2005).

The antiparallel nature of a DNA duplex poses a challenge to the continuous replication of both strands. DNA Pol III synthesises DNA in the 5' to 3' direction; therefore, the two polymerases move in opposite directions during replication: one in the same direction as the progressing fork, the other in the opposite direction. The coordination and colocalisation of both polymerases causes the formation of the trombone loop on the lagging strand (Figure 1.2) (Breier, Weier and Cozzarelli, 2005; Yao and O'Donnell, 2008). The synthesis rate of the leading and lagging strands was shown to be nearly identical. It has been recently revealed that the synchronicity between the leading-strand synthesis and the lagging-strand synthesis is not required and the DnaB helicase can continue unwinding DNA even when either of the polymerases is paused, albeit at a notably lower speed (Graham, Marians and Kowalczykowski, 2017).

1.6.1 Replication fork instability

During *E. coli* chromosome replication, progressing forks encounter various obstacles, such as DNA lesions, regions of complex DNA topology and DNA-protein complexes, the majority of which are represented by RNA polymerase elongation complexes or protein-bound regulatory sequences. Multiple mechanisms ensure the accuracy and successful completion of the replication process in *E. coli*.

The high processivity and fidelity of the replisome inherently diminish the ability to tolerate DNA lesions, and thus require an error-free DNA template. DNA lesions accumulate on the chromosome as a result of DNA interacting with damaging agents (electromagnetic irradiation, reactive oxygen species) or following a conflict between intracellular systems that work on DNA (transcription, gene expression regulation, chromosome segregation). Several DNA repair systems work to minimise the half-life of DNA lesions, such as DNA double-strand break repair (Bell and Kowalczykowski, 2016), mismatch repair (Jiricny, 2013), the nucleotide excision repair (Kisker *et al.*, 2013), and base excision repair (Dalhus *et al.*, 2009). When a DNA lesion is not repaired before the arrival of the replisome, the continuation of the arrested chromosome replication can proceed via either of two pathways. In one of the pathways, the primosome was shown *in vitro* to be reloaded past the lesion priming both leading and lagging-strand synthesis (Heller and Marians, 2006a). The other pathway utilises alternative DNA polymerases (Pol II, IV and V) that transiently replace Pol III to continue the replication via translesion synthesis through the damaged region on the DNA at the cost of a dramatically decreased fidelity. These polymerases have limited specificity with respect to the type of lesions they can bypass, responding predominantly to the local geometry of the DNA around the lesion and acting in a trial and error manner (Fuchs and Fujii, 2013). It is

currently unknown whether this pathway requires the SOS response activation or can act in an SOS-independent fashion. *polB*/*dinA* encoding Pol II and *dinB*/*dinP* encoding Pol IV are both expressed at a basal level in non-SOS-induced cells, but their expression is elevated 7 and 10-fold in response to SOS induction, respectively (Kim *et al.*, 2001). In contrast, under normal conditions, the synthesis of *umuDC* encoding Pol V is tightly repressed at several levels and biochemical assays were able to detect the presence of this polymerase only ~50 minutes after inducing an UV-dependent SOS response (Fuchs and Fujii, 2013).

DNA-bound proteins are considered to be the major source of replication fork pausing (Gupta *et al.*, 2013; Moolman *et al.*, 2016). Nucleoprotein complexes form covalent (with T4 pyrimidine dimer glycosylase/AP site lyase) or non-covalent (with lacO) (Dodson, Lloyd and Schrock, 1993; Brüning, Howard and McGlynn, 2014) bonds and require different mechanisms of resolution (Nakano *et al.*, 2007; Krasich *et al.*, 2015). While the frequency of naturally occurring covalent DNA-protein adducts are currently poorly understood, high-affinity non-covalent nucleoproteins in the form of regulatory, termination or transcription proteins were studied extensively (Michel, Ehrlich and Uzest, 1997; Bidnenko, Ehrlich and Michel, 2002; Merrikh *et al.*, 2012; Ivanova *et al.*, 2015; Mettrick and Grainge, 2015). Conflicts between the DNA replication and transcription complexes are inevitable, as both systems work on the same template and transcription is known to move 10-20 times slower than replication (Dennis *et al.*, 2009). If not resolved, in eukaryotic cells these conflicts can lead to gross chromosomal rearrangements (Lambert *et al.*, 2005; Schalbetter *et al.*, 2015) and potentially catastrophic genome instability associated with cancer or cell death. In contrast to eukaryotic cells, bacterial genomes show a striking bias towards co-directionality of the replication and transcription of essential and highly transcribed genes (Touchon and Rocha,

2016). While co-directional replication-transcription collisions are not benign as shown at highly transcribed rRNA genes in *B. subtilis*, these conflicts appear to arise only under fast-growing conditions (Merrikh *et al.*, 2011). The evolutionary pressure to maintain a certain orientation of essential genes suggest that head-on conflicts are substantially more detrimental (Merrikh *et al.*, 2012).

E. coli cells utilise several other approaches to resolve conflicts between replisomes and nucleoprotein complexes. (i) Constitutive expression of multiple factors (Mfd, NusA, ppGpp, DksA, Gre and Rho) that destabilise and facilitate the dissociation of DNA-protein barriers, as shown with the transcription-mediated conflicts, promote stability of replication and genome integrity (Trautinger *et al.*, 2005) (ii) The presence of at least two accessory helicases, Rep, UvrD or DinG, was shown to be essential for cell survival and ensures replication progress without disruptions (Boubakri *et al.*, 2010). While only Rep was shown to be associated with the replisome and to maintain rapid replication (Guy *et al.*, 2009), UvrD plays an important role in removing RecA filaments and preventing toxic recombination intermediates at stalled replication forks (Florés, Sanchez and Michel, 2005; Lestini and Michel, 2007). (iii) Finally, upon replisome collapse at a nucleoprotein barrier, DNA replication can be re-initiated in an origin-independent manner. If the barrier is no longer present, re-initiation occurs at the fork. Alternatively, prolonged replication stalling leads to either replication fork reversal or the collapse of subsequently arriving replication fork (Figure 1.3) (Larsen *et al.*, 2014; Azeroglu *et al.*, 2016; Hizume and Araki, 2019).

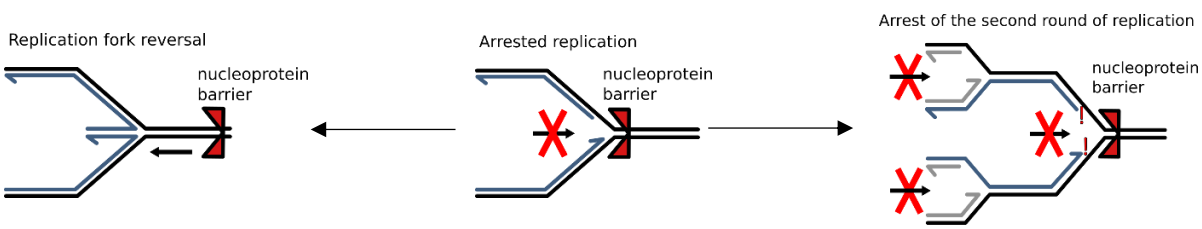

Figure 1.3
Schematic representation of consequences of prolonged replication stalling.

1.6.2 Stalled replication

In eukaryotic cells, replisomes at stalled replication forks were commonly regarded as stable due to the presence of checkpoint proteins (Casper *et al.*, 2002; Branzei and Foiani, 2007). It has since been shown that the replisome remains intact even in the absence of the key check-point ATR/Rad53 protein (De Piccoli *et al.*, 2012) is unable to recruit DnaB homolog, CMG helicase. Conflicting data exist showing different levels of stability of stalled replisomes in prokaryotes. A recent work of Mettrick and Grainge indicates that a stalled fork blocked by an array of *tetO* repressor-operator sequences dissociates within 3-5 minutes *in vivo* (Mettrick and Grainge, 2015). These data are supported by earlier *in vitro* experiments indicating that replisomes are blocked for 4 and 6 minutes by the accumulation of positive torsional stress and *lac* repressor-operator arrays, respectively, before dissociating from DNA template (Marians *et al.*, 1998; McGlynn and Guy, 2008). Conversely, *in vivo* experiments in Prof. Sherratt's laboratory showed prolonged stalling of replication forks at *tetO* or *lacO* repressor-operator arrays for up to 4 hours with a rapid re-activation of replication within 5 minutes after relieving the block by adding anhydrotetracycline or isopropyl-β-D-thiogalactopyranoside (Possoz *et al.*, 2006). This discrepancy was explained by the presence of the PriA-mediated replisome reloading machinery *in vivo* that would continually reload collapsed forks and provide the observed signal representing stalled replisome (Mettrick and Grainge, 2015). Yet, *in vivo* experiments utilizing an additional replication origin located halfway between *oriC* and *dif* on the clockwise replichore indicate that a replichore is stably bound (or is rapidly reloaded) at a Tus-*terC* block for at least ~30 minutes (Moolman *et al.*, 2016). Another study measured the stability of the replisome after a controlled collision with a halted transcription elongation complex. Surprisingly, even in the absence of the

primosomal proteins PriA/C, the stalled replisome remained active to continue synthesis immediately with the release of the block for 60 minutes after the collision (Pomerantz and O'Donnell, 2010). Highly contradictory data do not allow a conclusion to be drawn about the stability of a stalled replication complex at nucleoprotein barriers. Yet, it seems plausible that while in certain measurements it was the continuous replisome reloading that contributed to the observed duration of stalled replisome, in the case of arrest at the Tus-*ter* complex, specific protein-protein interactions could play a role in the maintained stability of the stalled fork.

1.6.3 Replication restart

Replication fork that upon removal of the block lacks replisome components can be rescued by the replication restart pathway. Unlike *oriC*-dependent replication initiation, the stochastic nature of the replisome collapse does not allow the restart pathway to rely on the presence of specific DNA sequences to reinitiate replication with the help of DnaA protein. Instead, replisome reassembling proteins recognise specific DNA structures (Heller and Marians, 2006b). The mechanism of origin-independent activation of replication relies on the action of the 3'-to-5' helicase PriA at abandoned forks or D-loops (Nurse, Liu and Marians, 1999; Tanaka and Masai, 2005; Gabbai and Marians, 2010). In the presence of SSB PriA effectively remodels the lagging-strand template arm in order to expose ssDNA (Jones and Nakai, 2001; Heller and Marians, 2005). This DNA conformation allows PriA to recruit PriB and DnaT or PriC and to form a multiprotein complex that facilitates the loading of DnaB-DnaC complex onto the exposed ssDNA (Michel and Sandler, 2017). The DnaB/DnaC complex then primes the substrate and re-initiates DNA synthesis (Yeeles and Marians, 2011). The PriA-PriB and the PriA-PriC pathways are redundant as was shown by the absence of phenotypic changes of either *priB* or *priC* mutants (Sandler *et al.*, 1999). The PriA-PriB

pathway is considered to be the dominant way to reinitiate replication, whereas PriC has a greater substrate specificity and acts preferentially at stalled forks with short ssDNA stretches between the nascent leading strand and the fork junction (Windgassen *et al.*, 2017).

1.6.4 Replication fork reversal

Additional pathway of fork reactivation in *E. coli* cells was proposed that does not in all cases rely on the PriA-dependent restart. The replication fork reversal pathway requires extensive fork remodelling to bypass the obstacle (McGlynn and Lloyd, 2002; Courcelle *et al.*, 2003). It occurs predominantly as a result of replication fork stalling, such as that at UV-induced DNA lesions, DNA-bound proteins in the absence of accessory helicase or unresolved topological stress ahead of the fork (Seigneur *et al.*, 1998; Sutherland and Tse-Dinh, 2010; Khan and Kuzminov, 2012). The fork reversal can occur via two different pathways: RecA-dependent re-annealing of parental leading- and lagging-strands at stalled forks that was shown to be induced only by the temperature-sensitive DnaB helicase (Seigneur *et al.*, 1998); and RuvAB-catalysed regression of replication fork with the subsequent generation of the four-way junction (Figure 1.3), observed *in vitro* (Baharoglu *et al.*, 2006; Gupta, Yeeles and Marians, 2014).

1.6.5 RecG-dependent DNA over-replication

Undesired DNA amplification can cause elevated occurrence of mutants and drug resistance and is characteristic of cancer (Engelman *et al.*, 2007; Sandegren and Andersson, 2009). *E. coli* cells have multiple layers of control that prevents unsanctioned chromosome replication initiation. Yet, replication can be initiated in PriA- and DnaA-independent manner at sites remote from *oriC*. DNA amplification was revealed in the terminus region (see 1.8) that was caused by the collision between two replisomes. As a result the 3’ end of

the nascent leading strand may be displaced to generate a branched DNA structure from which replication can be re-initiated leading to amplification of an already duplicated region (Hiasa and Marians, 1994; Krabbe *et al.*, 1997; Markovitz, 2005) The so-called stable DNA replication (SDR) was shown by Kogoma in *rnhA* mutants lacking RNase HI (Kogoma, 1997). In the absence of RNase HI SDR found to sustain genome duplication independently of *oriC*-initiated replication and, in fact, cells are viable in the absence of the whole *oriC* region due to the abundance of DNA-bound RNA 3' ends (Kogoma, 1997; Rudolph *et al.*, 2013; Dimude *et al.*, 2015). Later, SDR was characterised in cells lacking RecG helicase following DNA damage (Rudolph *et al.*, 2009) and shown to cause over-replication of double-strand break flanking regions (Azeroglu *et al.*, 2016). However, it was shown that DNA damage is not required for SDR in the absence of RecG, as the over-replication was detected in the terminus region of the chromosome between *terA* and *terB* replication terminator sequences (Rudolph *et al.*, 2013; Wendel, Courcelle and Courcelle, 2014; Azeroglu *et al.*, 2016). Several alternative scenarios were proposed to explain how the over-replication in the terminus is initiated (reviewed in Azeroglu and Leach, 2017). DNA flaps generated as a result of head-to-head collision between replication forks was proposed to generate additional replication forks (Rudolph *et al.*, 2010; Dimude *et al.*, 2016). The other observation indicated that SDR arises as a result of incorrect function of PriA in the absence of RecG and initiation of backwards-directed replication as a result of replication restart at Tus/*ter* barrier (Azeroglu *et al.*, 2016) . It should be noted that the over-replication in the absence of RecG is normally contained within the terminus region due to the presence of Tus-*ter* replication fork trap system.

1.7 UvrD helicase

DNA duplex unwinding is a critical part of genome replication and maintenance. Cells encode molecular motors, called translocases, that utilise the energy released by hydrolysis of nucleoside triphosphates, typically ATP, to move along ssDNA and dsDNA. DNA translocases that can couple their movement with the unwinding of two complementary DNA strands are called helicases (Singleton, Dillingham and Wigley, 2007; Lohman, Tomko and Wu, 2008; Bhattacharyya *et al.*, 2014). This process is complicated by the presence of DNA-bound proteins that have to be displaced before DNA can be unwound. RNA polymerase elongation complexes, transcription factors such as repressors and nucleoid-associated proteins are abundant in cells and present a major challenge to replication fork movement.

UvrD (also DNA helicase II) is a non-hexameric helicase/translocase of the SF1A superfamily. UvrD monomers translocate in the 3' to 5' direction along ssDNA at the speed of ~190 nt s^{-1} (Fischer, Maluf and Lohman, 2004; Tomko *et al.*, 2007, 2010; Lee *et al.*, 2013) using ATP hydrolyses as the primary source of energy (Tomko, Fischer and Lohman, 2012). UvrD monomers are primarily translocases (Ali, Maluf and Lohman, 1999; Fischer, Maluf and Lohman, 2004; Lee *et al.*, 2013; Yokota, Yuko Ayabe Chujo and Harada, 2013), while helicase activity requires formation of a UvrD dimer or the presence of accessory proteins such as mutL (Maluf, Ali and Lohman, 2003; Maluf, Fischer and Lohman, 2003; Yokota, Yuko Ayabe Chujo and Harada, 2013). The dimer molecule of uvrD unwinds dsDNA at approximately 70 bp s^{-1} rate (Ali and Lohman, 1997; Tomko *et al.*, 2010).

UvrD is structurally similar to *E. coli* Rep and *Bacillus subtilis* PcrA helicase proteins (Lohman, Tomko and Wu, 2008) and is involved in two important DNA repair pathways: methyl-directed mismatch repair and nucleotide excision repair (Oeda, Horiuchi and

Sekiguchi, 1982; Matson, 1991; Iyer *et al.*, 2004). In the mismatch repair pathway UvrD acts at DNA sequences nicked by MutH and remove the daughter strand containing the incorrectly incorporated nucleotide (Iyer *et al.*, 2006; Matson and Robertson, 2006). In the nucleotide excision repair pathway UvrD facilitates the removal of 12-13 bp oligonucleotides containing a pyrimidine dimer or a bulky adduct. UvrABC complex initiates the repair process and recruits UvrD at the final stage of it (Husain *et al.*, 1985).

More recent studies show that UvrD is directly involved in recombination reactions at replication forks (Johnson *et al.*, 2007; Lestini and Michel, 2007). In particular, it was demonstrated that UvrD assists in regression of nascent leading- and lagging-strands at arrested replication forks (Florés, Sanchez and Michel, 2005; Atkinson and McGlynn, 2009). Consistent with *in vitro* experiments, UvrD was shown to remove RecA filaments assembled on ssDNA at stalled forks to facilitate the fork reversal reaction (Morel *et al.*, 1993; Florés, Sanchez and Michel, 2005; Lestini and Michel, 2007). UvrD also has the ability to prevent unwanted recombination events by antagonising the action of RecA (Radman *et al.*, 1995; Petrova *et al.*, 2015). Unsurprisingly, UvrD-deficient cells are hyper-recombinogenic (Arthur and Lloyd, 1980), exhibit elevated rates of spontaneous mutagenesis and have reduced survival rate upon exposure to UV (reviewed in Yang, 2010).

Interestingly, UvrD was copurified with DNA polymerase III indicating some level of interaction with replication forks (Lahue, Au and Modrich, 1989), despite having no interaction with DnaB, unlike its close homolog, Rep. UvrD is implicated in facilitating Okazaki fragment processing in *polA* mutant cells together with other proteins of the nucleotide excision repair pathway (Moolenaar, Moorman and Goosen, 2000).

Finally, one of the least explored functions of UvrD is its ability to facilitate the removal of *ter*-bound Tus proteins that form a replication fork barrier in the terminus (review in detail Mechanism of the Tus-ter mediated fork arrest 1.8.2.2). Overall, these data suggest that UvrD is essential for displacing non-covalently bound DNA-protein complexes and genome maintenance processes.

1.8 Replication termination

Termination of chromosome replication poses a mechanistic challenge to in bacteria with a circular chromosome. Bidirectional movement of replisomes from the origin along the circular molecule should ultimately result in their head-to-head collision. If not carefully orchestrated, the event could lead to the formation of a branched DNA structure and to re-replication of the already replicated DNA (Hiasa and Marians, 1994; Markovitz, 2005). Another potentially deleterious consequence of bidirectional replication of circular molecules is the accumulation of positive supercoils ahead of the replication forks. Moreover, it was proposed that, during later stages of replication, positive supercoiling between the two replisomes becomes so frequent that the sister chromosomes form precatenanes as supercoils diffuse behind the forks (Wang, 1996; Lesterlin *et al.*, 2012; El Sayyed *et al.*, 2016). If not successfully resolved, the topological tension accumulated as a result of chromosome replications prevent normal nucleoid segregation and may lead to fork stalling and the formation of DNA double-strand breaks.

One type II DNA topoisomerases, the DNA gyrase, works on removing the topological stress from positive supercoils ahead of forks, while precatenanes and catenanes are resolved by another type II topoisomerase, the Topo IV (Zechiedrich, Khodursky and Cozzarelli, 1997; Joshi *et al.*, 2013). A coordinated action of the RecQ monomeric helicase and the Topo

III type Ia topoisomerase in the presence of SSB was also shown to resolve topological constrains between two replication forks (Suski and Marians, 2008). It is worth noting that the existence of precatenanes and the role of Topo IV in the resolution of such structures still remains questionable (Kleckner *et al.*, 2014).

While DNA topoisomerases regulate the accumulation of secondary structures during replication (supercoils, catenanes), potential DNA re-replication caused by two converging replisomes could be constrained by the presence of a "replication fork trap" in the chromosome terminus region (Mulcair *et al.*, 2006; Duggin and Bell, 2009).

1.8.1 Structure of the terminus region

The final stage of *E. coli* chromosome replication is confined within a ~400 kb region, called terminus region (*ter*), located opposite to the origin of replication. Terminus region contains numerous specific DNA sequences that interact with essential proteins orchestrating the intricate process of chromosome segregation .

Among those sequences, a repeating 13-mer imperfect palindrome, *matS*, is responsible for interacting with the MatP protein and defines the terminus macrodomain (Mercier *et al.*, 2008). Bound to *matS*, MatP is responsible for the condensation of the terminus DNA and plays an essential role in the terminus macrodomain dynamics. Together with ZapB, ZapA and FtsZ, MatP relocates the terminus to the mid-cell region during divisome assembly prior to septation (Espéli *et al.*, 2012; Kleckner *et al.*, 2014; Castillo *et al.*, 2016).

Another important component of the terminus region is FtsK-orienting polar sequences (KOPS). These are highly abundant 8 bp long sequences with a consensus of GGGNAGGG that are located predominantly on the leading-strand template of each replichore and are

polarised towards the middle point of the terminus region (Bigot *et al.*, 2005; Graham *et al.*, 2009).

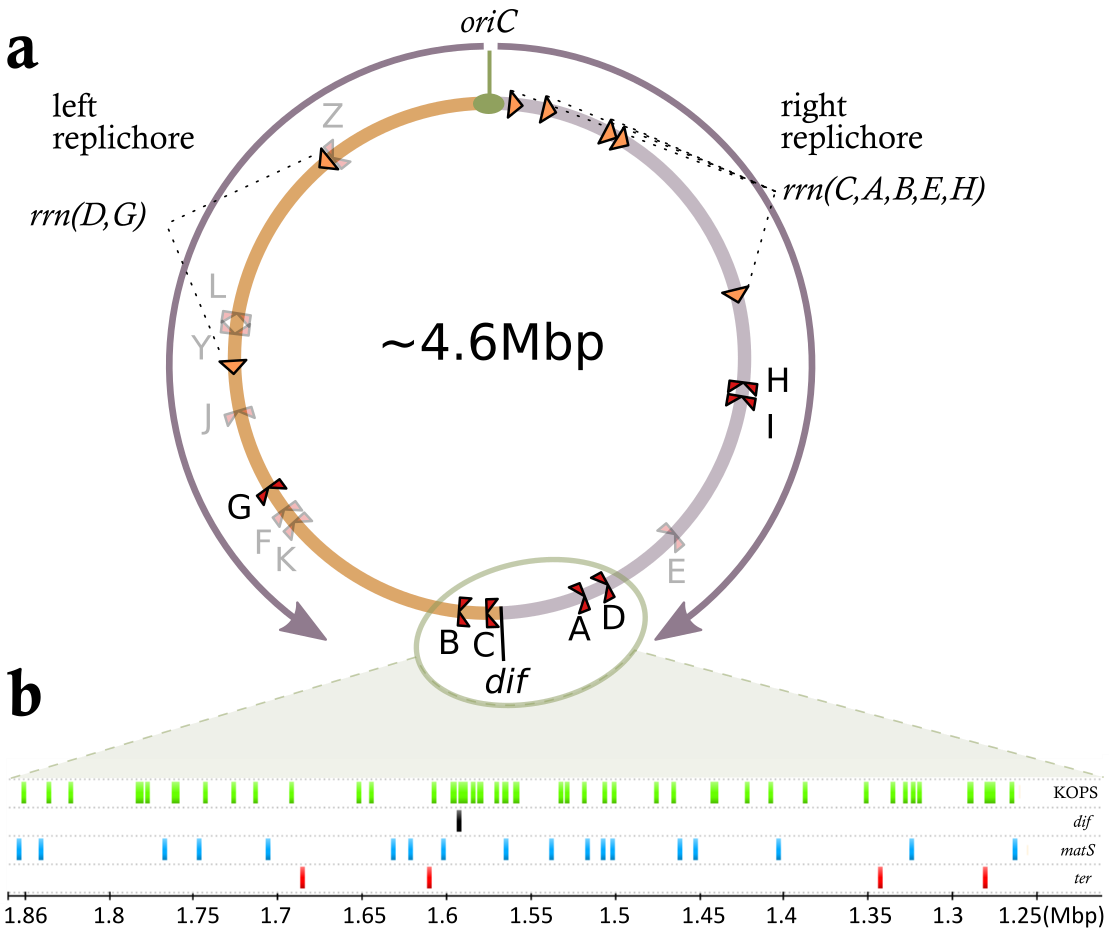

Figure 1.4

Schematic representation of the *E. coli* DL1777 chromosome terminus region. **(a)** *ter* sites arrangement on the chromosome. Direction of replication from the origin is indicated by grey arrows. The origin of replication, *oriC*, and the dimer resolution site *dif* are indicated. Active sites of replisome arrest (*ter*) and their respective names are shown as highlighted rectangles with the indent indicating the non-permissive side. Weak or non-functional *ter* sites are shown as faded triangles. **(b)** Detailed view of the terminus macrodomain. Vertical bars show the distribution of the indicated sequences. *terA-D* sites are arranged in the same way as in picture **(a)**. Numbers indicate the exact location on the chromosome in bp.

Despite their abundance across the whole genome, their density increases in the terminus region and only a certain number of repeats within a defined ~400kb region of the terminus interact with FtsK translocase (Bigot *et al.*, 2005; Stouf, Meile and Cornet, 2013). Directed by KOPS motifs, FtsK plays a key role in the final stage of chromosome segregation mediating decondensation of the terminus by removing MatP from *matS* sequences and promoting decatenation and the correct recombination pathway between chromosome dimers at *dif by* interacting with TopoIV and XerCD, respectively (Aussel *et al.*, 2002; Bonné *et al.*, 2009; Lee *et al.*, 2014).

The terminus region contains the chromosome dimer resolution site *dif*, a 28 bp sequence located directly opposite to the origin of replication (Roecklein, Pelletier and Kuempel, 1991). This sequence is recognised by two tyrosine recombinases, XerC and XerD, which cooperatively mediate recombination events at *dif* to convert chromosome dimers into monomers (Colloms *et al.*, 1990, 1996; Graham *et al.*, 2009). Finally, a series of short DNA sequences, called *ter* sites (Figure 1.4), are located in the terminus. *ter* sites are recognised by a small ~36 kDa monomeric protein, named *termination utilisation substance* (Tus) (Hill *et al.*, 1989; Natarajan, Kelley and Bastia, 1991; Roecklein, Pelletier and Kuempel, 1991). The resulting nucleoprotein complex functions as a replication arrest site.

1.8.2 Tus-*ter* system

1.8.2.1 Features and components

Due to the asymmetric nature of *ter* sequences, the resulting Tus-*ter* nucleoprotein complex forms a polar barrier on the DNA duplex that stalls replication forks in a direction-dependent manner allowing them to enter, but not to escape the terminus region, thus establishing a "replication fork trap" (Mulcair *et al.*, 2006; Duggin and Bell, 2009). 14 *ter* sites

have been identified in the *E. coli* chromosome with a GNRNGTTGTAAYKA consensus sequence (Duggin and Bell, 2009). However, under wild-type conditions, only one half of these *ter* sites (*terA-D*, *G-I*) (Figure 1.4-a, Figure 1.5) was found to be functional and capable of arresting approaching replisomes. The other seven *ter* sites (*terE*, *F*, *J-L*, *Y*, *Z*) were found to be either weak or non-functional under normal physiological conditions and were able to infrequently arrest forks but only in the presence of overproduced Tus protein to a level of ~5% of total cellular protein (Duggin and Bell, 2009). The majority of *ter* sites are oriented in a way that is consistent with the fork trap model, except for *TerZ* and *TerY*, which are located on the left-handed replichore in the oritentation that stops replication originating at *oriC*.

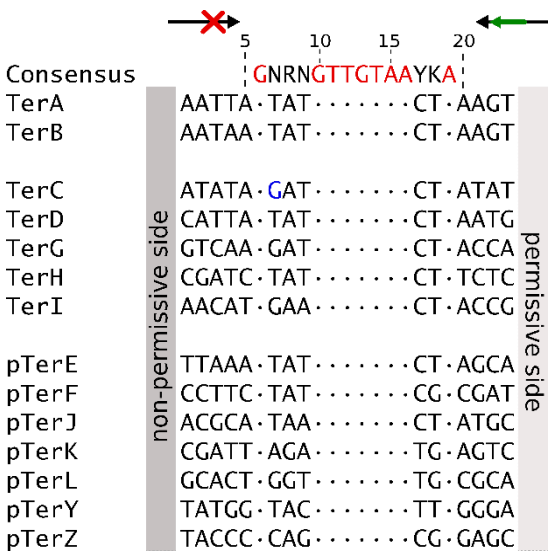

Figure 1.5

Sequences of *E. coli ter* sites. The core sequence for Tus recognition is shown at the top. *ter* sites, for which activity was shown to be either very low or non-detectable, are indicated as p*ter* sites. Strictly conserved nucleotides are indicated with red colour in the consensus sequence and with '·' symbol. The single nucleotide difference between conserved regions of *terB* and *terC* is indicated with blue colour.

Noteworthy, the *tus* gene is located in the terminus region adjacent to *terB*, and its expression is autoregulated. The promoter region of the *tus* gene contains the strong fork arrest sequence *terB* that overlaps with the TATAAT-box, the transcription start site and the ribosomal binding site of this gene. Thus, it is only when a replisome approaches the permissive side of the Tus/*ter* barrier from *OriC* and dissociates the complex, that the *tus* promoter region becomes derepressed, allowing *tus* mRNA synthesis to initiate (Roecklein, Pelletier and Kuempel, 1991).

1.8.2.2 Mechanism of the Tus-ter mediated fork arrest

The peculiar property of the Tus-*ter* complex is to arrest replisomes approaching from one direction while allowing forks from the other direction to disassemble the complex. This property was studied by X-ray crystallography of Tus bound to a truncated 16 bp long *terA* site (Kamada *et al.*, 1996; Mulcair *et al.*, 2006). Tus was found to make multiple contacts with both strands of the *ter* DNA duplex on the non-permissive side of the protein, while the permissive side interacted only with a single DNA strand. Thus, replisomes approaching the permissive face of the Tus/*ter* complex can unfold the Tus protein from the DNA and continue the synthesis without interruption. The non-permissive face of the Tus/*ter* complex arrests approaching replisomes with high efficiency, blocking their further movement for up to several minutes (Coskun-Ari and Hill, 1997; Mulcair *et al.*, 2006; Moreau and Schaeffer, 2013; Berghuis *et al.*, 2015; Elshenawy *et al.*, 2015; Pandey *et al.*, 2015).

17 amino acid residues of the Tus protein were shown to make sequence-specific contacts with the *terA* DNA, and about twice as many would promote non-specific interactions (Kamada *et al.*, 1996; Mulcair *et al.*, 2006; Elshenawy *et al.*, 2015). These studies

identified Tus-*ter* as the most stable complex of a monomeric sequence-specific protein and a DNA recognition sequence.

Upon interaction with the leading-strand template outside of the protein-DNA binding region that has been unwound by the approaching replisome, the Tus-*ter* complex changes its conformation to a "locked" state, which increases the half-life of the complex dramatically (Mulcair *et al.*, 2006; Elshenawy *et al.*, 2015; Pandey *et al.*, 2015). Extensive mutational studies were performed to determine the key nucleotide residues of *ter* and the amino acid residues of Tus that were responsible for the formation and stability of the Tus/*ter* complex (Coskun-Ari and Hill, 1997; Neylon *et al.*, 2000; Mulcair *et al.*, 2006; Elshenawy *et al.*, 2015). The strictly conserved cytosine at position 6 (Figure 1.5) of the *ter* site and His144 residue of Tus were proposed to be the key elements responsible for the formation of the locked state of the Tus/*ter* complex. These observations were confirmed when the crystal structure of the Tus protein bound to *terA* with the first several unpaired nucleotides was resolved (Mulcair et al., 2006). It was shown that, as a replication fork progresses towards the non-permissive side of the Tus/*ter* complex, the *ter* C6 residue on the lagging strand template rotates around the helical DNA axis and fits into a pocket in the Tus protein. Three hydrogen bonds between C(6) and His144, Gly149 with Leu150 of the pocket stabilise this conformation, while Phe140 and Glu49 outside of the pocket are responsible for the specificity and probability of the 'locked' state formation (Mulcair *et al.*, 2006; Berghuis *et al.*, 2015; Elshenawy *et al.*, 2015).

Interestingly, in experiments using the T7 phage replisome, Tus-*terB* was able to arrest the progressing Pol III polymerase at its non-permissive end, but not the isolated T7 polymerase, which would continue DNA synthesis after a short pause. However, the substrate with the unpaired C(6) (due to the nucleotide mismatch at this position) was shown to arrest

the isolated T7 polymerase completely. This suggests the existence of the specificity of Tus/*ter* lock formation towards the polarity of the DNA motor. Such specificity in the case of T7 polymerase could be explained by the occlusion of C(6) residue with the 3'-5' translocating protein, thus preventing the "locked" conformation of Tus-*ter* complex (Pandey *et al.*, 2015).

Another observation Tus/*terB* barrier bypass by a replication fork was done in the Michel lab (Bidnenko, Lestini and Michel, 2006). There, two ectopic *terB* sites were introduced in the middle of each replichore of the Δ*tus E. coli* strain. In the absence of the UvrD helicase the expression of Tus from an inducible arabinose promoter was lethal for these cells. UvrD was shown to restore viability, but this function was dependent on RecA- and RecBCD dependent homologous recombination. From these observations a model was proposed to explain the mechanism UvrD utilises to elicit the block at ectopic *terB* sites (Figure 1.6).

In the first step after replication arrest at an ectopic *terB* site, the second round of replication arrives at the blocked fork leading to replication run-off of two-forks. This results in two linear strands that are recognised and processed in RecBCD-dependent manner. Both strands are incorporated into the intact homologous sequences on the chromosome with the help of RecA and RecBCD. Repair-initiated forks are assembled by PriA pathway and DnaB along with UvrD are present at both forks on the lagging and leading strands, respectively.

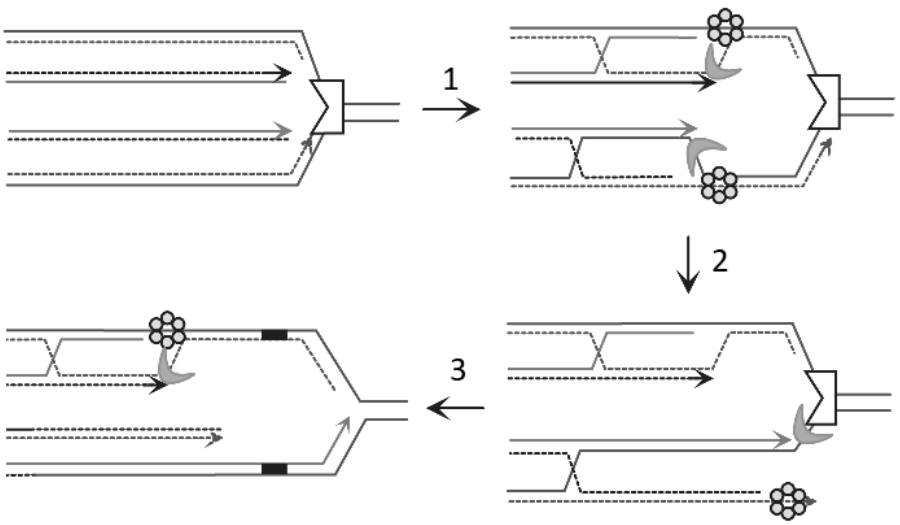

Figure 1.6

Model of Tus removal from ectopic *terB* sites by UvrD during the RecA-dependent homologous recombination. Full lines are the initial template strands. Dashed lines are strands generated by the second round of replication. Arrows indicate 3' ends. Indented rectangles indicate *ter* sites. Hexagon shaped rings – DnaB, crescent-shaped figures – UvrD (adapted from Bidnenko *et al.*, 2006, with modifications).

In the next stage (one of two scenarios is shown for simplicity) DnaB and UvrD unwind DNA towards the Tus/*terB* barrier. However, the strand DnaB is translocating on is discontinuous, which causes the helicase to run off. Meanwhile, UvrD approaches the Tus/*terB* barrier translocating in 3' to 5'direction and consequently does not trigger the locked state of the barrier and displaces Tus. Removal of the barrier by recombination-initiated replication indicates the absolute need for homologous recombination in this process.

1.9 About the thesis

Genome replication is sporadically challenged by obstacles that can result from DNA damage, topological stress or tightly bound proteins. Replication fork stalling at DNA-bound proteins can lead to collapse of the fork and promote mutation and genomic instability, a

hallmark of cancer cells. However, organisms have evolved barriers that cause replication forks to stall, and this may suggest that regulated fork stalling is preferable to un-regulated fork stalling. In this work we have quantified stalled replication forks at naturally occurring Tus/*ter* barriers in the *Escherichia coli* chromosome and have shown that the helicase UvrD (Srs2 in eukaryotes) specifically promotes bypass of the most commonly encountered barrier, *terC*, in the terminus.

The Tus/*ter* system allows replisomes to enter the terminus but prevents their escape into the opposite replichore, that is, towards *oriC*. This prevents collisions of replication forks with transcription complexes from highly transcribed genes (e.g. ribosomal RNA operons). UvrD helicase is involved in DNA repair pathways and the removal of DNA-bound proteins at replication forks. UvrD has been shown to allow bypass of an ectopic Tus/*terB* replication fork barrier introduced in the middle of a replichore, but only as a consequence of RecA-mediated homologous recombination (Bidnenko, Lestini and Michel, 2006). These findings suggest that UvrD has a unique function to facilitate replication fork bypass of Tus/*ter* barriers; however it is not known whether this function is retained under normal conditions in the terminus region. Therefore, the primary goal of this study has been to:

1. Characterise replication fork arrest at Tus/*ter* barriers in the terminus.
2. Determine whether replication fork bypass of Tus/*terC* occurs in the terminus under normal conditions.
3. Investigate the role of UvrD in the replication fork bypass of Tus/*terC* and identify underlying features that influence this process.

2 MATERIALS AND METHODS

2.1 Materials

2.1.1 Growth Media

Growth media were prepared using deionized H_2O (dH_2O), sterilized by autoclaving at 121˚C for 15 minutes, unless stated otherwise, and stored at room temperature. M9 media was always freshly prepared using the M9 salts 4X concentrated stock, $CaCl_2$ (0.5 M) and $MgSO_4$ (1 M) before use. Media composition is described in Table 2.1.

Table 2.1 Growth media.

Media	Composition
Luria-Bertani (LB)	1% Bacto-tryptone, 0.5% Oxoid yeast extract, 1% NaCl; pH 7.2
LB Agar	1% Bacto-tryptone, 0.5% Oxoid yeast extract, 1% NaCl, 1.5% Oxoid agar #3; pH 7.2
LC Bottom Agar	1% Bacto-tryptone, 0.5% Oxoid yeast extract, 0.5% NaCl, 1% Oxoid agar #3; pH 7.2
LC Top Agar	1% Bacto-tryptone, 0.5% Oxoid yeast extract, 0.5% NaCl, 0.7% Oxoid Agar #3; pH 7.2
SOC	2% Bacto-tryptone, 0.5% Oxoid yeast extract, 3.6% Glucose, 10 mM NaCl, 2.5 mM KCl, 20 mM $MgSO_4$, 20 mM $MgCl_2$; sterilised by autoclaving at 116˚C for 20 minutes
M9 salts stock (x4)	0.2 M Na_2HPO_4, 90 mM KH_2PO_4, 30 mM NaCl, 80 mM NH_4Cl
M9 minimal	50 mM Na_2HPO_4, 22.5 mM KH_2PO_4, 7.5 mM NaCl, 20 mM NH_4Cl, 0.2% casamino acids, 0.4% glucose, 1 mM $MgSO_4$, 0.1 mM $CaCl_2$; pH 7.2

M9 minimal Agar	1.2% Oxoid agar #3, 33.7 mM Na_2HPO_4, 22 mM KH_2PO_4, 8.55 mM NaCl, 9.35 mM NH_4Cl, 0.2% casamino acids, 0.4% glucose, 1 mM $MgSO_4$, 0.1 mM $CaCl_2$; pH 7.2

2.1.2 Media supplements and antibiotics

Media supplements listed in Table 2.2 were prepared using dH_2O, autoclaved at 121˚C for 15 minutes and stored at room temperature. Antibiotics listed in Table 2.3 were prepared using indicated solvents and stored at -20˚C. Melted agar media was cooled down to below 60˚C prior to addition of supplements and antibiotics. All supplements and antibiotics were added prior to use.

Table 2.2 Media supplements

Name	Abbreviated name	Stock concentration
Arabinose	Ara	20% (w/v)
Glucose	Glu	20% (w/v)
Glycerol	Gly	80% (w/v)
Sucrose	Suc	20% (w/v)

Table 2.3 Antibiotics

Name	Abbreviated name	Solvent	Stock concentration	Working concentration
Chloramphenicol	Cm	100% ethanol	50 mg/ml	50 µg/ml
Kanamycin	Km	dH_2O	50 mg/ml	50 µg/ml
Spectinomycin	Spec	dH_2O	50 mg/ml	50 µg/ml
Streptomycin	Str	dH_2O	50 mg/ml	50 µg/ml
Tetracycline	Tc	50% ethanol	15 mg/ml	15 µg/ml

2.1.3 Buffers and solutions

2.1.3.1 General purpose buffers and reagents

$CaCl_2$ (0.5 M)

0.55 g of $CaCl_2$ were dissolved in a final volume of 10 ml of dH_2O. Sterilised by passing through 0.22-µm filter (Merck). Stored in 2 ml aliquots at 4˚C.

$MgSO_4$ (1 M)

1.2 g of $MgSO_4$ were dissolved in a final volume of 10 ml of dH_2O. Sterilised by passing through 0.22-µm filter (Merck). Stored at room temperature.

Tris-HCl (1 M, pH 8.0)

121.14 g of Tris base were dissolved in ~800 ml of dH_2O. Adjusted the pH of the room temperature solution to 8.0 using concentrated HCl and made up to a final volume of 1 litre. Sterilised by autoclaving at 121˚C for 15 minutes. Stored at room temperature.

Ethylenediaminetetraacetic acid (EDTA) (0.5 M)

93.05 g of disodium EDTA dihydrate was dissolved in ~400 ml of dH_2O. Adjusted the pH to 8.0 using 10 N NaOH and made up to a final volume of 500 ml. Sterilised by autoclaving at 121˚C for 15 minutes; stored at room temperature.

TE buffer

100 ml of Tris-HCl (1 M, pH 8.0) and 20 ml of EDTA (0.5 M, pH 8.0) were mixed in a final volume of 1 litre of dH_2O for the 10X concentrated solution. The working concentration of TE was 1X (10 mM Tris-base, 1 mM EDTA). Sterilised by autoclaving at 121˚C for 15 minutes. Stored at room temperature.

TEN buffer

100 ml of Tris-HCl (1 M, pH 8.0), 20 ml of EDTA (0.5 M, pH 8.0), and 58.44 g of NaCl were mixed in a final volume of 1 litre of dH_2O for the 10X concentrated solution; the working concentration of TEN was 1X (100 mM NaCl, 10 mM Tris-base, 1 mM EDTA). Sterilised by autoclaving at 121˚C for 15 minutes. Stored at room temperature.

NDS buffer (pH 8.0)

0.6 g of Tris base, 93 g of disodium EDTA dihydrate, and 12 g NaOH were dissolved in 350 ml of dH_2O. 5 g of sodium N-lauroylsarcosine was dissolved in 50 ml of dH_2O separately. The two solutions were then mixed together. The pH was further adjusted to 8.0 using 10 N NaOH. The

volume of the solution was adjusted to 500 ml using dH_2O. The final concentrations of the ingredients were 10 mM Tris base, 0.5 M EDTA, and 34 mM sodium N-lauroylsarcosine.

Phage buffer

7 g of Na_2HPO_4, 3 g of KH_2PO_4, 5 g of NaCl, 0.25 g of $MgSO_4 \cdot 7H_2O$, 10 ml of 10 mM $CaCl_2$, and 1 ml of 1% (w/v) gelatine were mixed in a final volume of 1 litre of dH_2O. Dispensed in 100 ml aliquots and sterilised by autoclaving at 121˚C for 15 minutes. Stored at room temperature. The final concentrations of the ingredients were 49 mM Na_2HPO_4, 22 mM KH_2PO_4, 85 mM of NaCl, 1 mM of MgSO, 0.1 mM $CaCl_2$, and 0.001% (w/v) gelatine.

Tris-acetate buffer (TAE)

242.28 g of Tris base, 57 ml of glacial acetic acid, 18.61 g of disodium EDTA dihydrate were dissolved in a final volume of 1 litre of dH_2O for the 50X concentrated stock solution. Stored at room temperature. The working concentration of TAE was 1X (40 mM Tris base, 19 mM acetic acid, 1 mM EDTA).

Tris-borate buffer (TBE 10x)

108 g of Tris base, 55 g of boric acid, and 3.72 g of disodium EDTA dihydrate were dissolved in a final volume of 1 litre of dH_2O. Freshly prepared before use. The working concentration of TBE was 1X (89 mM Tris base, 89 mM acetic acid, 11 mM EDTA).

PBS (Phosphate-buffered saline)

8 g of NaCl, 0.2 g of KC1, 1.44 g of Na_2HPO_4 and 0.24 g of KH_2PO_4 were dissolved in a final volume of 1 litre of dH_2O. Sterilised by passing through 0.22-µm filter (Merck). Stored at room temperature. The final concentrations of the ingredients were 137 mM NaCl, 2.7 mM KCl, 10 mM Na_2HPO_4 and 2 mM KH_2PO_4.

2.1.3.2 Buffers and reagents for Southern blot and DNA-DNA hybridisation

SSC

175.3 g of NaCl and 88.2 g of tri-sodium citrate dihydrate were dissolved in a final volume of 1 litre of dH_2O for the 20X concentrated stock solution. The pH was adjusted to 7.0 using concentrated HCl. Stored at room temperature. The final concentrations of the ingredients were 3.0 M NaCl and 0.3 M sodium citrate.

Phosphate buffer (0.5 M)

142 g of Na_2HPO_4 and 3 ml of concentrated (85%, 15.2 M) H_3PO_4 were mixed in a final volume of 1 litre of dH_2O. The pH was adjusted to 7.2 using concentrated H_3PO_4. Sterilised by passing through 0.22-µm filter (Merck). Stored at room temperature.

Depurination solution

40 ml of concentrated (37%, 11.6 M) HCl was added to the final volume of 1 litre of dH_2O. Freshly prepared before use. The final concentration of HCl was 464 mM.

Transfer buffer

1 litre of SSC 20X and 40 g of NaOH pellets were mixed in a final volume of 2 litres of dH_2O. Stored at room temperature. The final concentrations of the ingredients were 1.5 M NaCl and 0.15 M sodium citrate.

Church-Gilbert buffer (hybridisation buffer)

200 µl of EDTA (0.5 M), 1 g of bovine serum albumin (BSA), and 7 g of Sodium dodecyl sulfate (SDS) were mixed in a final volume of 100 ml of phosphate buffer (0.5 M). Freshly prepared before use. The final concentrations of the ingredients were 0.5 M phosphate buffer, 1 mM EDTA, 1% (w/v) BSA and 7% (w/v) SDS.

Low stringency wash buffer

100 ml of SSC (20X) and 10 ml SDS (10% stock solution, Fisher Scientific) were mixed in a final volume of 1 litre of dH_2O. Stored at room temperature. The final concentrations of the ingredients were 2xSSC and 0.1% (v/v) SDS.

High stringency wash buffer

25 ml of SSC (20X) and 10 ml SDS (10% stock solution, Fisher Scientific) were mixed in a final volume of 1 litre of dH_2O. Stored at room temperature. The final concentrations of the ingredients were 0.5xSSC and 0.1% (v/v) SDS.

SSPE (20X)

175.3 g of NaCl, 27.6 g of $NaH_2PO_4 \cdot H_2O$ and 7.4 g of EDTA were dissolved in a final volume of 1 litre of dH_2O. Adjusted the pH to 7.4 using 10 N NaOH. Sterilised by autoclaving at 121˚C for 15 minutes. Stored at room temperature. The final concentrations of the ingredients were 3 M NaCl, 0.2 M NaH_2PO_4 and 20 mM EDTA.

Stripping buffer

50 ml of formamide (96% stock solution, Sigma-Aldrich) and 25 ml of SSPE (20X) were mixed in a final volume of 100 ml of dH_2O.

2.1.4 Oligonucleotides, plasmids and bacterial strains

Primer oligonucleotides, plasmids and bacterial strains used in the study are in Table 2.4, Table 2.5 and Table 2.6, respectively.

Table 2.4 Oligonucleotides

Name	Sequence (5`-3`)	Description
pKO F (2233)	AGGGCAGGGTCGTTAAATAGC	To sequence pTOF24 SalI-PstI inserts
pKO R (2234)	AGGGAAGAAAGCGAAAGGAG	
UvrD.F1 (3426)	AAAActgcagTGACCTCGCTGATATAATCA	To sequence the *uvrD* gene deletion
UvrD.R2 (3429)	AAAAgtcgacTCAGATACTGAAGATGGCGC	
RecG-F1 (1040)	AAAAgtcgacGCATTTTGATGGGACAGGAG	To sequence the *recG* gene deletion
RecG-R2 (1043)	AAAActgcagATGGGCAAAAACTACGATGC	
recO-KO-F1 (1249)	AAAAActgcagCGTGCGTAAGCATCTACCTG	To sequence the *recO* gene deletion
recO-KO-R2 (1252)	AAAAAgtcgacCATCGCGCATTTTGTCAC	
RecA-KO-F1 (1273)	AAAActgcagAACGCGGATTTGTCACCTAC	To sequence the *recA* gene deletion
RecA-KO-R2 (1276)	AAAAgtcgacCGCGGGAAATACCTTTCTG	

RecQ-KO-F1 (1311) RecQ-KO-R2 (1314)	AAAAActgcagATGTGGTGGGTAATA CTGACG AAAAAgtcgacTTTTCAGTGCACCACG TAGC	To sequence the *recQ* gene deletion
terA_XmnI_ps 1 F (4291) terA_XmnI_p R (4217)	AATAGCGCAACGAGAACAAGA GTTGGGTACATTAGGTGGTGC	To generate the DNA fragment used for *terA* region Southern blot probing
terB A F (3998) terB B R (3999)	TGGAAAGATTACTGCGTGGG TAACAACTCACCAACGTCCG	To generate the DNA fragment used for *terB* region Southern blot probing
terC A F[a] terC B R[a]	CCGGTACCCATTGTTATTGC GGTGCACAGTATCCAGAACG	To generate the DNA fragment used for *terC* region Southern blot probing
terD_long F (4537) terD_long R (4538)	TAAGGTGGCAGACATCGAAAC AGAAGTGCTGTTCATGTGACG	To generate the DNA fragment used for *terD* region Southern blot probing
terB_NcoI chkF (3993) terB_NcoI chkR (3994)	CTGCTCCTCACCTGATTA GATACAACTCACACAATGC	To sequence the NcoI cutting site insertion

terB_NcoI F (3989) terB_NcoI R (3990) terB_NcoI F2 (3991) terB_NcoI R2 (3992)	AAAAAgtcgacATTGGAACTTTGGCTTTT **TTTccatggACATCAGGCAATCTCGT** **T**ATCAAATGGTAAATAATAAG **AACGAGATTGCCTGATGTccatggAA** **A**TGTTTGGTCTTTCGTG AAAAActgcagAAGAGCGGATGGATAAC	To generate the insert by crossover PCR for the construction of pDL6501
uxaBter - R2 (3874) yneEter - F1 (3876)	AAAAAgtcgacTATGACCAAGTTCCGCACCC AAAAActgcagCGACCGTGAGGCAATCATC	To generate the insert by crossover PCR for the construction of pDL6356-6359, 6689, 7447-7449
yneEterB - R1 (3877) uxaBterB - F2 (3875)	**AACactttagttacaacatacttattGCC**TTTATCATTAACAGGT **GGCaataagtatgttgtaactaaagtGGT**GAAATAAGAAACCCGG	To generate the insert by crossover PCR for the construction of pDL6357
yneEnoter - R1 (3888) uxaBnoter - F2 (3889)	**TTTCTTATTTCACCGCC**TTTATCATTAACAGGT **TTAATGATAAAGGCGGT**GAAATAAGAAACCCGG	To generate the insert by crossover PCR for the construction of pDL6356

yneEchk – F (3890) uxaBchk – R (3891)	CTTCAGGCGTGGAAAAGTCG ACACCGTTACTTCTGAACCCG	To screen mutation of *terC*
yneEterB' - R1 (3896) uxaBterB' - F2 (3898)	**AACactttagttacaacatccttattGCC**TTTATCATTAACAGGT **GGCaataaggatgttgtaactaaagtGGT**GAAATAAGAAACCCGG	To generate the insert by crossover PCR for the construction of pDL6358
yneEterC' - R1 (3897) uxaBterC' - F2 (3899)	**AACatattagttacaacatactatatGCC**TTTATCATTAACAGGT **GGCatatagtatgttgtaactaatatGGT**GAAATAAGAAACCCGG	To generate the insert by crossover PCR for the construction of pDL6359
rstBTerchk - F1 (3922) tusTerchk - R1 (3923)	CATCCCGCAATTTACCTCTG ACCAATAGCTTGTGTTGCTC	To screen mutation of *terB*
rstBter - F1 (3924) tuster - R2 (3933)	AAAAAgtcgacATAATTTGCTCAATAACGCCC AAAAActgcagGTCTTGAGTTTATTGATGTGC	To generate the insert by crossover PCR for the construction of pDL6401-6403, 6414, 6501
rstBdter - R1 (3925)	**CATAATATTAACCTTA**TAGCACAGTCGTGGTG	To generate the insert by crossover PCR for

tusdter - F2 (3929)	**GACTGTGCTATAAGGT**TAATATTATGGCGCGT	the construction of pDL6401
rstBterC - R1 (3926)	**ACCatattagttacaacatcctatatTTA**TAGCACAGTCGTGGTG	To generate the insert by crossover PCR for the construction of pDL6402
tusterC - F2 (3930)	**TAAatataggatgttgtaactaatatGGT**TAATATTATGGCGCGT	
rstBterC' - R1 (3927)	**ACCatattagttacaacatactatatTTA**TAGCACAGTCGTGGTG	To generate the insert by crossover PCR for the construction of pDL6403
tusterC' - F2 (3931)	**TAAatatagtatgttgtaactaatatGGT**TAATATTATGGCGCGT	
rstBterB' - R1 (3928)	**ACCactttagttacaacatccttattTTA**TAGCACAGTCGTGGTG	To generate the insert by crossover PCR for the construction of pDL6414
tusterB' - F2 (3932)	**TAAaataaggatgttgtaactaaagtGGT**TAATATTATGGCGCGT	
yneECreT - R1 (4138)	**ACCatataggatgttgtaactaatatGCC**TTTATCATTAACAGGT	To generate the insert by crossover PCR for the construction of pDL6689
uxaBCreT - F2 (4139)	**GGCatattagttacaacatcctatatGGT**GAAATAAGAAACCCGG	
terC[fl1-B] - R1 (4539)	**ACCatattagttacaacatccttattGCC**TTTATCATTAACAGGT	To generate the insert by crossover PCR for the construction of pDL7447
terC[fl1-B] - F2 (4540)	**GGCaataaggatgttgtaactaatatGGT**GAAATAAGAAACCCGG	

terC[fl2-B] - R1 (4541) terC[fl2-B] - F2 (4542)	**ACCactttagttacaacatcctatatGCC**TTTATCATTAACAGGT **GGCatataggatgttgtaactaaagtGGT**GAAATAAGAAACCCGG	To generate the insert by crossover PCR for the construction of pDL7448
terC-B[fl1-C] - R1 (4543) terC-B[fl1-C] - F2 (4544)	**ACCactttagttacaacatactatatGCC**TTTATCATTAACAGGT **GGCatatagtatgttgtaactaaagtGGT**GAAATAAGAAACCCGG	To generate the insert by crossover PCR for the construction of pDL7449
terC-B[fl2-C] - R1 (4545) terC-B[fl2-C] - F2 (4546)	**ACCatattagttacaacatacttattGCC**TTTATCATTAACAGGT **GGCaataagtatgttgtaactaatatGGT**GAAATAAGAAACCCGG	To generate the insert by crossover PCR for the construction of pDL7450

[a] – These oligonucleotides were designed by Julia Mawer, Leach Lab. PstI and SalI restriction enzymes cutting sites and *ter* sites are in lower case; crossover PCR homology regions are **bold**.

Table 2.5 Plasmids

Name	Description	Source
pDL1605	pTOF24 Cm^R Km^R *rep*^{ts} Suc^S	(Merlin, Mcateer, and Masters 2002)
pDL2391	pTOF24 *uvrD* KO	J. Blackwood, Leach lab
pDL2429	pTOF24 *recG* KO	L. Wardrope, Leach Lab
pDL2710	pTOF24 *recO* KO	E. Okely, Leach Lab
pDL2711	pTOF24 *recA* KO	E. Okely, Leach Lab
pDL2765	pTOF24 *recQ* KO	E. Okely, Leach Lab
pDL6356	pTOF24_Δ*terC* Cm^R *rep*^{ts} Suc^S	This study
pDL6357	pTOF24_ *terC* →*terB* Cm^R *rep*^{ts} Suc^S	This study
pDL6358	pTOF24_ *terC* →*terB*[T7G] Cm^R *rep*^{ts} Suc^S	This study
pDL6359	pTOF24_*terC*[G7T] Cm^R *rep*^{ts} Suc^S	This study
pDL6401	pTOF24_Δ*terB* Cm^R *rep*^{ts} Suc^S	This study
pDL6402	pTOF24_ *terB* →*terC* Cm^R *rep*^{ts} Suc^S	This study
pDL6403	pTOF24_ *terB* →*terC*[G7T] Cm^R *rep*^{ts} Suc^S	This study
pDL6414	pTOF24_*terB*[T7G] Cm^R *rep*^{ts} Suc^S	This study
pDL6501	pTOF24_NcoI_*terB* Cm^R *rep*^{ts} Suc^S	This study
pDL6689	pTOF24_pCret Cm^R *rep*^{ts} Suc^S	This study
pDL7447	pTOF24_ *terC*[NP.fl-B] Cm^R *rep*^{ts} Suc^S	This study

pDL7448	pTOF24_ *terC*[P.fl-B] Cm^R rep^{ts} Suc^S	This study
pDL7449	pTOF24_ *terC* →*terB*[NP.fl-C] Cm^R rep^{ts} Suc^S	This study
pDL7450	pTOF24_ *terC* →*terB*[P.fl-C] Cm^R rep^{ts} Suc^S	This study

Cm^R - resistant to chloramphenicol; Km^R - resistant to kanamycin; rep^{ts} - temperature-sensitive replication; Suc^S - sensitive to products of sucrose metabolism; NP.fl-B/C and P.fl-B/C – the non-permissive flanking sequence of *terB*/*terC* and the permissive flanking sequence of *terB*/*terC*, respectively.

Table 2.6 *Escherichia coli* strains

Name	Genotype	Source
DL1719	*recA1 endA1 gyrA96 thi*-1 *hsdR17 supE44 relA1 lac* [F' *proAB lacIqZ* ΔM15 Tn10]	Stratagene
DL1777 (MG1655)	$lacI^q$ $lacZ_{\chi-}$ *fnr*-267 (Δ*ynaJ* Δ*ydaA* Δ*frn* Δ*ogt* Δ*abgT* Δ*abgB* Δ*abgA* Δ*abgR* Δ*ydaL* Δ*ydaM* Δ*ydaN* Δ*dbpA* Δ*ydaO*)	(Eykelenboom *et al.*, 2008)
DL6318	DL1777 Δ*terC*	PMGR with pDL6356
DL6319	DL6318 *terC* →*terB*	PMGR with pDL6357
DL6423	DL1777 Δ*terB*	PMGR with pDL6401
DL6436	DL6423 *terB* →*terC*	PMGR with pDL6402
DL6503	DL6436 Δ*terC*	PMGR with pDL6356
DL6504	DL1777 *fumC-fumA*::NcoI-cs	PMGR with pDL6501
DL6505	DL6319 *fumC-fumA*::NcoI-cs (*terC* →*terB*)	PMGR with pDL6501
DL6506	DL6436 *fumC-fumA*::NcoI-cs (*terB* →*terC*)	PMGR with pDL6501
DL6507	DL6503 *fumC-fumA*::NcoI-cs (Δ*terC*)	PMGR with pDL6501
DL6554	DL6504 Δ*recG* (NcoI-cs)	PMGR with pDL2429
DL6555	DL6505 Δ*recG* (NcoI-cs, *terC* →*terB*)	PMGR with pDL2429
DL6556	DL6506 Δ*recG* (NcoI-cs, *terB* →*terC*)	PMGR with pDL2429
DL6557	DL6507 Δ*recG* (NcoI-cs, Δ*terC*)	PMGR with pDL2429
DL6602	DL6504 Δ*terC* (NcoI-cs)	PMGR with pDL6356

DL6603	DL6504 Δ*terB* (NcoI-cs)	PMGR with pDL6401
DL6604	DL6504 Δ*recO* (NcoI-cs)	PMGR with pDL2710
DL6643	DL6504 Δ*uvrD* (NcoI-cs)	PMGR with pDL2391
DL6644	DL6604 Δ*recG* (Δ*recO,* NcoI-cs)	PMGR with pDL2429
DL6645	DL6604 Δ*uvrD* (Δ*recO,* NcoI-cs)	PMGR with pDL2391
DL6678	DL6602 Δ*recG* (Δ*terC,* NcoI-cs)	PMGR with pDL2429
DL6679	DL6603 Δ*recG* (Δ*terB,* NcoI-cs)	PMGR with pDL2429
DL6685	DL6643 *terC→terB* (Δ*uvrD*, NcoI-cs)	PMGR with pDL6357
DL6686	DL6643 Δ*terC* (Δ*uvrD*, NcoI-cs)	PMGR with pDL6356
DL6687	DL6643 *terB→terC* (Δ*uvrD*, NcoI-cs)	PMGR with pDL6402
DL6688	DL6687 Δ*terC* (*terB→terC,* Δ*uvrD*, NcoI-cs)	PMGR with pDL6356
DL6764	DL6645 Δ*recG* (Δ*uvrD*, Δ*recO,* NcoI-cs)	PMGR with pDL2429
DL6768	DL6644 Δ*uvrD* (Δ*recG*, Δ*recO,* NcoI-cs)	PMGR with pDL2391
DL6909	DL6504 $terC_{inverted}$ (NcoI-cs)	PMGR with pDL6689
DL6931	DL6504 Δ*recA* (NcoI-cs)	PMGR with pDL2711
DL6932	DL6602 Δ*recA* (Δ*terC,* NcoI-cs)	PMGR with pDL2711
DL6933	DL6643 Δ*recA* (Δ*uvrD*, NcoI-cs)	PMGR with pDL2711
DL6934	DL6686 Δ*recA* (Δ*terC*, Δ*uvrD*, NcoI-cs)	PMGR with pDL2711
DL7126	DL6504 *terC→terB* (NcoI-cs)	PMGR with pDL6357
DL7127	DL7126 Δ*recA* (*terC→terB* ,NcoI-cs)	PMGR with pDL2711

DL7128	DL6685 Δ*recA* (*terC*→*terB*, Δ*uvrD*, NcoI-cs)	PMGR with pDL2711
DL7395	DL6504 *terC*[G7T] (NcoI-cs)	PMGR with pDL6359
DL7396	DL6504 *terC*→*terB*[T7G] (NcoI-cs)	PMGR with pDL6358
DL7405	DL7395 Δ*recG* (*terC*[G7T], NcoI-cs)	PMGR with pDL2429
DL7406	DL7396 Δ*recG* (*terC*→*terB*[T7G], NcoI-cs)	PMGR with pDL2429
DL7455	DL6504 *terC*[NP.fl-B] (NcoI-cs)	PMGR with pDL7447
DL7456	DL6504 *terC*[P.fl-B] (NcoI-cs)	PMGR with pDL7448
DL7457	DL6504 *terC*→*terB*[NP.fl-C] (NcoI-cs)	PMGR with pDL7449
DL7458	DL6504 *terC*→*terB*[NP.fl-C] (NcoI-cs)	PMGR with pDL7450

2.2 Methods

2.2.1 Microbiology methods

2.2.1.1 Overnight cultures

A single colony from a freshly streaked solid agar plate was inoculated into a capped bottle with 5 ml of LB or M9 minimal medium containing antibiotics and supplements when required. Strains were incubated overnight (12-18 hours) under agitation at the appropriate temperature.

2.2.1.2 Long-term storage of strains

500 µl of an overnight culture was thoroughly mixed with 500 µl of glycerol (80%) in an Eppendorf tube. Each tube was sealed with Parafilm and stored at -80˚C.

2.2.1.3 Ultraviolet sensitivity assay

An overnight culture was diluted in fresh medium to adjust the OD_{600} to 1.0. 10-fold serial dilutions were prepared and 5 µl aliquots of each dilution were spotted onto agar plates with the appropriate medium and supplements. Plates were exposed to different doses of UV radiation prior to incubation at 30˚C or 37˚C for up to 24 hours.

2.2.1.4 Chemical transformation of bacterial strains

500 µl of the overnight culture was inoculated into 250 ml Erlenmeyer flask with 25 ml of pre-warmed LB medium containing antibiotics and supplements when required. The strain was incubated at 37˚C under agitation until it reached mid-log phase of growth. 1 ml of the culture was then transferred to an Eppendorf tube and centrifuged for 30 seconds at maximum speed (~14k g). The supernatant was discarded, and the cell pellet was resuspended in 500 µl of freshly made ice-cold 0.1 M $CaCl_2$. The cell suspension was incubated on ice for 30 minutes and then centrifuged for 30 seconds at the maximum speed. The supernatant was discarded, and the cell pellet was resuspended in 100 µl of ice-cold 0.1 M $CaCl_2$. 10-300 ng of plasmid DNA or 20 µl of a plasmid ligation reaction mix was added to the cell suspension. The cell suspension was incubated on ice for 30 minutes then put in a water bath at 42˚C for 2 minutes. 800 µl of room temperature LB or SOC medium was added to each tube. Cells were incubated at the appropriate temperature (30˚C for thermosensitive plasmid replication) for an hour under agitation and then centrifuged for 30 seconds at the maximum speed.

800 µl of the supernatant was discarded, cells were resuspended in the remaining 100 µl of the medium and spread on a solid LB medium containing antibiotics and supplements when required. Appropriate controls were prepared in parallel.

2.2.1.5 Plasmid mediated gene replacement

Plasmid mediated gene replacement (PMGR) method was used to introduce alterations in the chromosomal DNA sequence. The resulting strain does not require a selection marker and does not leave "scars" on the chromosome (Link *et al.*, 1997). Derivatives of the low copy number plasmid pTOF24 (Merlin *et al.*, 2002) are used in the technique. pTOF24 carries $repA^{ts}$ ecoding a temperature labile replication initiation protein, the levansucrase gene from *Bacillus subtilis*, *sacB*, the chloramphenicol resistance gene *cat*, the kanamycin resistance gene *aph*(3')-1 and a multiple cloning site (MSC) including PstI and SalI restriction endonuclease recognition sequences flanking *aph*(3')-1. PstI and SalI recognition sequences allows *aph*(3')-1 gene to be replaced with another DNA molecule (insert) flanked by PstI and SalI recognition sequences through restriction and ligation reactions generating derivatives of pTOF24 plasmid.

The insert contains the DNA sequence of interest (or the absence of it to produce a deletion) flanked by two approximately 400 bp fragments, PstI recognition sequence on one end and SalI on another. These ~400 bp fragments are copies of the two chromosomal regions adjacent to each side of the sequence that is intended to be modified in the chromosome. Each fragment was generated using PCR reaction. The insert was generated using crossover PCR (see Figure 2.1).

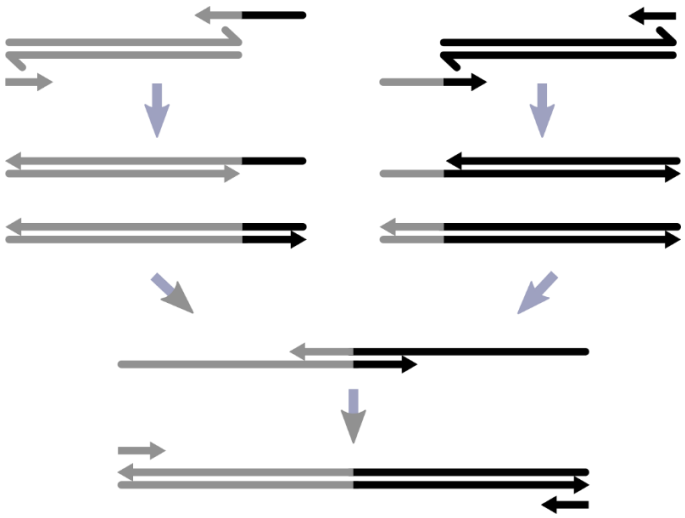

Figure 2.1
Schematic representation of crossover PCR method stages. RNA primers (black and grey arrows) are used to splice two DNA sequences (black and grey) together.

To introduce a modification into the chromosomal DNA using PMGR technique, the *E. coli* strain of interest was transformed with the desired derivative of pTOF24 plasmid. Transformed cells were grown on LB plates containing chloramphenicol at 30°C to permit plasmid temperature sensitive replication. Cells carrying the plasmid were purified once on LB plates containing chloramphenicol. A single colony was streaked on LB plates containing chloramphenicol and grown at 42°C. Plasmid replication is inhibited at this temperature and only cells with the plasmid integrated into the chromosome via either of the 400 bp homologous regions are able to grow. Cells carrying the integrated plasmid were purified once on LB plates containing chloramphenicol at 42°C. A single colony was incubated overnight in liquid LB medium at 30°C to permit plasmid replication and excision from the chromosome. The liquid culture was serially diluted in LB medium, 100 µl of 10^{-4} and 10^{-5} dilutions were spread on LB plates containing sucrose (5%) and incubated at 30°C. Cells carrying the plasmid expressed levansucrase from the *sacB* gene which produced toxic levan polysaccharide from sucrose, severely retarding cell growth. Cells that lost the plasmid grew normally and were checked for chloramphenicol sensitivity by replica plating on LB plates containing sucrose (5%) and chloramphenicol with sucrose (5%). Cells in which the plasmid insertion and excision happened via different homologous regions kept the desired alteration in the chromosome. This was confirmed by PCR and gel electrophoresis migration analysis of the resulting fragments/or Sanger sequencing of the modified locus. Colonies were purified once on LB plates and their viability examined using UV sensitivity assay where necessary.

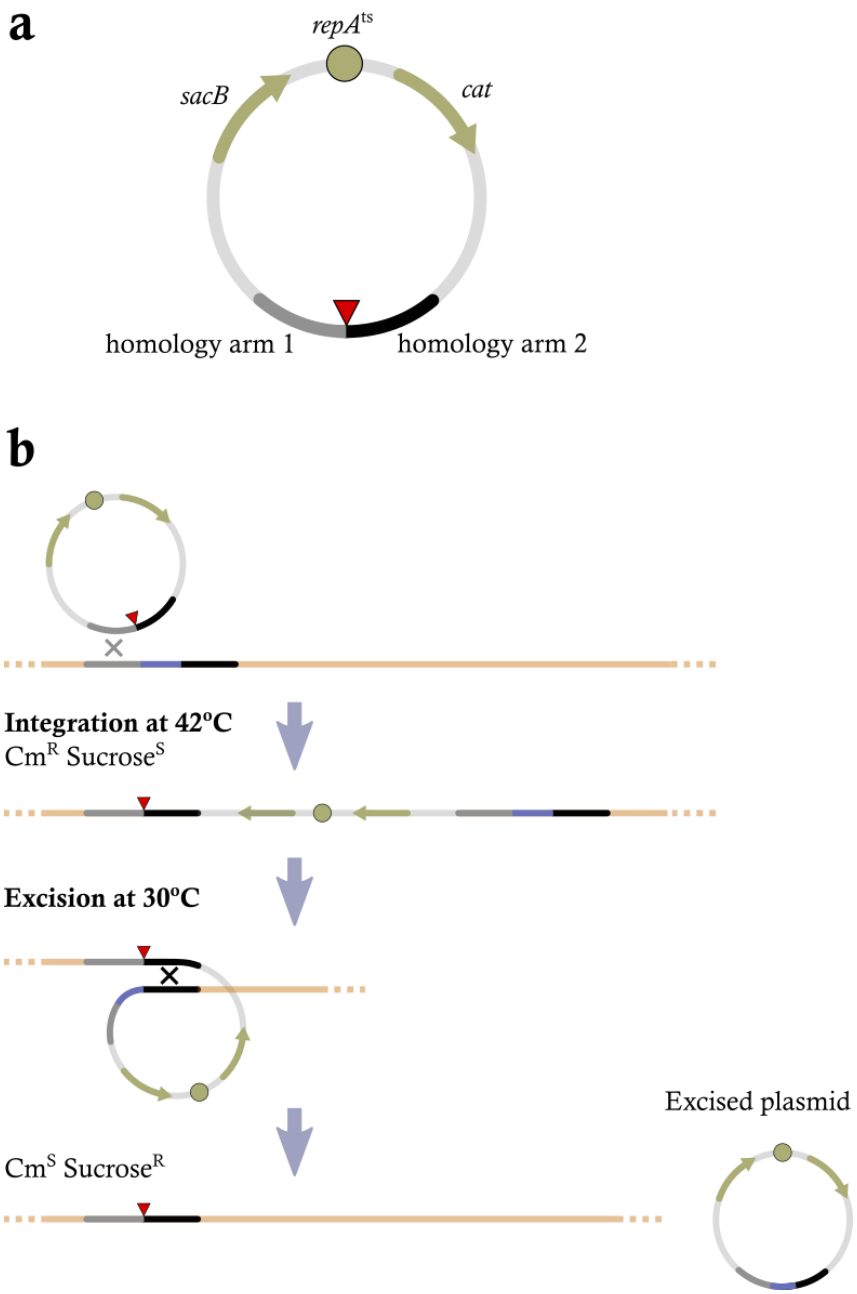

Figure 2.2
Plasmid mediated gene replacement method diagram. **(a)** Schematic representation of a temperature sensitive PMGR vector. Gene *cat* encodes chloramphenicol resistance, *sacB* encodes Levansucrase, and *repA*^{ts} encodes a temperature sensitive RepA protein (pSC101 replicon). The red triangle indicates a DNA sequence to be integrated into the chromosome (a small deletion in this case). **(b)** Diagram of main stages involved in PMGR. Recombination events are indicated by a grey and black crosses.

2.2.1.6 Growth rate assay

All dilutions in growth experiments were done using the appropriate fresh pre-warmed medium containing required supplements. An overnight culture was diluted to adjust the OD_{600nm} to 0.01 and grown at the appropriate temperature under agitation until the early/mid log-phase of growth (OD_{600} 0.15-0.3). Cells were diluted to the OD_{600nm} of 0.01 again and incubated at the appropriate temperature under agitation. The OD_{600nm} was measured every 30 minutes for 6 hours. To maintain cells in the early log growth phase the culture was diluted to OD_{600nm} 0.01 whenever it reached OD_{600nm} 0.2-0.3.

2.2.1.7 P1 lysate preparation

1 ml of an overnight culture of the strain carrying the mutation of interest linked to a selective marker gene was added to a 125 ml Erlenmeyer flask with 9 ml of pre-warmed LB medium supplemented with $CaCl_2$ (2.5 mM). Diluted cells were grown at the appropriate temperature under agitation for 2 hours. A stock P1 lysate was serially diluted in Phage buffer to obtain 10^{-1} to 10^{-5} dilutions. 200 µl of the cell culture were mixed with 100 µl of 10^{-1} to 10^{-5} stock P1 lysate dilutions and incubated at the appropriate temperature under gentle agitation for 30 minutes to allow phage attachment to cell walls. 2.5 ml LC top agar supplemented with $CaCl_2$ (5 mM) and cooled down to 50°C was mixed with each cell-phage mix suspension and poured onto solid LC bottom agar supplemented with $CaCl_2$ (5 mM). Once the LC top agar solidified, plates were incubated in a non-inverted orientation at the appropriate temperature overnight. The plate with the phage dilution that produced confluent lysis was selected and 5 ml of Phage buffer was poured onto the agar. LC top agar was scraped with the Phage buffer into a 5 ml sterile bottle. 100 µl of chloroform were added to the bottle, gently mixed and left for 30 minutes at 4°C. The agar was centrifuged at 5,000 rpm for 5 minutes at room temperature and the supernatant containing phage particles was carefully extracted and added to a sterile 5 ml bottle containing 100 µl of chloroform. The resulting P1 stock was stored at 4°C in the dark.

2.2.1.8 P1 transduction

A single colony of the desired strain was inoculated into 50 ml test-tube containing 5 ml LB medium supplemented with $CaCl_2$ (2.5 mM) and grown overnight at the appropriate temperature. 1 ml of the overnight culture was then transferred to an Eppendorf tube and centrifuged for 30 seconds at the maximum speed (~14k g). The supernatant was discarded, and the cell pellet was resuspended in 100 µl of LB medium supplemented with $CaCl_2$ (2.5 mM). 3 cell suspensions were prepared and 1

µl, 10 µl or 100 µl of the desired stock phage lysate was added to each suspension and incubated for 20 minutes at room temperature. Appropriate controls were prepared in parallel. 800 µl of LB medium supplemented with sodium citrate (2 mM final concentration) were added to each tube to inhibit new rounds of infection. Cells were incubated at the appropriate temperature under agitation for an hour and then centrifuged for 30 seconds at the maximum speed. 800 µl of the supernatant was discarded, cells were resuspended in the remaining 100 µl of medium and spread on a solid LB medium containing appropriate antibiotics and supplements where required. Plates were incubated at the appropriate temperature until colonies were visible (1-2 days). Individual colonies were purified on LB agar plates containing appropriate antibiotics and supplements twice. The resulting strain was confirmed to carry the desired mutation by PCR and UV sensitivity assays when possible.

2.2.2 Molecular biology methods

2.2.2.1 Routine DNA extraction

Genomic DNA was extracted from stationary phase cell cultures using Promega Wizard Genomic DNA purification kit according to the manufacturer's instructions. Plasmid DNA was extracted from stationary phase cell cultures using QIAGEN QIAprep Miniprep plasmid extraction kit according to the manufacturer's instructions. Extracted DNA was stored at -20°C.

2.2.2.2 Polymerase chain reaction

Routine PCRs were done in 20 µl reaction volume containing 0.2 µ M of dNTPs, 0.25 µM of each primer oligonucleotides, 1X GoTaq Reaction Buffer (Promega), 0.5 unit of Go-Taq G2 DNA Polymerase (Promega) and 1-100 ng of template DNA. For high fidelity reactions 1X Herculase II Reaction Buffer (Agilent) and 0.5-1 µl of Herculase II Fusion DNA Polymerase (Agilent) were used instead of 1X GoTaq Reaction Buffer (Promega) and Go-Taq G2 DNA Polymerase (Promega), respectively. Temperature cycling program was set according to the manufacturer's instructions and the melting temperature of oligonucleotides. Samples were stored at 4°C.

2.2.2.3 DNA purification

DNA samples were purified using QIAGEN PCR Purification kit or QIAGEN Gel Extraction kit according to the manufacturer's instructions and stored at -20°C.

2.2.2.4 Sanger sequencing of DNA

The sequencing reactions of purified DNA fragments and plasmids were performed using the BigDye Terminator v3.1 Cycle-Sequencing kit (Applied Biosystems) according to the manufacturer's instructions. The samples were analysed using ABI 3730XL instrument in the Edinburgh Genomic Facility. The resulting chromatograms were visualised using Unipro UGENE Software and the DNA sequences were verified manually.

2.2.2.5 DNA restriction and ligation

DNA restriction and ligation reactions were performed using NEB enzymes according to the manufacturer's instructions. DNA was purified after each restriction reaction by colomn purification (see 2.2.2.3).

2.2.2.6 DNA agarose gel electrophoresis

DNA fragments were separated in 0.8-1.5% (w/v) agarose (Melford) gel supplemented with SafeView (NBS Biologicals) DNA staining compound in 1X TAE buffer at 2-5 V/cm applied voltage. The size of the DNA fragments was determined by comparing with an appropriate commercial DNA size marker ladder (NEB).

2.2.2.7 Two-dimensional native gel electrophoresis

An overnight culture was diluted in pre-warmed medium to adjust the OD_{600nm} of 0.01 and grown at the appropriate temperature under agitation until the early log-phase of growth (OD_{600} 0.15-0.3). Cells were diluted to the OD_{600nm} of 0.01 again and incubated at the appropriate temperature under agitation until the OD_{600nm} value reached 0.2. 80 ml (70 ml for Δ*recG* strains) of the OD_{600nm} 0.2 cells were then rapidly cooled in an ice-water bath and centrifuged at ~4000 g at 4°C for 10 minutes. The cell pellet was twice resuspended in 3 ml of ice-cold TEN buffer and centrifuged at ~4000 g at 4°C for 5 minutes. The washed cell pellet was resuspended in 140 µl of ice-cold TEN buffer and allowed to stand at room temperature for 30 seconds. 170 µl of low melting point (LMP) agarose 0.8% (w/v) (Thermo Fischer Scientific) freshly prepared with TEN and cooled down to 38°C was added to the resuspended cells and mixed thoroughly. The cell-agarose mix was divided between four PFGE plug moulds (Bio-Rad) evenly, 85 µl each, and was let solidify at 4°C for 20-30 minutes. Cell-agarose plugs were carefully extracted from the mould and incubated in 4 ml of NDS buffer supplemented with Proteinase K (1 mg/ml, Promega) under gentle agitation for 18 hours at 37°C. NDS buffer with

added Proteinase K was replaced with a fresh 4 ml of NDS buffer supplemented with Proteinase K and plugs were incubated under the same conditions for another 18 hours. NDS buffer with added Proteinase K was replaced with 6 ml of TE buffer and plugs were incubated under the same conditions for 1 hour. The TE wash was repeated 5 times. TE buffer was then replaced with 4 ml of Buffer 3.1 (NEB) and plugs were incubated under the same conditions for 1 hour. The four plugs were separated into two pairs and each pair was placed into a fresh 50 ml falcon tube containing 2 ml of Buffer 3.1 supplemented with 150 units of either NcoI or NsiI restriction endonuclease. Plugs were incubated under gentle agitation for 9-12 hours at 37°C.

The digested chromosomal DNA trapped in agarose plugs was separated in a first agarose gel dimension according to the weight of each molecule. Plugs were attached to gel electrophoresis comb teeth with 15 µl of 0.4% (w/v) cooled down to 38°C melted agarose (Melford) prepared with 1X TBE buffer. DNA fragments were separated according to their weight in 0.4% (w/v) agarose (Melford) gel in 1X TBE buffer at 0.9 V/cm applied voltage for 36 hours at 4°C. The lane with the 1kb DNA size marker ladder (NEB) was cut from the gel and the distance between the different size molecules was measured in cm upon staining with EtBr. 8 cm long fragments of lanes containing separated chromosomal DNA were cut from the gel in a way that ensures the presence of the DNA locus of interest in each slice.

Slices of lanes were placed into another gel-casting tray in a way perpendicular to the electrical current flow in the second electrophoresis dimension. DNA fragments were separated according to their weight and molecule topology in 1% (w/v) agarose (Melford) gel in recirculated 1X TBE buffer supplemented with 0.3 µg/ml of EtBr (Sigma-Aldrich) at 1.8 V/cm applied voltage for 14 hours at 4°C.

2.2.2.8 Southern blot

Separated DNA fragments were transferred from the agarose gel to a positively charged nylon membrane (NYLM-RO, Sigma-Aldrich), using Southern blot technique. The gel was rinsed in dH_2O and incubated in depurination solution for 20-25 minutes at room temperature. The gel was rinsed in dH_2O again and incubated in transfer buffer for 45-60 minutes at room temperature. Inverted capillary transfer was assembled using 3M Whatmann paper sheets and stacks of paper towels. After 18 hours, the transfer stacks were disassembled, and the membrane was carefully peeled from the gel. The membrane was let to dry for 1 hour at room temperature and the DNA-carrying side was exposed to 100 mJ/cm^2 of UV light to cross-link DNA to the membrane surface. The membrane with the cross-

linked DNA was stored between two sheets of 3M Whatmann paper in a sealed plastic bag at 4°C for up to three weeks.

The membrane was soaked in a 2X SSC solution, drained and placed into a pre-warmed to 65°C 200 ml hybridisation roller bottle. 25 ml of the pre-warmed to 65°C hybridisation buffer were added to the bottle, and the membrane was incubated at 65°C for 4-8 hours in a hybridisation oven under rotation. Hybridisation buffer was decanted and fresh 25 ml of pre-warmed to 65°C hybridisation buffer were added to the bottle supplemented with 25 µl of the appropriate ^{32}P-labelled DNA probe. The membrane was incubated at 65°C for 8 hours in a hybridisation oven under rotation.

The hybridisation buffer with the unbound probe was decanted and 80 ml of pre-warmed to 60°C low-stringency wash buffer were added to the bottle. The membrane was incubated at 60°C for 10 minutes in the hybridisation oven under rotation. This step was repeated 3 times replacing the low-stringency wash buffer with a fresh one each time. The membrane was washed the same way with the high-stringency wash buffer three times. The washed membrane was rinsed with a 2X SSC solution, drained, wrapped in Azpack Sarogold PRO Cling Wrap Film and placed under an autoradiographic phosphor screen (GE Healthcare) with the DNA-carrying side facing the screen. After 2-8 hours of exposition the phosphor screen was scanned using Typhoon FLA 7000 (GE Healthcare). The digital image was analysed using ImageQuant TL Toolbox v8.2.0.

2.2.2.9 Preparation of ^{32}P-labelled DNA probes

Visualisation of chromosomal loci of interest on the membrane was done using ^{32}P-labelled 3-3.7 kb DNA probes. Probes were amplified with terA_XmnI_ps1 and terA_XmnI_p R, terB A F and terB B R, terC A F and terC B R, terD_long F and terD_long R primer pairs from *E. coli* K-12 DL1777 chromosomal DNA using the PCR method and purified following electrophoretic separation in an agarose gel. 5 µl of 5 ng/µl purified DNA probes were mixed with 4 µl of sterile milli-Q water and 5 µl of random 9-mer oligonucleotides (Prime-it II Random Primer labelling kit, Agilent) in a 200 µl PCR reaction tube. The mix was incubated at 95°C for 5 minutes and let to cool down to room temperature on the bench. 5 µl of the 5X dATP buffer (Prime-it II Random Primer labelling kit, Agilent), 2.5 µl of Buffer 2 (NEB), 2.5 µl of ^{32}P-labeled ATP (Perkin Elmer) and 1 µl of Exo(-) Klenow DNA polymerase (5 units/ µl, NEB) were added to the reaction mix with the polymerase being added last, and thoroughly mixed. The reaction mix was incubated at 37°C for 1 hour. The labelled DNA probe sample was diluted with 75 µl of sterile milli-Q water and purified by running through a GE Healthcare Illustra Microspin G-25 Column according to the manufacturer's instructions. DNA

probes were stored at -20°C. DNA probes were denatured at 95°C for 5 minutes and rapidly cooled in an ice-cold water bath for 2 minutes before use.

2.2.2.10 Stripping of a ^{32}P-labelled DNA probe from a membrane

To remove non-covalently bound DNA probe, the membrane was incubated in a 200 ml hybridisation roller bottle containing 50 ml of stripping buffer for 1 hour at 65°C in a hybridisation oven under rotation. The stripping buffer was decanted, and the membrane was washed 3 times with low-stringency buffer and 3 times with high-stringency buffer as described in the section 2.2.2.8. The membrane was rinsed with a 2X SSC solution, drained, wrapped in Azpack Sarogold PRO Cling Wrap Film and placed under autoradiographic phosphor screen (GE Healthcare) with the DNA-carrying side facing the screen. The screen was scanned after 24 hours of exposition to verify the absence of any residual probe on the membrane.

3 REPLICATION FORK ARREST AT TER SITES IN THE TERMINUS REGION

3.1 Introduction

The circularity of the *E. coli* chromosome ensures that bidirectionally progressing replication forks eventually meet in the region opposite from the replication origin, called the terminus (Neylon et al., 2005). The terminus region is approximately 800 kb long and carries four replication termination sites, *terA* and *terD* on the right replichore, and *terB* and *terC* on the left replichore. *Ter* sites are 23 bp long sequences with a highly conserved 13 bp core (Hidaka, Akiyama and Horiuchi, 1988; Coskun-Ari and Hill, 1997). They are recognized by the terminator protein Tus to form a simple 1:1 Tus/*ter* nucleoprotein complex (Coskun-Ari et al., 1994). This complex forms a polar barrier that allows replication forks to pass when approached from the permissive side but arrests their movement through the opposite non-permissive side. *Ter* sites on the right replichore, *terA* and *terD*, arrest counter-clockwise moving forks that have replicated completed left replichore whereas *terB* and *terC* on the left replichore arrest clockwise moving forks that have replicated the complete right replichore. This orientation of *ter* sites on both replichores creates a fork "trap" that allows replication forks to enter the terminus region unimpeded but prevents their exit (Duggin et al., 2008). The polarity of *ter* barriers is mediated by protein-DNA interactions between Tus and *ter*. These interactions are triggered by an approaching replication fork from a non-permissive side and result in the "locked" stated of the Tus/*ter* complex (Mulcair et al., 2006; Berghuis et al., 2015). The resulting nucleoprotein complex works as a physical barrier that prevents further movement of replication forks.

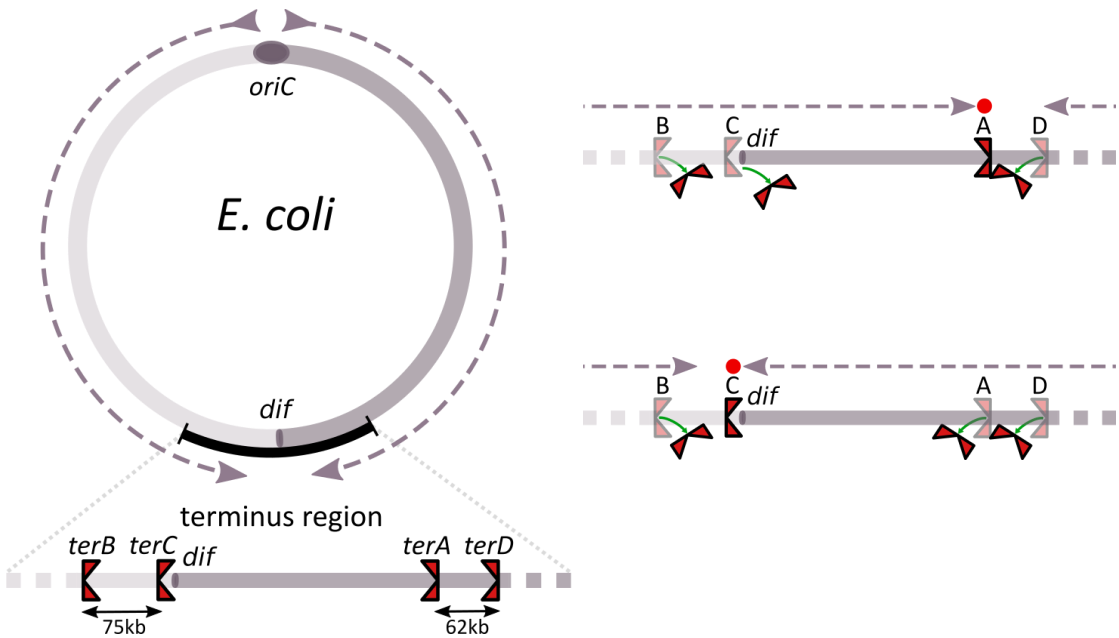

Figure 3.1

Schematic representation of the *E. coli* K-12 DL1777 chromosome. The terminus region of the chromosome is marked with the black line and is shown below zoomed. Distances between four *ter* sites are shown below horizontal arrows. The direction of the replication fork movement is shown as dashed arrows. Right panel shows anticlockwise replication passing through *terB* and *terC* in permissive direction and being arrested in the right replichore at *terA* (top), or clockwise replication passing through *terA* and *terD* and being arrested in the left replichore at *terC* (bottom).

One of the ways to study Tus/*ter*-mediated replication arrests is based on the careful quantification of the amount of paused forks at *ter* sites and relies on the neutral two-dimensional gel electrophoresis method (2D GE). Branched and other nonlinear dsDNA molecules migrate in agarose gels differently when compared with a linear dsDNA molecule of the same mass (Bell and Byers, 1983; Brewer and Fangman, 1987). This difference can be

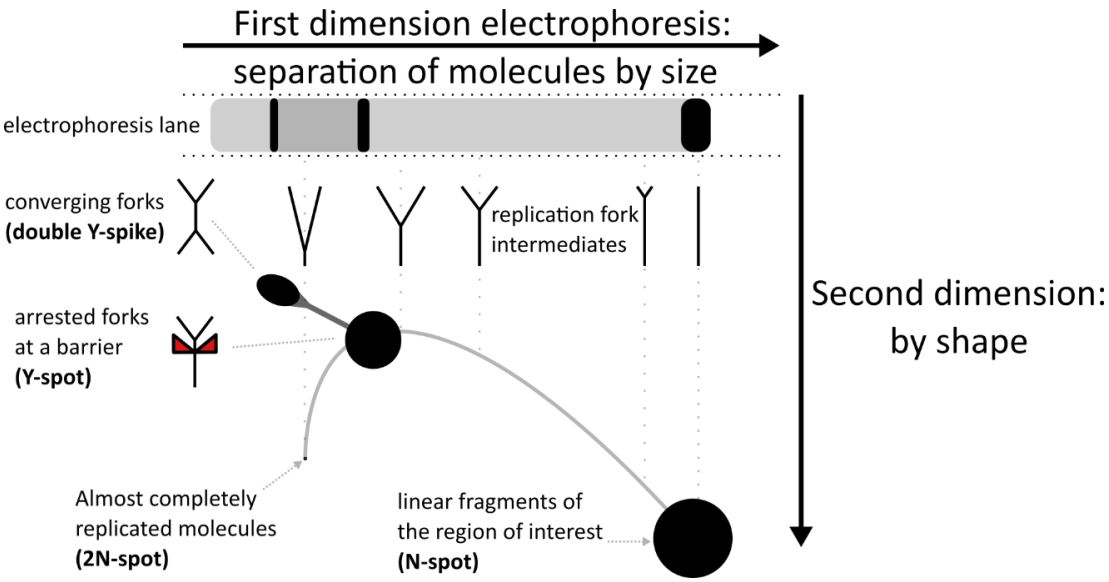

Figure 3.2

Schematic representation of 2-D gel hybridisation patterns generated by replication intermediates. Black arrows indicate the direction of the applied electrical current.

minimised or maximised by increasing or decreasing the voltage, the agarose concentration and/or a DNA intercalating agent concentration. This principle is utilised to separate branched copies of a chromosomal fragment from their linear counterparts in an agarose gel (Figure 3.2). In the first dimension, low voltage is applied to separate DNA in low agarose concentration (0.4%) to minimize the effect of the shape of molecules on electrophoretic migration. Then the gel slice containing the lane of separated DNA fragments is rotated counter-clockwise 90°, embedded in a higher concentration (1%) agarose gel containing the intercalating agent EtBr, and higher voltage is applied to maximise the effect of shape on the separation of DNA fragments during the second dimension.

The accumulation of paused replication forks at *ter* sites depends on the frequency of fork arrest and the bypass of the barrier. Several factors can affect those events such as (i) the probability of Tus binding with *ter* site, (ii) the intrinsic strength of protein-DNA interactions of a Tus/*ter* complex on its non-permissive side and (iii) the frequency at which replication forks reach each side of ter.

However, the replication fork arrest at Tus/*ter* is not permanent and some replication forks may resume progress past the barrier. This was shown for ectopic Tus/*terB* barriers inserted in the middle of each replichore in the orientation that arrests *oriC*-originated replication forks. The bypass was dependent on the presence of homologous recombination proteins RecA, RecBC and RuvC as well as the accessory helicase UvrD (Flores et al., 2001; Bidnenko, Lestini and Michel, 2006). Another observation was done using marker frequency analysis of the chromosome replication of *E. coli* Δ*recG* strain that suggested that replication forks may bypass endogenous Tus/*terC* barrier in the terminus (Azeroglu et al., 2016). However, it was still unclear whether a replication fork can bypass Tus/*terC* in the wild-type strain and what mediates the bypass.

A combination of two-dimensional (2-D) agarose gel electrophoresis (GE) and Southern blotting was used to identify and visualise DNA replication intermediates that accumulate in the chromosomal loci containing *terC* and the following *terB* site. This chapter provides detailed characterization of the in vivo replication fork arrest efficiency of the *terC* site and the dependence of the location and sequence on the fork pausing activity and bypass.

3.2 Replication termination in the *terC* locus

3.2.1 Introduction

The *terC* site is located on the left replichore close to the chromosome dimer resolution site, *dif*. Its orientation allows counter-clockwise moving replication forks to progress unimpeded while clockwise moving forks are arrested at its non-permissive side. *terC* is only 5 kb away from the middle point of the chromosome relative to the *oriC* and may be involved in the termination of the normal replication of the chromosome. First, it was necessary to determine whether replication termination occurs in the *terC* locus. Using neutral 2-D GE method replication forks in the *terC* locus were visualized and characterized.

3.2.2 Construction of Δ*terC* and inverted-*terC* strains

In order to study the role of the *terC* site in the replication arrest and to determine the movement direction of replication forks prior to the arrest in the *E. coli* DL1777 strain, two control strains were constructed: Δ*terC* strain DL6318 and the strain DL6910 in which the *terC* sequence was inverted. First, pDL6356 and pDL6689 plasmids were constructed. Two homology fragments were amplified from the chromosomal DNA of *E. coli* DL1777 strain using primer pairs yneEter - F1 and yneEnoter - R1, uxaBnoter - F2 and uxaBter - R2 for the construction of pDL6356 and primer pairs yneEter - F1 and yneECret - R1, uxaBCret - F2 and uxaBter - R2 for the construction of pDL6689. The resulting homology fragments were first fused by cross-over PCR (see Figure 2.1) using, in both cases, primers yneEter - F1 and uxaBter - R2 and then cloned into the PstI and SalI restriction sites of pDL1605 (pTOF24). The cloned sequences in the plasmids were sequenced using pKO-F and pKO-R2 primers to ensure that no mutations were introduced during the construction. pDL6356 and pDL6689 were then used to transform *E. coli* K-12 strain to generate the Δ*terC* strain DL6318 and the inverted-*terC*

strain DL6910 using the PMGR method, respectively. Successful introduction of *terC* mutations in the chromosome were confirmed by gel electrophoresis migration analysis of chromosomal DNA generated by PCR using yneEter - F1 and uxaBter - R2 primers.

3.2.3 Replication fork arrest in the terC locus

E. coli strains DL1777 (wild-type), DL6318 (Δ*terC*) and DL6910 (inv.*terC*) were grown in LB rich media at 37°C under agitation until cells reached mid-exponential phase of growth (OD_{600}=0.2) as explained in the paragraph 2.2.2.7. 80 ml of cells were harvested, washed twice in ice-cold TEN buffer at 4°C and mixed in 1:1 ratio with cooled to 37°C 0.8% agarose to form 4 plugs with 4 OD of cells in each. Embedded cells were lysed in the presence of 1 mg/ml of proteinase-K and the released DNA within plugs was then digested with 150 U of NcoI restriction endonuclease. DNA fragments were separated using 2-D GE and the 6.6 kb region containing *terC* was visualised by Southern blotting using the terC_A-B probe (Figure 3.3a and b).

The visualised *terC* locus of the wild type, Δ*terC* and inverted-*terC* strains are shown in Figure 3.3d, e and f, respectively. The linear molecules are represented by the large spot at the bottom-right corner of each panel and constitute the majority of the labelled DNA. Molecules of higher mass migrated at a slower rate and formed characteristic patterns depending on their branched structure. Two types of branched intermediates are clearly visible in strains DL1777 and DL6910 (Figure 3.3e and f, respectively) and form a distinctive arc, Y-arc, and a spot at the top of the arc, Y-spot. The Y-arc was formed by Y-shaped DNA molecules with different branching points that represent a population of *terC* locus fragments that were being replicated when the cells were harvested.

(a)

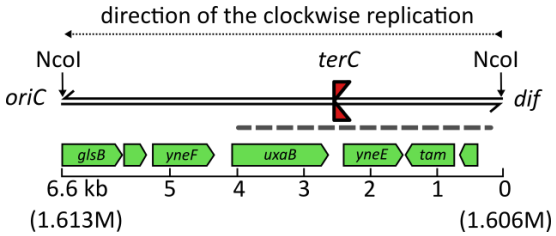

(b)

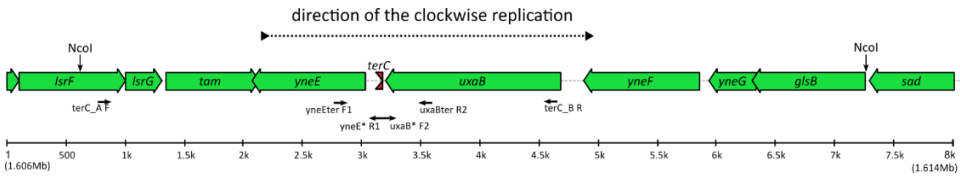

(c)

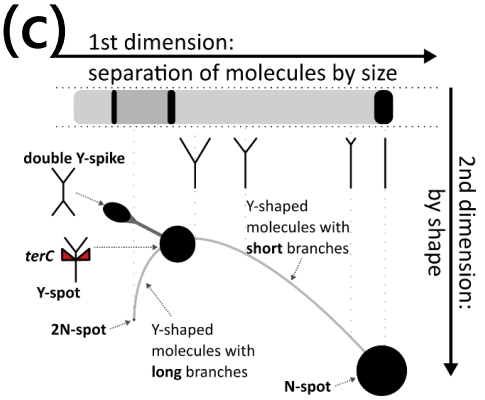

(e) wild-type

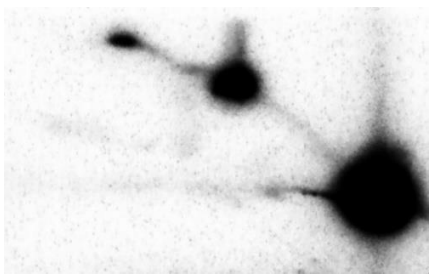

(d) Δ*terC*

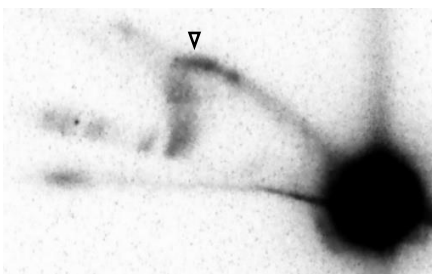

(f) inv.*terC*

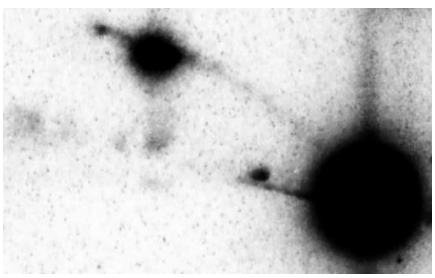

Figure 3.3

Detection of replication fork intermediates in the *terC* locus of *E. coli* DL1777 strains. **(a,b)** Schematic representation of the *terC* chromosomal locus. NcoI restriction sites are indicated by vertical arrows. The Tus/*terC* barrier is shown as the red figure with the flat side representing the permissive side and the sharp convex representing the non-permissive side. The terC_A-B probe is indicated below the respective binding region as a dashed horizontal grey line. Genes are indicated by green arrows. **(c)** Explanatory illustration of the observed 2-D patterns. **(d, e, f)** The *terC* locus of *wt* DL1777 **(c),** Δ*terC* DL6318 **(d)** and inverted-*terC* DL6910 strains revealed after Southern blotting hybridisation with the terC_A-B probe. Black triangles (▽) indicate regions of high signal intensity on the Y-arc in the absence of *terC* barrier.

The spot on the top of the Y-arc was formed by the accumulation of Y-shaped replication intermediates of a specific size. In the DL6318 strain where the *terC* sequence was deleted no Y-spot could be observed (Figure 3.3d), confirming that *terC* is responsible for the accumulation of these arrested forks.

The asymmetric location of the *terC* in the NcoI chromosomal fragment makes it possible to differentiate between clockwise and counter clockwise moving replication forks arrested at the Tus/*terC* barrier. In the wild-type strain DL1777 counter clockwise-moving forks approach the Tus/*terC* barrier from the permissive side and should replicate through the barrier. Clockwise-moving forks should accumulate as Y-shaped molecules with branches of ~2.5 kb length and the unreplicated part of ~4 kb. Molecules with short branches constitute the right half of the Y-arc closer to the N-spot (Figure 3.3c). Indeed, as can be seen on the Figure 3.3e, in the wild-type strain the Y-spot on the arc was located before the inflection point closer to the N-spot, confirming that arrested replication forks were moving in the clockwise direction prior to the arrest. Y-shaped structures with longer replicated wing form the left half of the Y-arc with the 2N-spot at the terminal point. In the DL6910 strain, where the *terC* sequence was inverted, counterclockwise-moving forks approach the non-permissive

side of the Tus/*terC* barrier and should accumulate as Y-shaped molecules with 4 kb long branches and 2.5 kb long unreplicated DNA. As can be seen in the Figure 3.3f, the Y-spot was located on top of the arc closer to the 2N-spot. This correlates with the expected size of counter clockwise-moving forks paused at Tus/*terC.*

The intensity of the signal was not uniform along Y-arcs of all strains, with the area partly occluded by the Y-spot in the wild type strain noticeably darker in the Δ*terC* strain. In the absence of the active Tus/*terC* barrier, replication forks were not arrested, however their progress appears to be slowed considerably. This could be a result of the accumulation of torsional stress between two forks approaching the meeting point at *terC* in the absence of the Tus/*terC* barrier.

Another type of branched molecules that can be clearly seen in the presence of *terC* were converging fork intermediates, which are represented by a straight line coming out from the Y-arc (double Y-spike, Figure 3.3d). This structure is formed by two replication forks, one of which being arrested at the Tus/*terC* barrier while the other is approaching it from the opposite side. The length of the unreplicated chromosomal DNA between the two converging forks is different in each cell in the population, forming a straight line of hybridization signal instead of a round dot. Interestingly, an oval-shaped spot can be seen at the end of the double Y-spike. This double Y-spot represents structures formed by the accumulation of converging replication forks that are close to fusion. The accumulation of the double Y-spot suggests that these structures are relatively stable and require more time to be resolved. Several factors can contribute to the persistence of the double Y-spot. It is known that replication forks accumulate positive supercoiling ahead of the replisome. Such supercoiling may require special pathways to be resolved when accumulating between forks just prior to fusion, as was

shown to be the case for plasmids (Suski and Marians, 2008). Also, if one of the replisomes reached Tus/*terC* from the non-permissive side and triggered the locked state of the Tus/*terC* barrier, the approaching replisome from the permissive side must have an active 5'-3' translocating helicase in order to displace the Tus protein from the complex (Mulcair *et al.*, 2006; Pandey *et al.*, 2015). Interestingly, in the absence of the *terC* site, a faint signal similar to a double Y-spike can still be observed (Figure 3.3e). This can be attributed to the stochastic fusion of replication forks that converge at random locations in the *terC* locus, suggesting that fork fusion occurs at this location even in the absence of the Tus/*terC* barrier in the exponential growth phase of *E. coli*.

3.3 Tus/*terC* nucleoprotein barrier is permeable in the terminus

3.3.1 Introduction

The ability of the replication machinery in bacteria to overcome obstacles on the DNA is important for the timely completion of genome duplication. Secondary DNA structures, template damage or DNA-bound proteins are potential barriers that can arrest movement of the replication forks. Replication arrest can lead to the loss of replisome function and its disassembly. However, replication fork arrest does not necessarily result in replisome collapse and arrested forks can resume movement eventually removing or bypassing the obstacle (Boubakri *et al.*, 2010; Georgescu, Yao and O'Donnell, 2010; Yeeles and Marians, 2011). It is therefore critical for the cell to find a balance between complete arrest and barrier bypass of forks in order to maintain accurate transmission of genetic information.

The replication terminator protein, Tus, binds to a 23 bp *ter* sequence and forms the most stable nucleoprotein complex known between a monomeric protein and a sequence it recognizes on a double-stranded DNA (Berghuis *et al.*, 2015). Its remarkable feature to block *E. coli* replisomes only at its non-permissive side prevents replication escape from the chromosomal terminus (Mulcair *et al.*, 2006; Moolman *et al.*, 2016). The *terC* site is the first *ter* on the left replichore encountered in the non-permisive orientation by fork that has replicated right replichore, and it is followed by *terB*. To determine if replication forks bypass the Tus/*terC* barrier and reach *terB* in the wild type strain DL1777, 2-D GE method was used to quantify and compare the replication arrest at *terC* and at the following *terB* site.

3.3.2 Construction of DL6504 *fumC-fumA*::NcoI strain

2-D GE method relies on the restriction endonuclease cleavage of chromosomal DNA.The *terB* locus contains two XmnI sites that generate a 4.9 kb fragment upon enzymatic

cleavage reaction and was used in studies in literature. However, the XmnI enzyme is inefficient in restriction reactions of DNA embedded in agarose and partially digested fragments were frequently observed (Duggin and Bell, 2009; Iurchenko E., personal communication). To overcome this problem, the NcoI restriction enzyme was chosen for the digestion of chromosomal DNA embedded in agarose plugs. The *terB* locus contains a single NcoI restriction endonuclease recognition site upstream from the *terB* sequence. The intergenic region of the *fumA-C* operon outside of the published rho-independent termination sequence of *fumA* and the promoter sequence of *fumC* was chosen for integration of the second NcoI recognition sequence (Figure 3.4) (Miles and Guest, 1984; Park and Gunsalus, 1995; Cunningham, Gruer and Guest, 1997).

First, the pDL6501 plasmid was constructed. Two homology fragments were amplified from the chromosomal DNA of *E. coli* DL1777 strain using primer pairs terB_NcoI F and terB_NcoI R, and terB_NcoI F2 and terB_NcoI R2. The resulting homology fragments were fused by cross-over PCR using primers terB_NcoI F and terB_NcoI R2 and then cloned into PstI and SalI restriction sites of pDL1605 (pTOF24). pDL6501 was then transformed into the *E. coli* K-12 DL1777 strain to generate *fumA-fumC*::NcoI strain DL6504 by PMGR method. Successful integration of the NcoI restriction recognition site in the *terB* locus was confirmed by gel electrophoresis migration analysis of chromosomal DNA generated by PCR using terB_NcoI F and terB_NcoI R2 primers.

3.3.3 Replication fork arrest in the *terB* locus

E. coli strains DL6504 was grown in LB rich media at 37°C under agitation until cells reached mid-exponential phase of growth (OD_{600}=0.2) as explained in detail in the paragraph

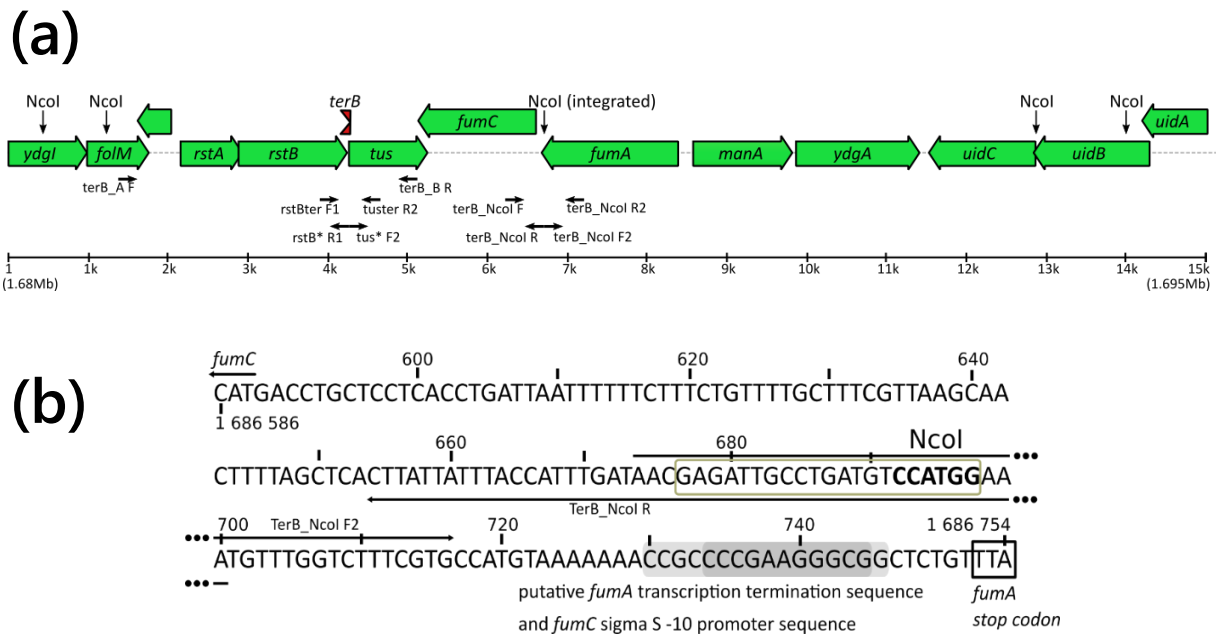

Figure 3.4

Schematic representation of *terB* region of the *E. coli* K-12 DL1777 chromosome. **(a)** Illustration of the *terB* region. Genes are indicated by green arrows. NcoI restriction sites are indicated by vertical arrows. The Tus/*terC* barrier is shown as the red figure with the flat side representing the permissive side. Primer binding sites are indicated by horizontal arrows. **(b)** The *fumA-fumC* intergenic region. The integrated 21 bp sequence containing NcoI restriction recognition sequence is indicated by the horizontal black line at the position 1686692. The start codon of the *fumC* gene is indicated by the black arrow at the position 1686588. The stop codon of the *fumA* gene is indicated by the black box at the position 1686752. The published *fumA* transcription termination sequence and *fumC* -10 promoter sequence are indicated by grey and dark grey boxes, respectively.

2.2.2.7. The chromosomal DNA was prepared as described in the paragraph 3.2.3. DNA fragments were separated using 2-D GE and the 5.5 kb region containing *terB* was visualised by Southern blotting using the *terB* A-B probe (Figure 3.5a).

Several types of replication intermediates were visualised in the *terB* locus of the wild type strain (Figure 3.5Figure 3.3c). A faint Y-arc and a prominent N-spot in the bottom right

corner of the image can be seen. The presence of a Y-spot on the Y-arc demonstrates the accumulation of arrested replication forks in the *terB* locus.

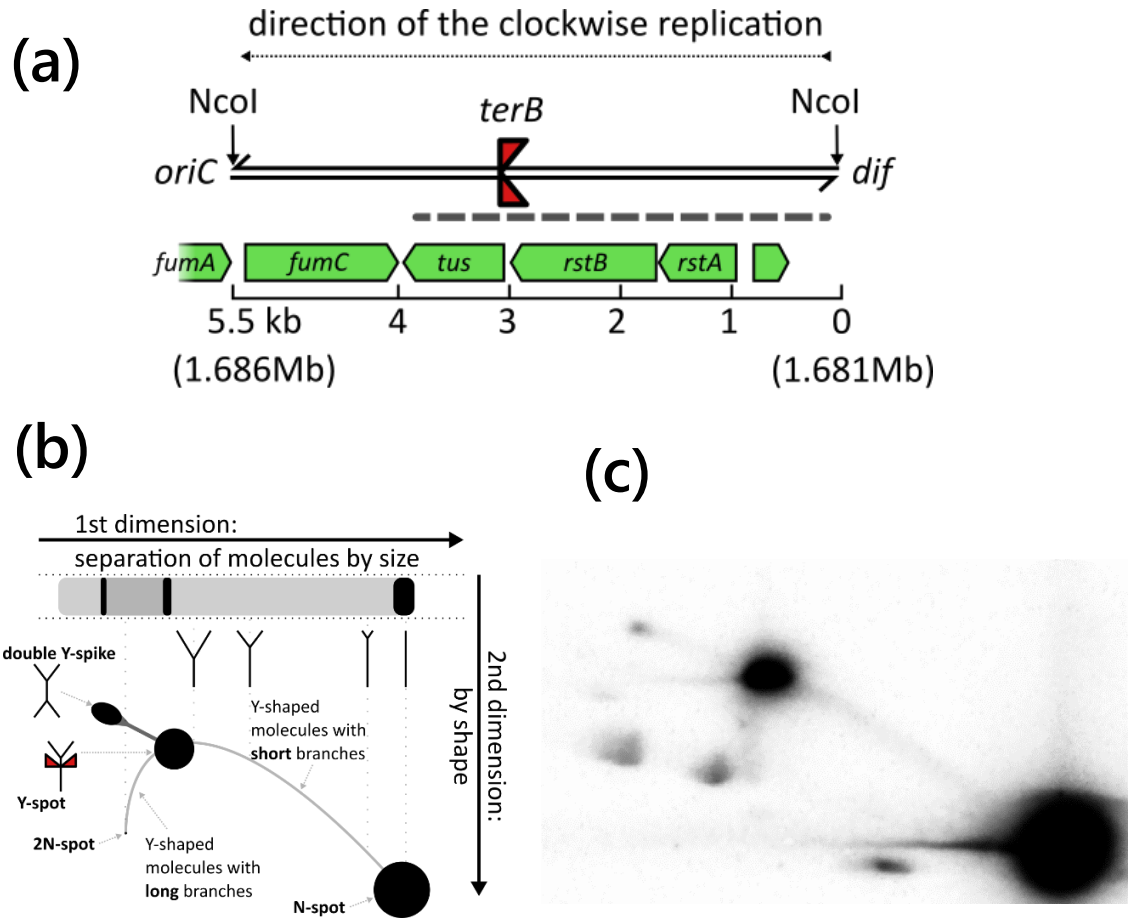

Figure 3.5

Detection of replication fork intermediates in the *terB* locus of *E. coli* DL1777 strains. **(a)** Schematic representation of the *terB* chromosomal locus. NcoI restriction sites are indicated by vertical arrows. The Tus/*terC* barrier is shown as the red figure with the flat side representing the permissive side and the sharp convex representing the non-permissive side. The terB A-B probe is indicated below the respective binding region as the dashed grey horizontal line. Genes are indicated by green arrows. **(b)** The explanatory illustration of the observed 2-D patterns. **(c)** The *terB* locus of the *wt* DL6504 strain revealed after Southern blotting hybridisation with the terB A-B probe.

Clockwise-moving replication forks arrested at the *terB* site are expected to accumulate as Y-shaped molecules with 3.1 kb long branches and 2.4 kb unreplicated part. The position of the Y-spot at the inflection point of the Y-arc shows that it was formed by NcoI fragments replicated past their midpoint. The position of the Y-spot correlated with the size of clockwise-moving replication forks arrested at the *terB* site. It should be noted, that those replication forks first had to pass the *terC* sequence in order to reach the *terB* barrier. Another type of branched structures formed by two converging replication forks with an unreplicated DNA between them was also detected. These molecules represent termination intermediates and form the Y-spike on the blot. The most abundant of these termination intermediates had a very short fragment or no unreplicated DNA between the two forks and are represented by a double Y-spot at the highest point of the Y-spike. The presence of termination intermediates in the *terB* locus shows that replication fork fusion happens not only at *terC*, as shown in the paragraph 3.2.3, but also at the Tus/*terB* barrier. The two weak hybridization signals on the left of the 2N-spot were formed by two larger NcoI fragments. Those fragments could be generated as a result of cross-hybridisation of the TerB A-B probe with another NcoI chromosomal fragment or of incomplete chromosomal DNA cleavage by the NcoI endonuclease. A hybridisation reaction with another probe that was homologous to a different region within the NcoI fragment of the *terB* locus did not affect the presence of two unidentified spots. A 5-fold increase in the NcoI enzyme concentration during the digestion stage of the experiment did not abolish the incomplete cleavage of the *terB* locus. Occlusion of the NcoI cutting site in the *fumA-fumC* intergenic region by the nearby *fumC* -10 promoter sequence could be the cause of the incomplete NcoI endonucleolytic reaction that is not affected by the increased concentration of the enzyme.

3.3.4 Large fraction of clockwise-moving replication forks bypass *terC* and reach *terB*

One of the advantages of the 2-D GE method is that it allows the direct observation and quantification of replication intermediates accumulated as Y-spots corresponding to the arrested forks.

E. coli strains DL6504 was grown in LB rich media at 37°C under agitation until cells reached mid-exponential phase of growth (OD_{600}=0.2) as explained in detail in the paragraph 2.2.2.7. The chromosomal DNA was prepared as described in the paragraph 3.2.3 and the resulting four plugs with the embedded chromosomal DNA were divided in two pairs. One pair was used for the *terC* locus visualization and the other for the *terB* locus. DNA fragments were separated using 2-D GE and the 6.6 kb region containing *terC* and the 5.5 kb region containing *terB* were visualised by Southern blotting using the terC_A-B and terB_A-B probe, respectively (Figure 3.6a and Figure 3.6b).

Due to the variable amount of DNA present in each sample the quantification of the signal strength of arrested forks had to be normalised before it could be used in comparative analysis. The normalisation was done by calculating the ratio of the signal of arrested replication forks represented by Y and double Y-spots (marked with dashed lines) to that of the total labelled DNA (solid and dashed lines together) on the blot as shown on the Figure 3.6a and b.

The quantification of the arrested replication forks at *terC* and *terB* loci initially revealed notable fluctuations of ratio values, making it difficult to infer conclusions from the obtained data. In order to minimize the impact each biological repeat has on results, samples from a single liquid culture were used for both *ter* sites. This allows to determine the distribution of arrested replication forks across multiple *ter* sites in the terminus in a population. The resulting

ratio values represent the fraction of chromosomes in the culture that had replication arrested at either the *terC* or the *terB* site. The experiment was repeated four times to obtain the average value for each *ter*. Under wild-type conditions, the proportion of replication forks arrested at the Tus/*terC* barrier was the greatest and reached 2.05% of the total amount of DNA in the locus, whereas the fraction of arrested forks at the Tus/*terB* barrier was half as much and reached 1.02% (Figure 3.6c). The double Y-spike and the double-Y spot in the *terB* locus shows that the termination of replication and eventual fusion of two converging forks can also happen at the *terB* site. The simplest explanation of the presence of arrested replication forks at *terB* is that clockwise-moving replication forks bypass *terC* from the non-permissive side before eventually being arrested at the following terminator site, *terB*. The bypass of the Tus/*terC* barrier by the clockwise-moving fork could help avoid potentially deleterious effects of a permanent replication arrest of these forks at the *terC* site.

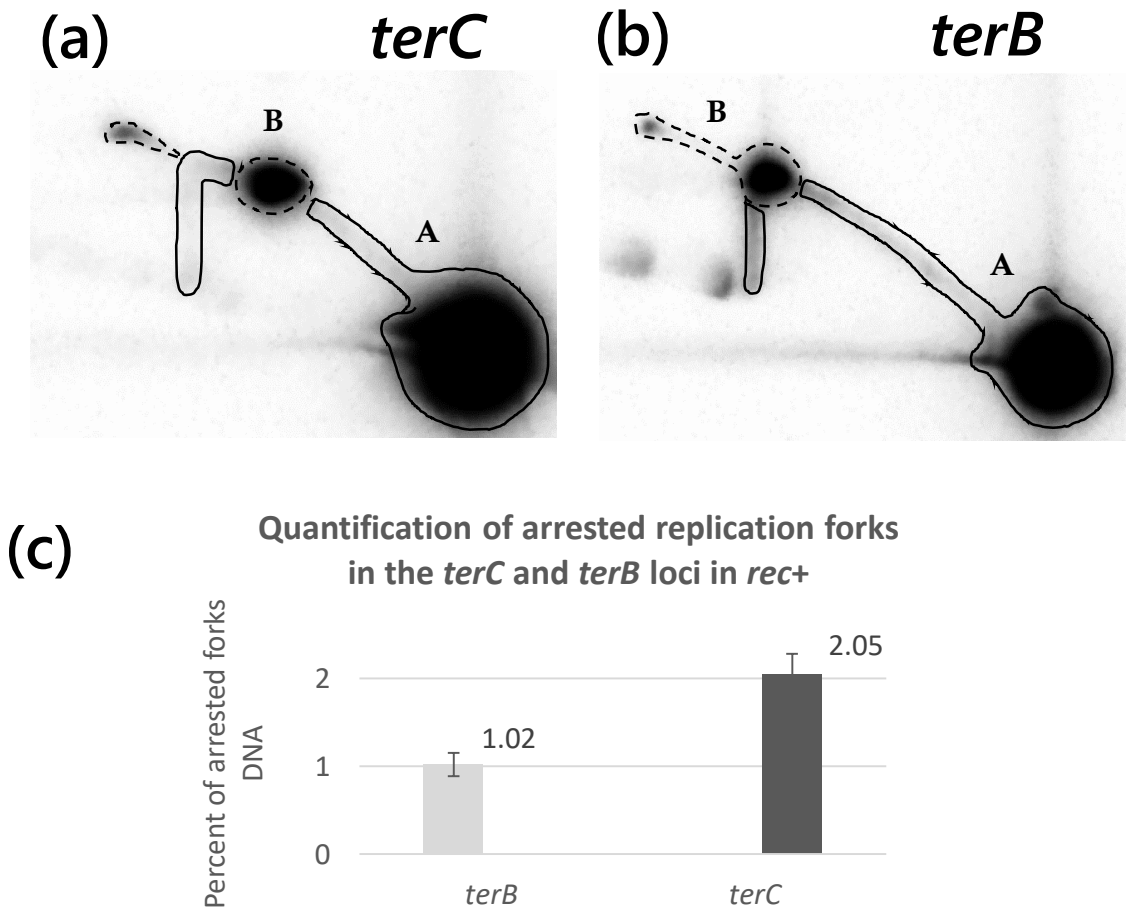

Figure 3.6

Quantification of arrested replication forks in the *terC* and *terB* loci of the *E. coli* K-12 DL1777 strain DL6504. **(a,b)** 2-D GE of the *terC* and *terB* loci of the DL6504 and the areas used in the quantification of arrested replication forks. Areas occupied by Y, double Y-spots and Y-spike molecules are marked with the dashed line (B). Areas occupied by linear and Y-arc molecules are marked with the solid line (A). **(c)** The percent of arrested forks relative to the total DNA signal at each *ter* site. The calculation of the ratio (R) is done using the formula: R=B/(A+B). The average of four indepedent repeats is shown. Error bars represent the standard deviation of the distribution of each data set.

3.4 Position and sequence dependence of *terC* on the replication fork arrest

3.4.1 Introduction

The degree of fork pausing is determined by the equilibrium between accumulation and fusion of arrested replication forks at Tus/*ter*. While the process of fork fusion at *ter* sites is poorly understood, the accumulation of arrested forks is well studied *in vitro*. According to the replication fork trap model of the Tus-*ter* system (Mulcair *et al.*, 2006), the accumulation of arrested forks at *ter* sites depends on the strength of protein-DNA interactions of Tus/*ter,* and on the frequency of forks approaching each side of Tus/*ter*. For all four *ter* sites in the terminus region, *terA-D,* the dissociation constant and the half-life of Tus/*ter* complexes was shown to be similar (Moreau and Schaeffer, 2012). However, in the locked state the half-life of the Tus/*terC* complex was found to be twice shorter, as well as its dissociation constant twice higher than that of the Tus/*terB* (Mulcair *et al.*, 2006). The observed difference in the thermodynamic and kinetic data suggests that the sequence of *ter* sites could play an important role in the efficiency of fork arrest *in vivo*. The *terC* is located 4.2 kb away from the middle point of the chromosome and is the first *ter* site that clockwise replication forks approach from the non-permissive side. The position of *terC* is unique in that it places it almost exactly at the point where two origin-initiated replication forks should normally meet. In contrast, *terB* is located almost 80 kb away from the midpoint of the chromosome and should only arrest clockwise-moving forks when the counter clockwise-moving forks are delayed.

3.4.2 Construction of DL6505, DL6507, DL6602

First, to test whether *ter* sequence affects replication fork arrest efficiency, the strain where the *terC* sequence is replaced with *terB* was constructed (Figure 3.7b). As a result, it was expected that the amount of arrested replication forks in the *terC* locus would change. For that pDL6357 plasmid was made. Two homology fragments were amplified from the chromosomal DNA of the background strain *E. coli* DL6504 (Figure 3.7a) containing NcoI recognition site in the *terB* locus using primer pairs yneEter - F1 and yneEterB - R1, uxaBterB - F2 and uxaBter - R2. The resulting homology fragments were first fused by cross-over PCR

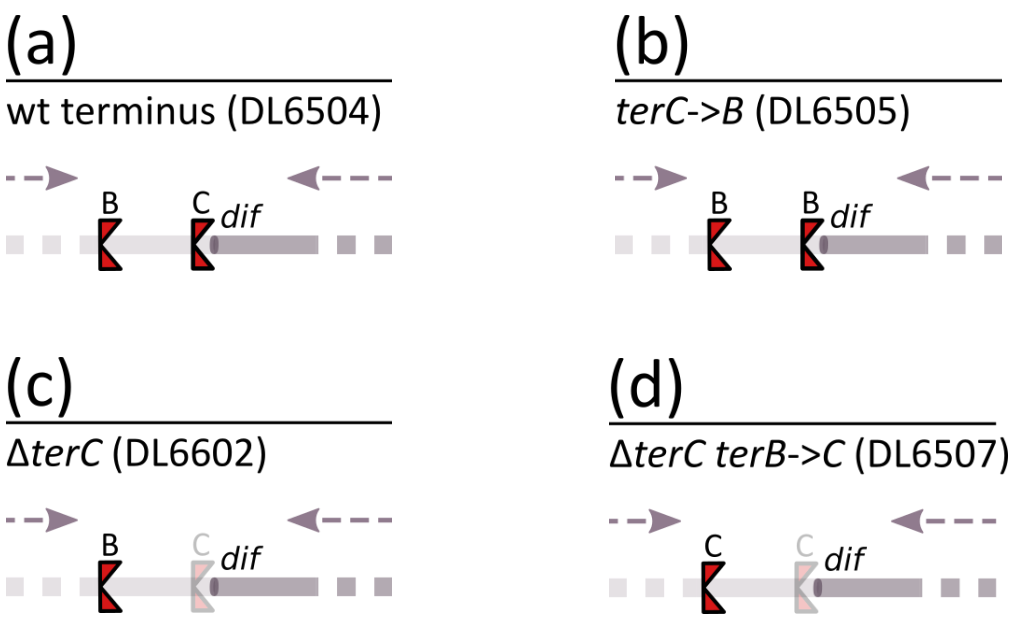

Figure 3.7

Schematic representation of the terminus region of DL6504 (wt), DL6505 (*terC→terB*), DL6602 (Δ*terC*) and DL6507 (Δ*terC terB→terC*) strains. The direction of the replication fork movement is shown as dashed arrows. The Tus/*terC* barrier is shown as the red figure with the flat side representing the permissive side and the sharp convex representing the non-permissive side. Transparent Tus/*ter* barriers represented deleted *ter* sequences.

using, in both cases, primers yneEter - F1 and uxaBter - R2 and then cloned into the PstI and SalI restriction sites of pDL1605 (pTOF24) to geneate pDL6357. The cloned sequences in the plasmids were sequenced using pKO-F and pKO-R2 primers to ensure that no mutations were introduced during the construction. In the first step, pDL6356 (see 3.2.2) was used to transform the background strain DL6504 to generate the Δ*terC* DL6602 strain (Figure 3.7c). The resulting DL6602 strain was transformed with pDL6357 to generate the *terC*→*terB* strain DL6505 using the PMGR method. Successful integration of *terB* in the place of *terC* was confirmed by gel electrophoresis migration analysis of chromosomal DNA generated by PCR using yneEter - F1 and uxaBter - R2 primers.

In addition, to test whether *ter* site location is important for the efficiency of replication fork arrest at the Tus/*terC* barrier, a strain where the *terC* sequence was removed from its native location and inserted into the *terB* locus in place of the *terB* sequence was constructed (Figure 3.7d). If the location of *terC* is important for the efficiency of replication fork arrest, it was expected that the quantity of arrested replication forks in the *terB* locus of the resulting strain would be different when compared with that of the Δ*terC* strain. For that pDL6401 and pDL6436 plasmids were made. Two homology fragments were amplified from the chromosomal DNA of *E. coli* DL6504 strain using primer pairs rstBter - F1 and rstBdter - R1, tusdter - F2 and tuster - R2 for the construction of pDL6401 and primer pairs rstBter - F1 and rstBterC - R1, tusterC - F2 and tuster – R2 for the construction of pDL6402. The resulting homology fragments were first fused by cross-over PCR using, in both cases, primers rstBter - F1 and tuster - R2 and then cloned into the PstI and SalI restriction sites of pDL1605 (pTOF24). The cloned sequences in the plasmids were sequenced using pKO-F and pKO-R2 primers to ensure that no mutations were introduced during the construction. First, pDL6401

was used to transform the strain DL6602 with already deleted *terC* to generate the Δ*terC* Δ*terB* strain DL6508 using the PMGR method. Then the strain DL6508 was transformed with the pDL6402 plasmid to generate the Δ*terC terB→terC* strain DL6507 also using the PMGR method. Successful integration of *terC* in the place of *terB* was confirmed by gel electrophoresis migration analysis of chromosomal DNA generated by PCR using rstBter - F1 and tuster - R2 primers. The replication fork arrest in *terC* and *terB* loci of resulting strains were analysed using 2-D GE method.

3.4.3 The sequence, but not the location, determines the efficiency of replication arrest at *terC* and *terB*

E. coli strains DL6504 (background), DL6505 (*terC→terB*), DL6507 (Δ*terC terB→terC*) and DL6602 (Δ*terC*) were grown in LB rich media at 37°C under agitation until cells reached mid-exponential phase of growth (OD_{600}=0.2) as explained in detail in the paragraph 2.2.2.7. The chromosomal DNA was prepared as described in the paragraph 3.2.3 and the resulting four plugs with embedded chromosomal DNA were divided in two pairs. One pair was used for the visualization of the *terC* locus and the other for the visualization of the *terB* locus. DNA fragments were separated using 2-D GE and the 6.6 kb region containing *terC* and the 5.5 kb region containing *terB* were visualised by Southern blotting using the terC_A-B and terB_A-B probe, respectively.

The results and quantified data are shown in Figure 3.8. The normalisation was done by calculating the ratio of the signal of arrested replication forks represented by Y and double Y-spots to that of the total labelled DNA on the blot as described in paragraph 3.3.4. The resulting ratio values represent the fraction of chromosomes in the culture that had replication arrested at either the *terC* or the *terB* site.

(a)

wt terminus (DL6504)

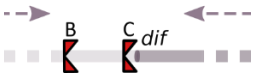

Quantification of arrested forks at *terC* and *terB* in the DL6504

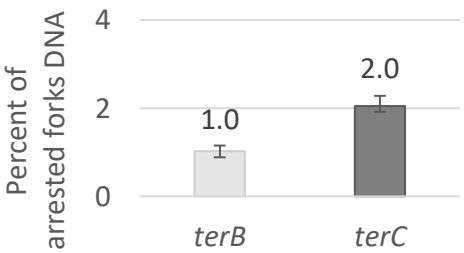

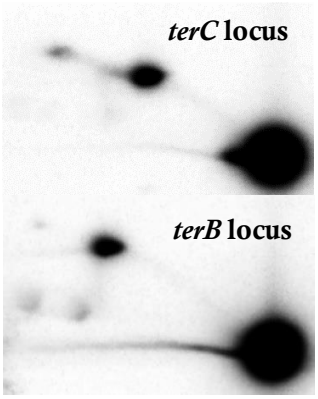

(b)

terC->B (DL6505)

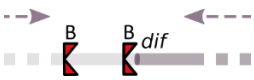

Quantification of arrested forks at *terC* and *terB* in the DL6505

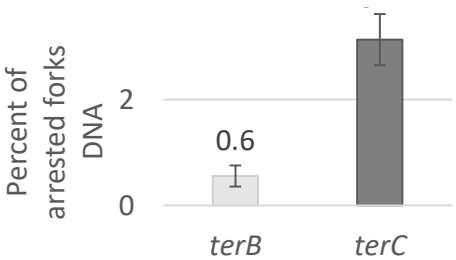

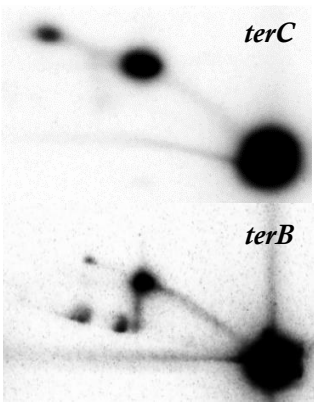

(c)

ΔterC (DL6602)

Quantification of arrested forks at *terC* and *terB* in the DL6602

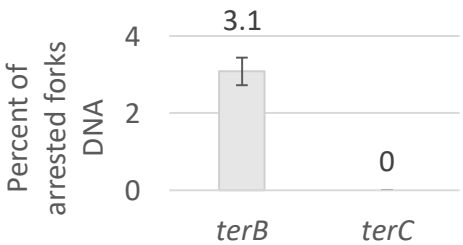

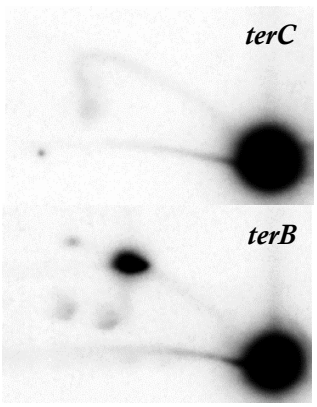

(d)

ΔterC terB->C (DL6507)

Quantification of arrested forks at *terC* and *terB* in the DL6507

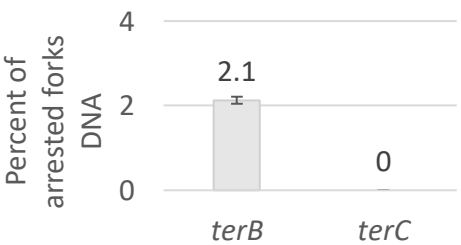

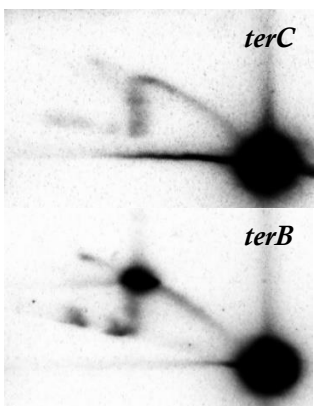

Figure 3.8

Quantification of arrested replication forks in *terC* and *terB* loci of *E. coli* DL6504 (wt), DL6505 (*yneE-uxaB*::*terB*), 6602 (Δ*terC*) and DL6507 (Δ*terC rstB-tus*::*terC*) strains. **(a-d)** Schematic representation of the terminus region of each strain is shown on the left (described as on Figure 3.7). 2-D gels of *terC* and *terB* loci are shown on the right. The quantification of arrested replication forks is shown in the middle. The percent of arrested forks relative to the total DNA signal at each *ter* site. The calculation of the ratio (R) is done using the formula: R=B/(A+B). The average of three independent repeats is shown. Error bars represent the standard deviation of the distribution of each data set.

The experiment was repeated three times to obtain the average value for each *ter*. Arrested replication forks represented by Y-spots were detected in *ter* loci of all strains, except DL6602 and DL6507 strains where the *terC* sequence was deleted. In the DL6505 strain where the *terC* sequence was replaced with *terB* the percentage of arrested replication forks in the *terC* locus reached to 3.2% of the total DNA. In comparison with the background strain DL6504, the amount of arrested replication forks in DL6505 (*terC*→*terB*) was notably higher (~55% stronger signal), demonstrating that the accumulation of replication forks in the *terC* locus depends on the sequence of the *ter* site.

The quantity of arrested replication forks in the *terB* locus varied greatly among four strains. In the absence of the terminator sequence in the *terC* locus, replication forks should be able to reach the *terB* locus unimpeded. Indeed, both Δ*terC* and Δ*terC rstB-tus*::*terC* strains (Figure 3.8-c, d) had the greater degree of fork pausing in the *terB* locus than the other two strains. Interestingly, in the presence of a terminator sequence in the *terC* locus, the observed fraction of arrested replication forks in the *terB* locus were also different. If replication forks have to bypass Tus/*ter* barrier in the *terC* locus before they can reach the *terB* locus, then the observed difference in the efficiency of fork arrest between *terC* and *terB* sequences should also affect the quantity of forks that reach the second Tus/*ter* barrier. In the background strain

DL6504 the quantity of arrested forks in the *terB* locus was shown to be ~1% of the total DNA. Expectedly, in the the *terC→terB* strain the degree of fork arrest in the *terB* locus was markedly lesser and reached only 0.6% of the total DNA. It should be noted, that the quantity of arrested replication forks in the *terB* locus of Δ*terC* (3.1%) was similar to that in the *terC* locus of the *terC→terB* strain (also 3.1%) despite the different position of these *ter* sites in the terminus. Similarly, no difference was detected in the degree of fork pausing at the *terC* sequence of the Δ*terC terB→terC* strain (2.1%) and the background strain (2.0%).

3.5 Discussion

In the present study, arrested replication forks were separated from the bulk of chromosomal DNA using native 2-D GE and then visualized using Southern blot method. The comparative analysis of the position of the Y-spot on the blot confirmed that under the wild-type conditions *terC* functions as the replication arrest site for replication forks moving in the clockwise direction. Replication forks in the *terC* locus were shown to form replication termination structures represented by two converging replication forks close to fusion (see Figure 3.3c). The majority of the visualized double-Y molecules had little to no unreplicated chromosomal DNA between the two converging forks. The accumulation of converging replication forks very close to fusion might indicate that such structures require more time to be resolved. Chromosome replication is accompanied by the accumulation of positive supercoiling ahead of the fork. In eukaryotes it was shown that during the bidirectional replication of circular molecules, the distance between converging forks reaches the point when the remaining stretch of parental DNA becomes too short to form supercoils or permit topoisomerase binding (Schalbetter *et al.*, 2015; Deegan *et al.*, 2019). Therefore, it is

conceivable that one of the reasons behind the persistence of double-Y molecules could be unresolved supercoiling that accumulated between converging replisomes. Suski and Marians showed that bidirectionally replicating minichromosomes accumulate intermediate structures formed by two opposed forks separated by ~130 bp in the final stage of replication. RecQ, Topoisomerase III and SSB were required to resolve these intermediates (Suski and Marians, 2008). This observation raises the possibility that the resolution of the double-Y molecules in the *terC* locus also happens via a similar pathway. It should be noted, that the weak cone-shaped signal resembling the double-Y spike in the Δ*terC* strain (see Figure 3.3d) suggests that the stochastic fusion of replication forks can happen in the region even in the absence of *terC*. The fact that the stochastic fork fusion does not form strong signal on the blot indicates that Tus/*ter* complex is directly involved in the accumulation of double-Y molecules and the replication fork fusion.

Analysis of the replication intermediates in the *terB* locus revealed the accumulation of clockwise-moving replication forks arrested at the *terB* sequence. The subsidiary positioning of *terB* in the terminus requires clockwise-moving forks to encounter the non-permissive side of the Tus/*terC* barrier before arriving at *terB*. The presence of clockwise-moving forks in the *terB* locus can potentially be explained by either the existence of an ectopic replication origin in the region between *terC* and *terB* or the innate ability of replication forks to bypass Tus/*ter* barriers. The search for the origin responsible for constitutive stable DNA replication (cSDR), the so-called *oriK*, failed to identify any in the region between *terC* and *terB* (Maduike *et al.*, 2014). Conversely, it has been previously indirectly shown on several occasions that clockwise moving replication forks can progress through the first Tus/*terC* barrier (Ivanova *et al.*, 2015; Azeroglu *et al.*, 2016; Moolman *et al.*, 2016). The quantification of arrested replication forks

in the *terC* and the *terB* loci demonstrated that the majority of forks were arrested at the Tus/*terC* barrier, whereas twice fewer accumulated at the following *terB* site despite the fact that *terB* was shown to have the highest intrinsic arrest efficiency when taken outside of the terminus (Duggin and Bell, 2009). The lower frequency of arrest at *terB* compared with *terC* observed in the present study may be due to the position of *terB* after *terC* in the fork trap.

Analysis of the replication fork arrest in the Δ*terC terB→terC* strain in which *terC* was deleted and the *terB* sequence was replaced with *terC* showed that the efficiency of the fork arrest of Tus/*terC* is not affected by its location in the terminus; it is still weaker than *terB*. This can be explained by the fact that the distance between the *terC* and the *terB* loci is too short to allow a considerable number of forks to meet before reaching *terB*. Assuming that the average speed of replication fork movement in *E. coli* is approximately 650-1000 nt/s (Pham *et al.*, 2013; Soubry, Wang and Reyes-Lamothe, 2019) it would take ~1.5 minutes for a normal fork to traverse from *terC* to *terB*. The same conclusion is valid for the *terB* sequence as seen in the comparison of fork arrest efficiency in the *terC→terB* strain in which the *terC* sequence was replaced with *terB* and the Δ*terC* strain. Quantification of arrested replication forks in the *terC→terB* strain demonstrated that the degree of fork pausing depends on the sequence of the *ter* site. Indeed, the presence of the stronger terminator sequence *terB* in the *terC* locus resulted in the greater number of arrested forks observed. At the same time, fewer replication forks were detected in the *terB* locus of the *terC→terB* strain when compared to the background strain. The simplest explanation is that the intrinsic strength of the terminator sequence determines not only the quantity of arrested forks but also the rate of the replication fork bypass. Taken together, these results support the hypothesis that a fraction of clockwise-

moving replication forks can bypass the first Tus/*ter* barrier in the *terC* locus and that the bypass frequency depends on the *ter* sequence.

4 REPLICATION FORK ARREST AT TUS/*TER* DURING RECG-DEPENDENT OVER-REPLICATION OF THE TERMINUS

4.1 Introduction

This chapter presents an investigation of the replication fork trap work in the *E. coli* terminus in the situation of induced DNA over-replication. One of the proposed biological functions of the Tus-*ter* system is to prevent replication from moving out of the terminus region in the direction towards the origin. Failure to do so results in the increased frequency of replication-transcription collisions as over 90% of highly transcribed genes encoding ribosomal proteins are oriented co-directionally with the DNA replication (Brewer, 1988; McLean, Wolfe and Devine, 1998). A replication fork that failed to meet its pair could potentially escape the terminus. This could happen when one of the two *oriC*-initiated forks is delayed because of a lesion or an obstacle on the DNA. Alternatively, non-*oriC* replication initiation could also cause replisome to escape from the terminus region. However, dispensability of the Tus-*ter* system without a loss of viability (Roecklein, Pelletier and Kuempel, 1991) suggests that such events may not be common in normal conditions. To investigate the replication fork arrest in the terminus in response to the non-*oriC* replication the phenomenon of the terminus over-replication was utilised. It has been previously shown that in the absence of the RecG helicase *E. coli* cells carry multiple copies of the chromosome terminus region (Rudolph, Upton and Lloyd, 2009; Rudolph *et al.*, 2013; Azeroglu *et al.*, 2016). Increased number of non-*oriC* replication forks responsible for the generation of additional copies of the terminus is expected to interact with Tus/*ter* barriers in the terminus.

This approach helps to understand how non-*oriC* initiated replisomes interact with the replication fork trap.

Marker frequency analyses (MFA) published by Rudolph and colleagues revealed that in Δ*recG* strains the over-replicated region of the terminus is confined between *terB* and *terA* sites (Rudolph *et al.*, 2013). Frequent replication fork bypass of the Tus/*terC* indicated that a considerable fraction of non-*oriC* replication forks interact differently with the innermost *ter* sites, *terA,* and *terC*. Here, I provide a detailed characterisation of the replication fork arrest in the terminus region of Δ*recG* strains. For this purpose, DNA replication intermediates in four *ter* loci in the terminus, *terA*, *terB*, *terC,* and *terD*, in the presence and absence of RecG were separated from the bulk of chromosomal DNA using 2-D GE and visualised using Southern blotting. The changes in the degree of fork pausing and the distribution of arrested forks across four *ter* sites as a result of over-replication of the terminus are shown by quantifying the visualised arrested forks. Finally, in the study of mutants with alternated positions and sequences of *ter* sites, I demonstrate the effect of the *ter* site location on the degree of fork arrest. In summary, I present evidence of the Tus/*terC* barrier bypass and the work of the replication fork trap in the presence of non-*oriC* initiated replication forks.

4.2 Quantification of arrested replication forks at *terC* and *terB* in Δ*recG* cells

4.2.1 Introduction

It has been shown that in the absence of RecG, abnormal DNA replication is detected in the terminus region (Rudolph *et al.*, 2013; Wendel, Courcelle and Courcelle, 2014). In the presence of Tus, cells carry multiple copies of the chromosome terminus restricted by *ter* sites. To determine whether non-*oriC* initiated replication forks pause at *ter* sites, replication fork intermediates in *terC* and *terB* loci were visualised and quantified. For that, the background strain DL6504 was transformed with pDL2429 plasmid to introduce Δ*recG* mutation using the PMGR method (described in 2.2.1.5), and the resulting strain was named DL6554. Successful deletion of *recG* was confirmed by the UV sensitivity assay and by electrophoresis analysis of the chromosomal DNA amplified by PCR using recG - F1 and recG - R2b primers. The Δ*recG* mutant strain exhibited no change in the growth rate in the growth rate assay (described in 2.2.1.6).

2-D GE experiments were performed as described in paragraph 2.2.2.7. Cells were collected from exponentially growing DL6554 culture and cooled on ice. Chromosomal DNA was prepared as described in paragraph 3.3.3. Resulting fragments were separated using 2-D GE, and the 6.6 kb region containing *terC* and the 5.5 kb region containing *terB* were visualised by Southern blotting using the terC_A-B and terB_A-B probe, respectively.

4.2.2 Elevated accumulation of arrested replication forks in Δ*recG* cells

Visualised Southern blots of *terC* and *terB* loci are presented in Figure 4.1c and d. Collected data were normalised to exclude the variability introduced by the inconsistent amount of DNA in each sample. The normalisation was done by calculating the ratio of the signal of arrested replication forks represented by Y and double Y-spots to that of the total labelled

DNA. The resulting ratio values represent the fraction of chromosomes in the culture that had replication arrested at either the *terC* or the *terB* site. The experiment was repeated at least three times to obtain the average value for each *ter*.

Specific branched intermediates were evident in fragments containing *terC* and *terB* sequences. The position of Y-spots on the arc of branched intermediates corresponded to the position of *ter* site in each locus. Most obvious effect was the increase of paused forks at *terC* and *terB* (Figure 4.1-e) in Δ*recG* strains (Figure 3.6-c). Under the condition of the terminus over-replication, the strongest Y-spot signal was detected at the Tus/*terB* barrier. Approximately a quarter (26.7%) of all DNA visualised in the *terB* locus was associated with arrested replication forks. Notably fewer, but still a considerable amount (9.3%) of DNA at *terC* contained arrested fork structures. In contrast, the proportion of arrested replication forks at Tus/*terB* and Tus/*terC* in the wild type strain was 26 times (1%) and 4.5 times (2%) less, respectively.

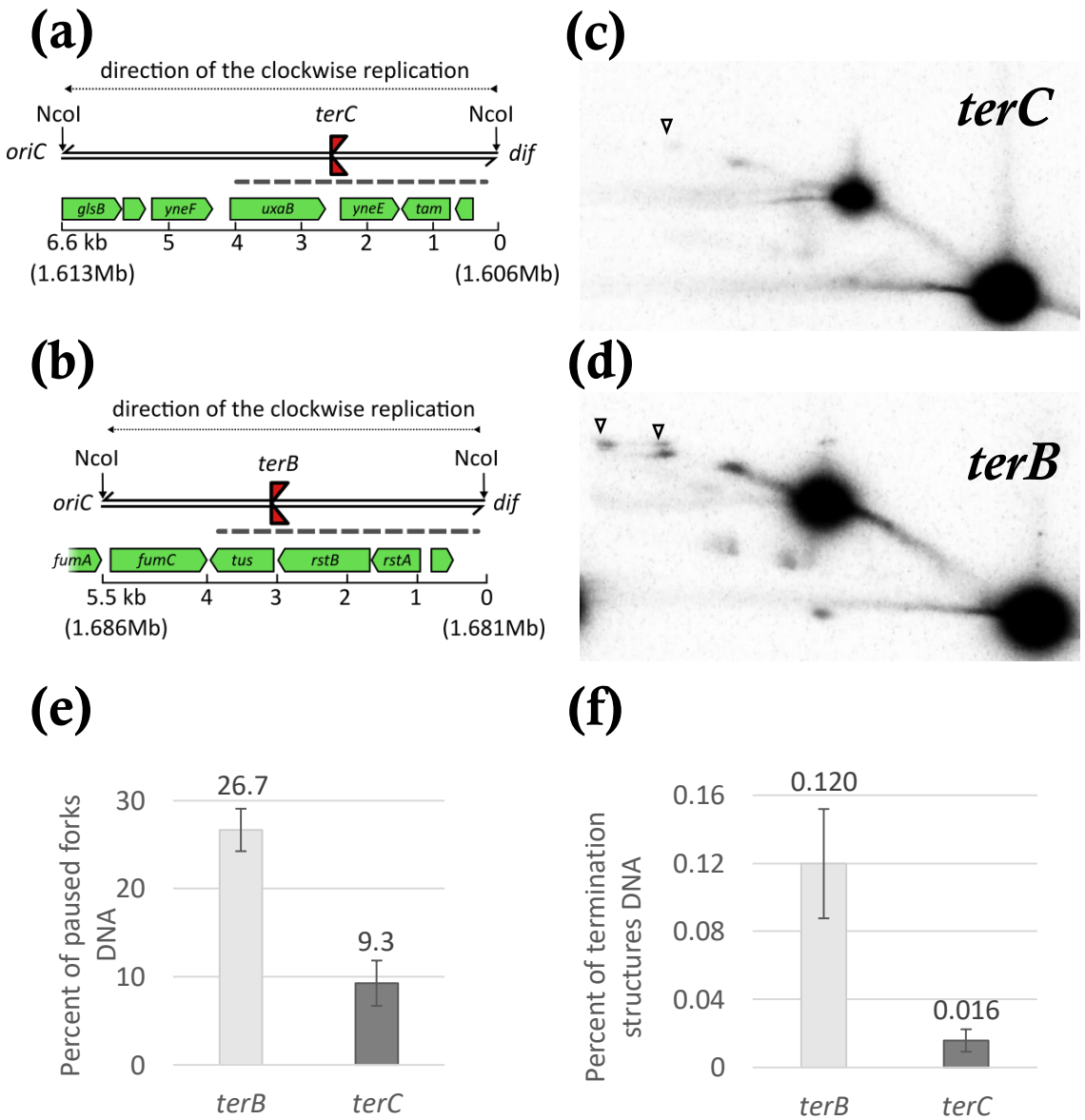

Figure 4.1

Arrested replication forks in *terC* and *terB* loci of the *E. coli* Δ*recG* strain DL6554. **(a,b)** Schematic representation of NcoI fragments of the *terC* (a) and *terB* (b) chromosomal loci (previously described in Figure 3.3 and Figure 3.5). **(c,d)** Southern blots of replication intermediates in the *terC* (c) and *terB* (d) loci visualised with *terC*_A-B and *terB* A-B probes, respectively. Black triangles (▽) indicate secondary and tertiary termination structures (explained in text). **(e,f)** Quantification of the percent of arrested forks (e) and termination structures (f) relative to the total DNA signal at each *ter* site. The quantification is done by calculating the ratio of the signal of arrested replication forks represented by Y and double Y-spots (e) or double Y-spots (f) to that of the total labelled DNA. The average of three repeats is shown. Error bars represent the standard deviation of the distribution of each data set.

The elevated amount of arrested replication forks in Δ*recG* cells indicates the presence of additional replication forks in the terminus that were caught at *terC* and *terB* sites. Under wild-type conditions, the majority of clockwise-moving replication forks are arrested at the first terminator sequence, *terC*, as they enter the left replichore. Conversely, in the absence of RecG, almost three times more arrested forks were detected at the subsidiary *terB* site than at *terC*. These observations correlate with the replication fork bypass of the Tus/*terC* barrier when the terminus is over-replicated in the absence of RecG. Furthermore, double Y-spots were detected at both *ter* sites. These double Y-spots represent converging replication forks separated by a stretch of unreplicated DNA and are indicative of fork fusion events at *terC* and *terB*. The strength of double Y-spot signals was relatively high, compared to double Y-spots in *recG*$^+$ cells, which allowed these structures to be quantified reliably. Values were normalised by calculating the ratio of the signal of termination structures represented by all double Y-spots to that of the total labelled DNA on each blot. The amount of termination structures in each *ter* locus is presented in Figure 4.1f. A markedly greater number of termination structures were detected at the *terB* site. This implies that the majority of replication termination events in the left replichore occurs in the *terB* locus when the terminus is over-replicated. Unfortunately, while termination structures at *terC* and *terB* sites in *recG*$^+$ cells were visible (e.g. Figure 3.5, Figure 3.8), the signal was often below the detection threshold of the blot scanning machine and was poorly reproducible.

4.3 Distribution of arrested replication forks in the terminus region

4.3.1 Introduction

In the absence of RecG, the majority of the amplified copies of the terminus region are limited by *terB* and *terA* sites. A considerable proportion of replication forks bypass the Tus/*terC*, one of the two innermost *ter* sites in the terminus. *terA* is the other innermost *ter* site in the terminus that terminates counter-clockwise replication and is located on the right replichore 253 kb away from the middle point of the *E. coli* K-12 DL1777 chromosome. The sequence of *terA* and the neighbouring *terD* are oriented in a way that allows Tus/*terA* and Tus/*terD* barriers to arrest counter clockwise-moving forks while clockwise-moving forks should bypass these barriers unimpeded. Interestingly, despite the presence of two *ter* sites (*terA* and *terD*) in the right replichore, over-replication was limited by the first *ter* site, *terA,* rather than the following one, *terD* (Azeroglu *et al.*, 2016). In contrast, most replication forks in the left replichore were arrested at the second *ter* site, *terB*. To determine whether *terA* arrests most of the counter clockwise-replication forks, replication fork intermediates in *terA* and *terD* loci were visualised and quantified. For that, the background strain DL6504 and the Δ*recG* strain DL6554 were used in the 2-D GE experiment.

2-D GE experiments were performed independently of experiments from Chapter 3 and as described in paragraph 2.2.2.7. Cells were collected from exponentially growing DL6504 and DL6554 cultures and cooled on ice. Chromosomal DNA was prepared as described in paragraph 3.3.3. The resulting four plugs with embedded chromosomal DNA obtained from a single culture were used to visualise each of the four *ter* loci. For that, one pair of plugs were incubated with NcoI restriction endonuclease to obtain chromosomal fragments containing *terC* and *terB* sites, while the other pair was incubated with NsiI restriction endonuclease to

obtain chromosomal fragments containing *terA* and *terD* sites. Resulting fragments were separated using 2-D GE. The 6.6 kb NcoI fragment containing *terC* and the 5.5 kb NcoI fragment containing *terB* were visualised separately by Southern blotting using terC_A-B and terB_A-B probes, respectively (Figure 4.2a, b). The 3.7 kb NsiI fragment containing *terA* and the 6 kb NsiI fragment containing *terD* were visualised by Southern blotting using terA_XmnI_ps1-p (generated with terA_XmnI_ps1 F and R primer pair) and terD_long (generated with terD_long F and R primer pair) probes, respectively (Figure 4.2c, d). This approach allowed to determine the distribution of arrested replication forks across four *ter* sites in the terminus in a single culture.

4.3.2 Arrested replication forks accumulate predominantly at *terB* and *terA* in Δ*recG* cells

Visualised fragments containing *terB*, *terC*, *terA*, or *terD* of the wild type strain DL6504 are presented in Figure 4.2. Specific branched structures formed by arrested replication forks were evident in all four loci. The detailed characterisation of replication intermediates at *terC* and *terB* loci in *recG*$^+$ background was presented in paragraph 3.2.3 and 3.3.3, respectively. Accumulation of arrested replication forks at *terA* and *terD* sites demonstrates that under normal conditions replication forks reach the more distant *ter* sites on the right replichore. A prominent signal formed by termination structures at the *terA* and *terD* sites indicates that replication fork fusion events also take place in more distant *terA* and *terD* loci. These *ter* sites are located 260 (*terA*) and 322 (*terD*) kb away from the midpoint of the chromosome in the right replichore may indicate a notable delay of clockwise-moving replication forks in some cells in the population. Fragments containing each *ter* site of the Δ*recG* strain DL6554 were visualised and presented in Figure 4.3. As expected, arrested replication forks formed large Y-spots in all four *ter* loci. Interestingly, two types of termination structures were revealed.

On the left replichore, an additional double Y-spot can be seen at both *ter* sites. It is arranged in line with the one closer to the Y-spot. On the right replichore an additional double Y-spot was also detected at both *ter* sites. However, it had a different position and was located below the other double Y-spot.

Quantification of arrested replication forks in *recG*$^+$ cells at each of the *ter* loci is shown in Figure 4.4a. The obtained values of arrested forks at the Tus/*terC* and Tus/*terB* correlated with the values reported in paragraph 3.3.4. The degree of fork arrest at *ter* sites on the right replichore is notably lower, as the distance replication forks must travel before fusing with its pair replisome is several times greater than on the left replichore. To evaluate the distribution of replication forks across four *ter* sites, the obtained values of replication fork arrest signals from each repeat indiviadually were normalised by calculating the contribution of each arrest site in the total sum of all four *ter* sites in the terminus. Then the resulting values across three repeats were averaged and shown in percentage. The results are presented in Figure 4.4b. Under normal conditions, *terC* functions as the main site of the replication termination accumulating the majority of replication forks. A considerable amount of replication forks was arrested at *terB* and *terD* sites, where at least a third of replisomes bypassed either the Tus/*terC* or the Tus/*terA* barrier and reached the following *ter* sites. Quantification of arrested replication forks and their distribution across four *ter* sites in the terminus of the Δ*recG* strain is shown in Figure 4.5a and b. Replication arrest at *terC* and *terB* was discussed in detail in paragraph 4.2.2. An elevated quantity of arrested forks accumulated at *terA* and *terD* sites in response to the terminus over-replication demonstrates that *ter* sites on both replichores are involved in the prevention of the replication escape from the terminus. In the left replichore, the majority of replication forks were able to bypass *terC* and reach the following site, *terB*. In

contrast, over-replication of the terminus region did not alter the replication arrest efficiency of the innermost *ter* site on the right replichore, *terA*. Most counter clockwise-moving replication forks were arrested at the *terA* site and only approximately one-fifth of forks were able to reach the Tus/*terD*.

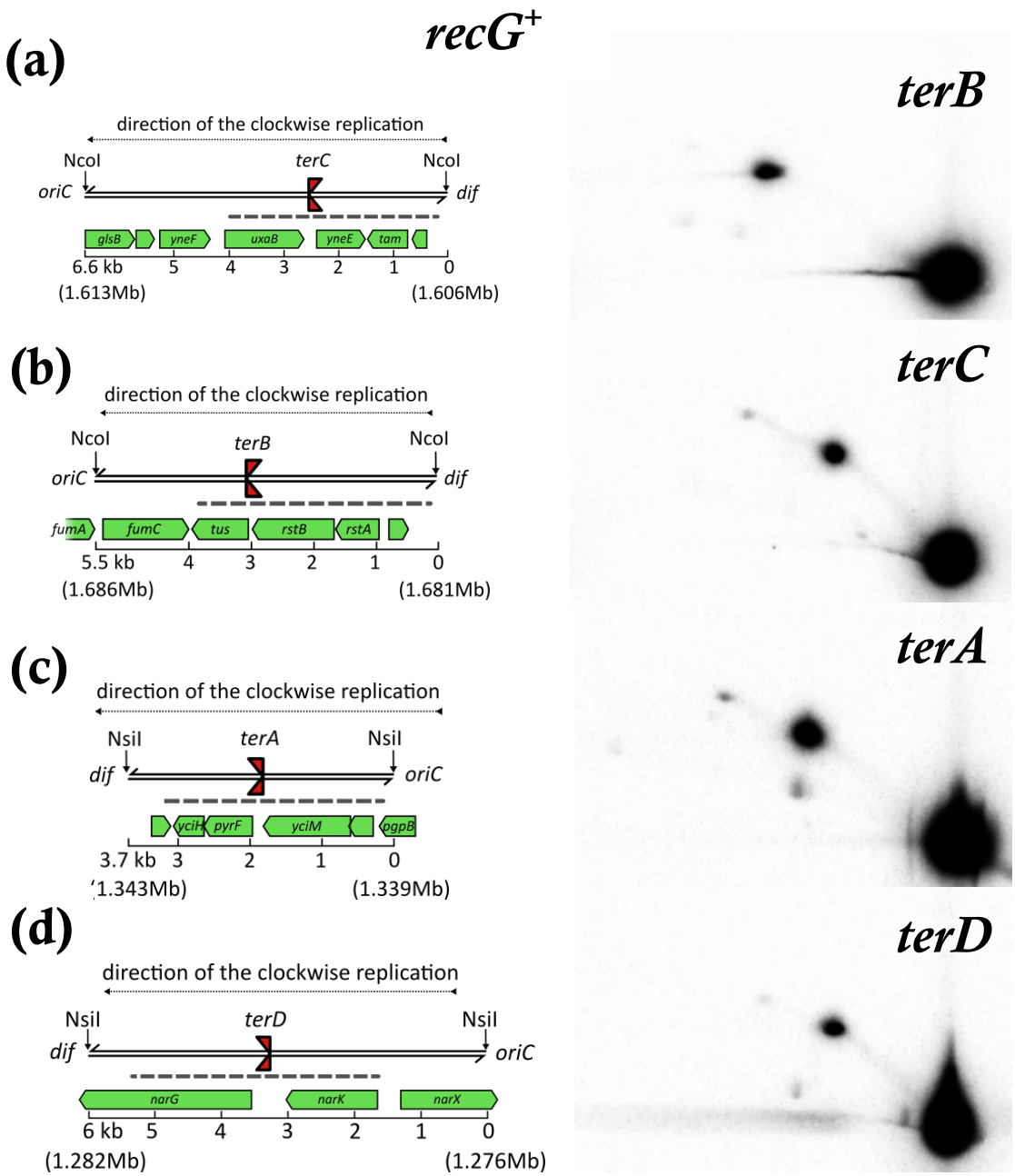

Figure 4.2

Replication fork intermediates in the terminus of the wild type DL6504 strain. **(a-d)** Schematic representation of the NcoI fragment containing the *terB* (a), *terC* (b) site (left panels). Southern blots of replication intermediates in the *terB* (a) and *terC* (b) loci visualised with terC_A-B and terB_A-B probes, respectively (right panels). Schematic representation of the NsiI fragment containing the *terA* (c), *terD* (d) site (left panels). Southern blots of replication intermediates in the *terA* (c) and *terD* (d) loci visualised with terA_XmnI_ps1-p and terD_long probes, respectively (right panels).

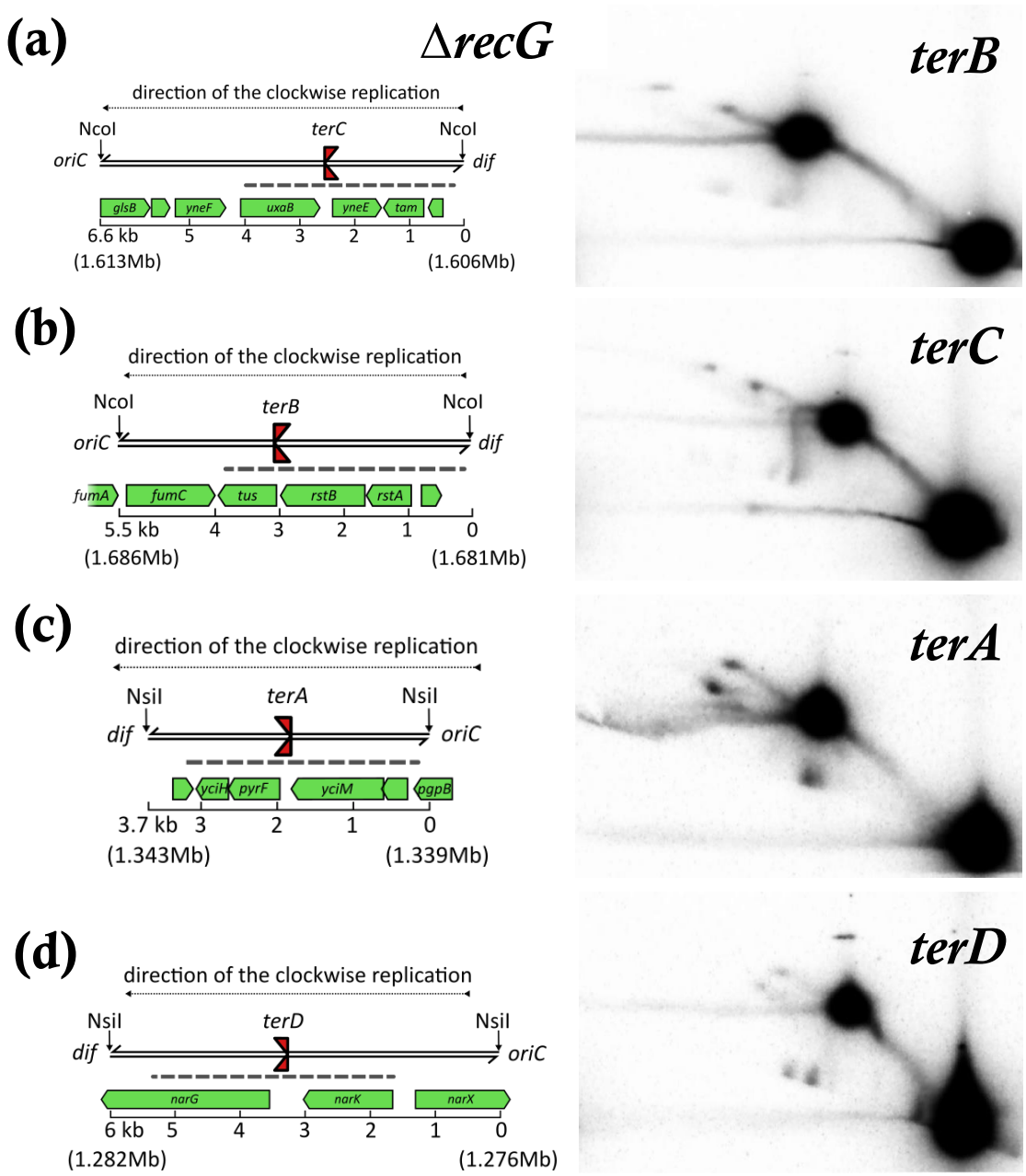

Figure 4.3

Replication fork intermediates in the terminus of the Δ*recG* DL6554 strain. **(a-d)** Schematic representation of the NcoI fragment containing the *terB* (a), *terC* (b) site (left panels). Southern blots of replication intermediates in the *terB* (a) and *terC* (b) loci visualised with terC_A-B and terB_A-B probes, respectively (right panels). Schematic representation of the NsiI fragment containing the *terA* (c), *terD* (d) site (left panels). Southern blots of replication intermediates in the *terA* (c) and *terD* (d) loci visualised with terA_XmnI_ps1-p and terD_long probes, respectively (right panels).

(a)

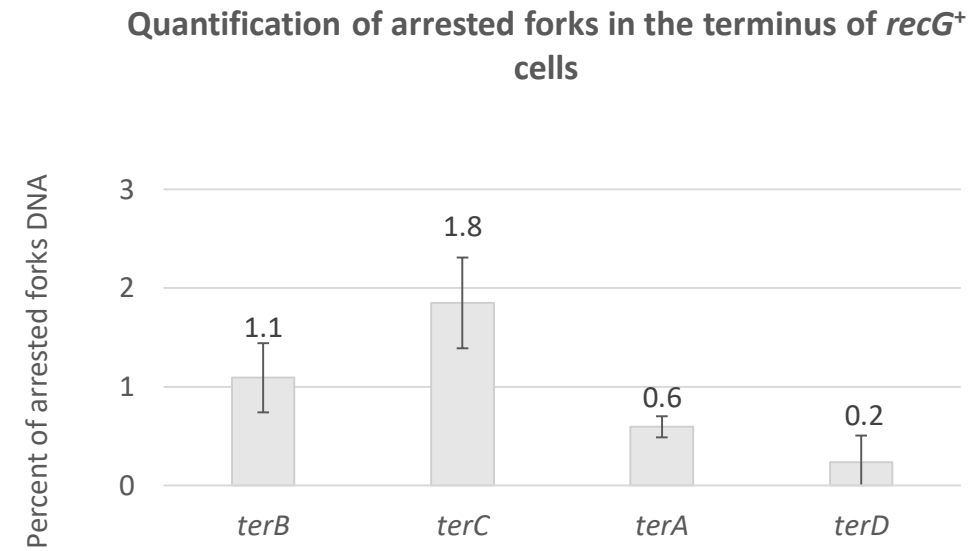

(b)

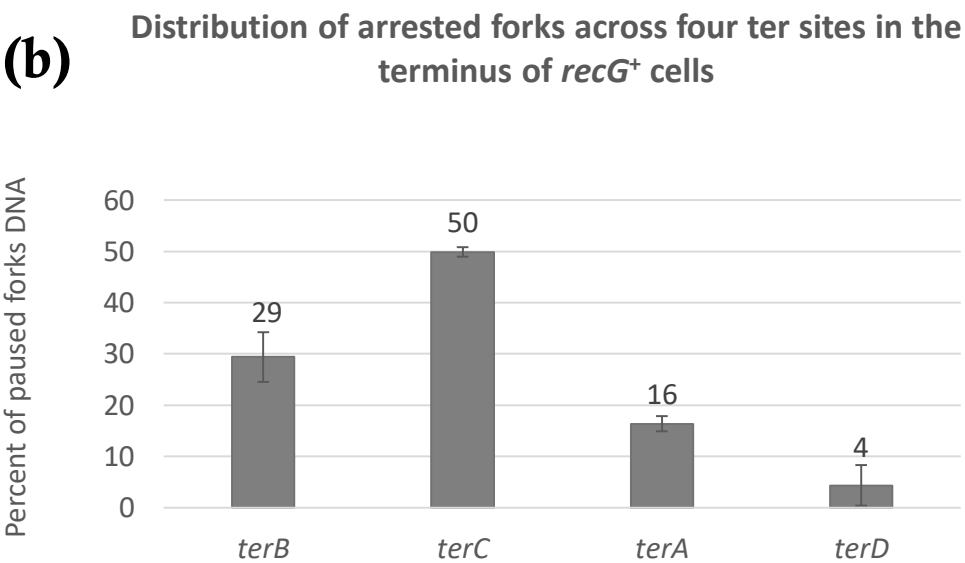

Figure 4.4

Quantification of arrested replication forks in the terminus of the wild type strain DL6504. **(a)** Percent of arrested forks relative to the total DNA signal at each *ter* site. The calculation is done as described in Figure 4.1. **(b)** Distribution of arrested forks across the terminus. Normalisation is done by calculating the contribution of each individual arrest site in the total sum of all four *ter* sites in the terminus in percentage (explained in detail in the chapter 4.3.2). The average of three repeats is shown. Error bars represent the standard deviation of the distribution.

(a)

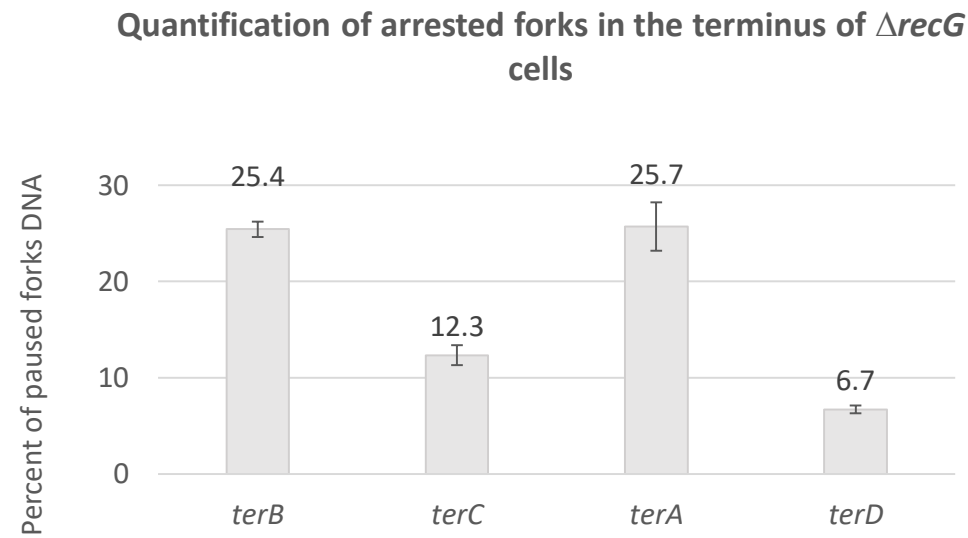

(b)

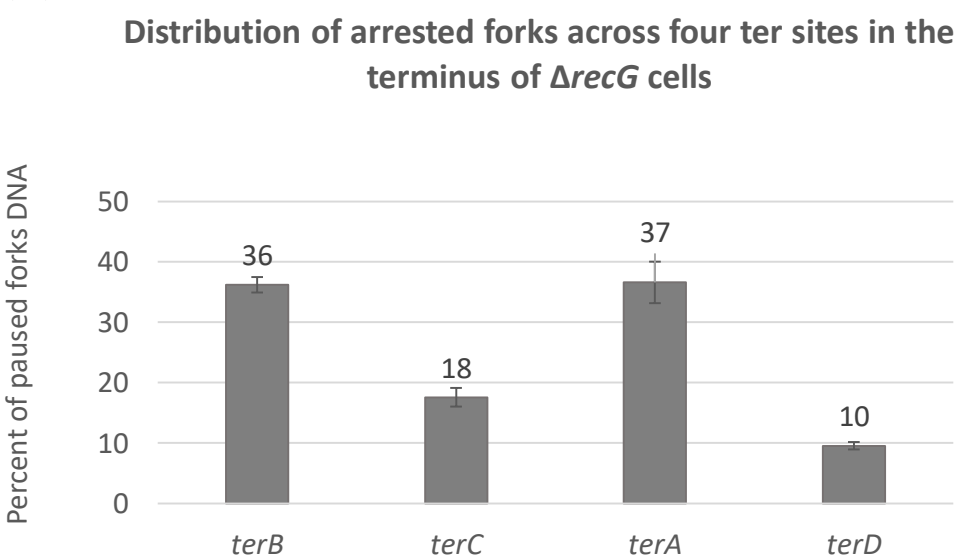

Figure 4.5

Quantification of arrested replication forks in the terminus of the Δ*recG* DL6554 strain. **(a)** Percent of arrested forks relative to the total DNA signal at each *ter* site. The calculation is done as described in Figure 4.1. **(b)** Distribution of arrested forks across the terminus. Normalisation is done by calculating the contribution of each individual arrest site in the total sum of all four *ter* sites in the terminus in percentage. The average of three repeats is shown. Error bars represent the standard deviation of the distribution.

4.4 The sequence and position effect on the replication fork accumulation frequency

4.4.1 Introduction

The difference between the *terC* and *terB* sequence in the efficiency of replication fork arrest observed in paragraph 3.4.3 suggested that the sequence plays a critical role in the fork bypass of Tus/*ter* barriers. Over-replication of the terminus notably changes the efficiency of the fork arrest of the Tus/*terC* barrier, as has been shown in the previous paragraph. To test whether the sequence of the Tus/*ter* barrier in the *terC* locus is important for the replication fork bypass, several strains that carried mutations in the sequences of *terC* and *terB* sites were made *recG*$^-$. pDL2429 was used to introduce Δ*recG* mutation into the strains DL6505 (*terC*→ *terB*), DL6507 (Δ*terC*, *terB*→*terC*), and DL6602 (Δ*terC*) via the PMGR method as described in 2.2.1.5. The resulting strains were named DL6555, DL6557, and DL6678, respectively. Successful deletion of *recG* was confirmed by UV sensitivity assay and by electrophoresis analysis of the chromosomal DNA amplified by PCR using recG - F1 and recG - R2b primers.

2-D GE experiments were performed as described in paragraph 2.2.2.7. The resulting fragments were separated using 2-D GE, and the 6.6 kb region containing *terC* and the 5.5 kb region containing *terB* were visualised by Southern blotting using the terC_A-B and terB_A-B probe, respectively.

4.4.2 The sequence and location influence the efficiency of replication arrest at *terC* and *terB* in Δ*recG* strains

The results and quantified data are shown in Figure 4.6. The normalisation was done by calculating the ratio of the signal of arrested replication forks represented by Y and double Y-spots to that of the total labelled DNA on the blot as described in 3.3.4.

ΔrecG

(a)

wt terminus (DL6554)

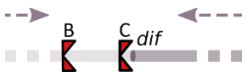

Quantification of arrested forks at *terC* and *terB* in the DL6554

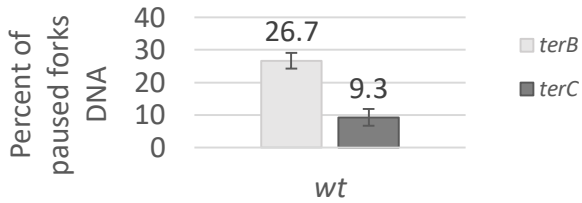

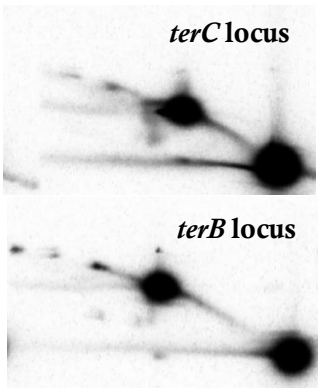

(b)

terC->B (DL6555)

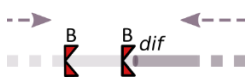

Quantification of arrested forks at *terC* and *terB* in the DL6555

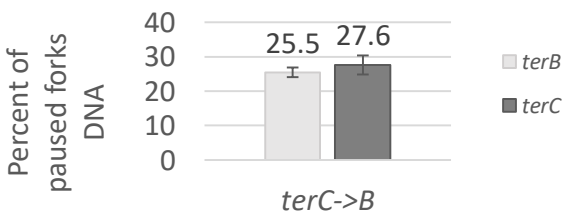

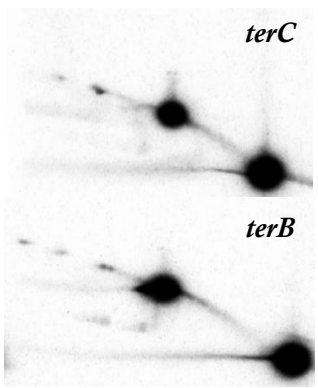

(c)

ΔterC (DL6678)

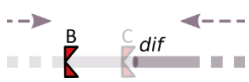

Quantification of arrested forks at *terC* and *terB* in the DL6678

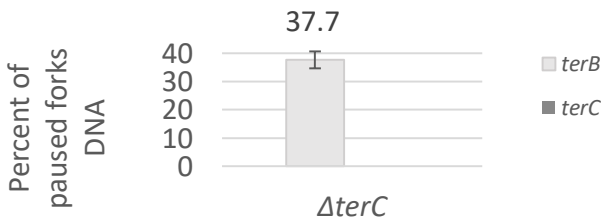

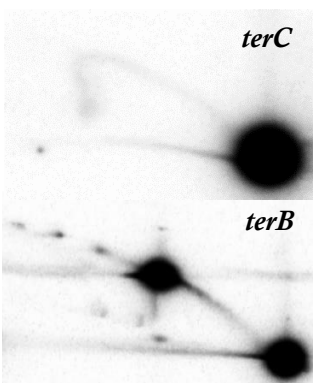

(d)

ΔterC terB->C (DL6557)

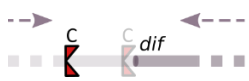

Quantification of arrested forks at *terC* and *terB* in the DL6557

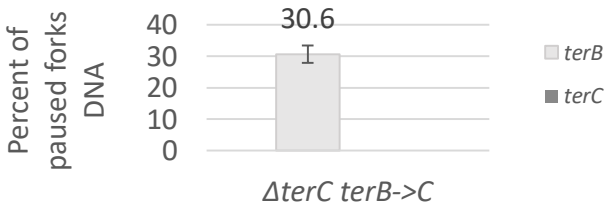

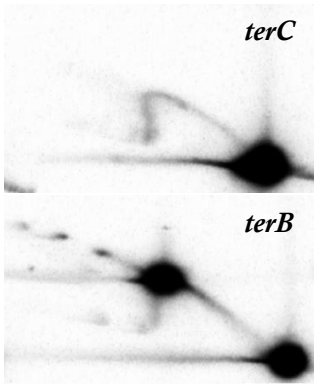

Figure 4.6

Quantification of arrested replication forks in *terC* and *terB* loci of *E. coli* DL6554 (Δ*recG*), DL6555 (Δ*recG terC→terB*), 6678 (Δ*recG* Δ*terC*) and DL6557 (Δ*recG* Δ*terC*, *terB→terC*) strains. **(a-d)** Schematic representation of the terminus region of each strain is shown on the left (described as on Figure 3.7). 2-D gels of *terC* and *terB* loci are shown on the right. The quantification of arrested replication forks is shown in the middle. The percent of arrested forks relative to the total DNA signal at each *ter* site. The calculation of the ratio (R) is done using the formula: R=B/(A+B). The average of three repeats is shown. Error bars represent the standard deviation of the distribution.

The resulting ratio values represent the fraction of chromosomes in the culture that had replication arrested at either the *terC* or the *terB* site. The experiment was repeated three times to obtain the average value for each *ter*. Arrested replication forks represented by Y-spots were detected in *ter* loci of all strains, except where the *terC* sequence had been deleted. In the DL6555 strain where the *terC* sequence was replaced with *terB,* the percentage of arrested replication forks in the *terC* locus reached 27.6% of the total DNA. In comparison with the Δ*recG* strain DL6554, the amount of arrested replication forks at the *terC* locus in DL6555 (Δ*recG terC→terB*) was markedly higher, demonstrating that the accumulation of replication forks in the *terC* locus depends on the sequence of the *ter* site.

The quantity of arrested replication forks in the *terB* locus varied greatly among the four strains. In the absence of the terminator sequence in the *terC* locus all replication forks should be able to reach the *terB* locus unimpeded. However, the strength of arrested replication forks signal at the *terB* site of Δ*terC* was notably greater than that at the *terB* site of the Δ*recG terC→ terB* strain (Figure 4.6c and d). Similarly, a greater quantity of forks was detected at the *terB* locus containing *terC* sequence of the Δ*recG* Δ*terC terB→terC* strain than in the Δ*recG* strain with unperturbed *ter* sites. This can be explained by the greater availability of the Tus protein

in the absence of one of the *ter* sites in the left replichore. Indeed, as a result of over-replication of the terminus the copy number of *ter* sequences increases. This leads to the rapid sequestration of the available Tus in the cell. Thus, in the absence of one of the *ter* sequences, the remaining *ter* is likely to be occupied by Tus more frequently.

4.5 Discussion

The data presented in this chapter showed that elevated degree of replication fork arrest is detected as a result of the terminus over-replication in Δ*recG* cells. It has been recently proposed that in the absence of RecG, abnormal backwards-directed DNA replication is initiated from *terA* and *terB* sites in the terminus (Azeroglu *et al.*, 2016). The presence of non-*oriC* replication forks in the terminus revealed important differences in the function of the Tus/*ter* replication fork trap. Under normal conditions, replication forks are arrested predominantly in the *terC* locus, and approximately one-third can bypass the first barrier and reach the *terB* locus. In contrast, I observed the opposite scenario in cells lacking RecG. Almost 75% of arrested replication forks were arrested at the second terminator sequence, *terB*, in the left replichore. The simplest explanation of such a massive bypass of the *terC* block is the sequestration of the Tus protein. As a result of the terminus over-replication, multiple copies of *ter* can accumulate in cells. *tus* gene is autoregulated and was shown to produce very few copies of short-lived *tus* mRNA at the end of each successful round of replication (Natarajan, Kelley and Bastia, 1991; Roecklein and Kuempel, 1992). It is conceivable that *terB* located within the promoter region of *tus* is more likely to be occupied by Tus, than *terC* positioned further away. However, the observation provided in this chapter demonstrated the strength of the *terA* site even when the terminus is over-replicated. The *terA* locus is located

much further away from *terB* (~330 kb) than *terC* (~74 kb) and should be even less likely occupied by Tus. Alternatively, the association of UvrD with non-*oriC* replication forks in the terminus can also potentially explain the bypass of Tus/*terC*. It has been previously shown in the Michel laboratory that the UvrD helicase can promote the bypass of a synthetically introduced Tus/*terB* replication fork barrier (Bidnenko, Lestini and Michel, 2006). No evidence was found in favour of the continuous association of UvrD with normal *oriC*-initiated replication forks. However, repair-initiated forks generated in the absence of RecG could potentially be assisted by the UvrD helicase (Boubakri *et al.*, 2010). Finally, in the absence of RecG, the backwards-initiated DNA synthesis from the *terB* locus should arrive at Tus/*terC* from the permissive side and eventually remove the barrier further contributing to the observed Tus/*terC* replication fork bypass.

The presence of non-*oriC* originated replication forks is expected to change the distribution of fork arrest events between the left and right replichores, as an uneven number of forks would be present in each round of replication in the terminus. Data of the distribution of arrested replication forks in the terminus of the *recG*$^{+}$ strain revealed that approximately 80% of all fork arrest events were localised in the left replichore at *terC* and *terB* sites and the remaining 20% in the right replichore at *terA* and *terD* (Figure 4.4b). This can be explained by the distance between the midpoint of the chromosome and innermost *ter* sites in each replichore. *oriC*-initiated counter clockwise-moving replication forks have to traverse almost 60 times greater distance (~260 kb) past the chromosome midpoint, which is equal 5.5% of the length of the chromosome, to reach *terA* than clockwise-moving forks that have to replicate 4.2 kb fragment before reaching *terC*. In contrast, in Δ*recG* cells only about 55% arrested forks were detected at *ter* sites in the left replichore and more than 45% at *ter* sites in

the right replichore. Consequently, it can be inferred that under the condition of the terminus over-replication the distribution of arrested forks between two replichores approaches 50:50 ratio, whereas under normal conditions this ratio is strongly skewed towards the left replichore.

One of the interesting observations of the replication termination at *terC* and *terB* was the presence of secondary, and sometimes tertiary, termination structures. One of the possible explanations of the appearance of such complex molecules in Δ*recG* cells is the innate slow resolution of termination structures at *ter* sites (observed in chapter 3) combined with the increased number of replication forks traversing the terminus. When a replication fork runs into a termination structure formed by another two fusing forks, a larger branched molecule with retarded gel migration speed could be generated, thus appearing as a secondary termination structure on the gel.

Finally, the quantification of the replication arrest efficiency at *terC* and *terB* of several Δ*recG* strains (DL6554, DL6555, DL6678, and DL6507) provided further evidence of the role of *ter* sequence in the efficiency of Tus/*ter* barrier. Previously, I showed that in *recG*$^{+}$ strains changing the *terC* sequence to *terB* resulted in a greater fraction of paused forks in the *terC* locus and fewer in the *terB* locus. The decrease of paused forks at *terB* can be explained by the requirement to bypass Tus/*ter* barrier in the *terC* locus in order to reach *terB*. Interestingly, the three-fold increase in the fraction of arrested forks in the *terC* locus observed in the DL6555 strain (Δ*recG terC→terB*) had no effect on the fraction of arrested forks detected in the *terB* locus (Figure 4.6, compare a and b). This is unexpected because the stronger barrier in the *terC* locus should further limit the bypass. One of the possible explanations is the greater stability of the Tus/*terB* barrier in the locked state (Mulcair *et al.*, 2006; Elshenawy *et al.*, 2015). In the

condition of the limited availability of Tus the observed 3-fold increase of the fraction of arrested forks in the *terC* locus may not be because more copies of the *ter* sequence in the *terC* locus are occupied. Instead, if the quantity of Tus proteins in the Δ*recG* and Δ*recG terC→terB* strain is the same, the longer half-life of the *terB*-bound Tus (Mulcair *et al.*, 2006; Moreau and Schaeffer, 2012) may contribute to the observed signal strength of the Y-spot by accumulating more forks at both permissive and non-permissive sides before the Tus dissociation from *ter*.

Taken together, this chapter provides evidence that the Tus/*ter* replication fork trap limits the abnormal DNA synthesis to the terminus region. Importantly, the data also suggest that non-*oriC* initiated replication interacts differently with the Tus/*terC* and Tus/*terB* barriers, confirming the previously observed replication fork bypass of Tus/*terC* in marker frequency analysis experiments of Δ*recG* strains (Rudolph *et al.*, 2013; Wendel, Courcelle and Courcelle, 2014; Azeroglu *et al.*, 2016).

5 ROLE OF UVRD IN THE REPLICATION FORK BYPASS OF *TERC* IN THE TERMINUS

5.1 Introduction

DNA replication forks are frequently challenged by DNA lesions, topological stress and DNA-bound proteins (reviewed in Marians, 2018). To promote replication through physical obstacles on DNA replisomes recruit accessory helicases, such as Rep, DinG or UvrD (reviewed in Brüning, Howard and McGlynn, 2014). However, when accessory helicases fail to clear DNA-bound proteins, replisome movement will be arrested. Blocked replication forks at tightly bound DNA-protein complexes can be broken and consequently cause DNA degradation and recombination, potential sources of DNA rearrangements (Bierne, Ehrlich and Michel, 1997; Michel, Ehrlich and Uzest, 1997).

The ability of the Tus-*ter* complex to form a fork barrier on DNA was used to study the consequences of replication arrest on chromosome stability and the fate of replication forks at natural impediments (Horiuchi and Fujimura, 1995; Bidnenko, Ehrlich and Michel, 2002). It has been shown that an ectopic Tus/*terB* barrier outside of the terminus promotes illegitimate recombination in plasmids and RecBCD-dependent chromosome rearrangements. However, the study of *E. coli* strains with the *terB* sequence introduced in the middle of each replichore suggested that replication forks can progress through ectopic Tus/*terB* barriers (Bidnenko, Lestini and Michel, 2006). It was demonstrated that the UvrD helicase is responsible for the ectopic Tus/*terB* bypass, but only as a consequence of RecBCD-dependent recombination reaction. Whether UvrD facilitates replication fork bypass of the Tus/*terC* barrier in the terminus is presently unknown, however a considerable increase of one-ended double-strand breaks was noticed in the *terC* locus in Δ*uvrD* Δ*recG* strain compared

with Δ*recG* suggesting elevated frequency of replication fork arrest at Tus/*terC* in the absence of UvrD (Azeroglu *et al.*, 2016; Azeroglu, personal communication). In this chapter, a detailed analysis of the replication fork arrest efficiency of *ter* sites in the terminus region of Δ*uvrD* strains is presented. Using 2-D GE method it was demonstrated that in the absence of UvrD, replication forks interact with the *ter* sites differently compared to wild-type. Also, by analysing the distribution of arrested replication forks across *ter* sites in the terminus, it was shown that the UvrD helicase is important for the replication through Tus/*terC*. Finally, using the mutational analysis of *terC* and *terB* non-consensus regions the importance of the non-permissive flanking region in the fork bypass of Tus/*ter* was demonstrated. In summary, data in this chapter present evidence that UvrD facilitates replication fork bypass of the Tus/*terC* barrier and the first five nucleotides of the *ter* sequence are critical for the UvrD-Tus/*terC* interaction.

5.2 Quantification of arrested replication forks at *terC* and *terB* in Δ*uvrD* cells

5.2.1 Introduction

It has been reported that UvrD facilitates replication through a synthetically introduced Tus/*terB* replication fork barrier in the middle of the right replichore (Bidnenko, Lestini and Michel, 2006). To evaluate the arrest efficiency of Tus/*terB* and Tus/*terC* barriers in the terminus in the absence of the UvrD helicase, replication fork intermediates in the *terB* and *terC* loci were visualised and quantified. For that, the Δ*uvrD* mutation was introduced in the background strain DL6504 (NcoI-cs inserted bear *terB*) using the PMGR method with pDL2391 plasmid (described in 2.2.1.5), and the resulting strain was named DL6643. The

uvrD gene deletion was confirmed by the UV sensitivity assay and by the electrophoresis analysis of the chromosomal DNA amplified by PCR using UvrD.F1 and UvrD.R2 primers. The Δ*uvrD* DL6643 strain growth rate profile was identical to that of the wild-type, as determined by the growth rate assay (described in 2.2.1.6). 2-D GE experiments were performed as described in paragraph 2.2.2.7. TerC_A-B and terB_A-B probes were used in Southern blotting to visualise chromosomal fragments containing the *terC* and *terB* locus, respectively.

5.2.2 Elevated accumulation of arrested replication forks in Δ*uvrD* cells

The results and quantified data are shown in Figure 4.1. The normalisation was done by calculating the ratio of the signal of arrested replication forks represented by Y and double Y-spots to that of the total labelled DNA on the blot as described in 3.3.4. The resulting ratio values represent the percentage of chromosomes in the culture that had replication arrested at either the *terC* or the *terB* site. The experiment was repeated three times to obtain the average value for each *ter*.

Branched intermediates formed by arrested replication fork were visualised in both *terC* and *terB* loci (Figure 4.1-c, d). The position of Y-spots on the arc of branched intermediates corresponded to the position of *ter* site in each locus. Quantification of the Y-spot signal (Figure 4.1-e) revealed that the majority of clockwise-moving replication forks were arrested at the first *ter* site in the left replichore, *terC*, similar to the wild-type strain (compare to Figure 3.8). The percentage of forks arrested in the *terC* locus (8.8%) was higher than under the wild type conditions (2%) and indicated the presence of additional replication forks in the terminus. The arrested fork signal at the Y-spot in the *terB* locus was approximately 2.3% of the total DNA.

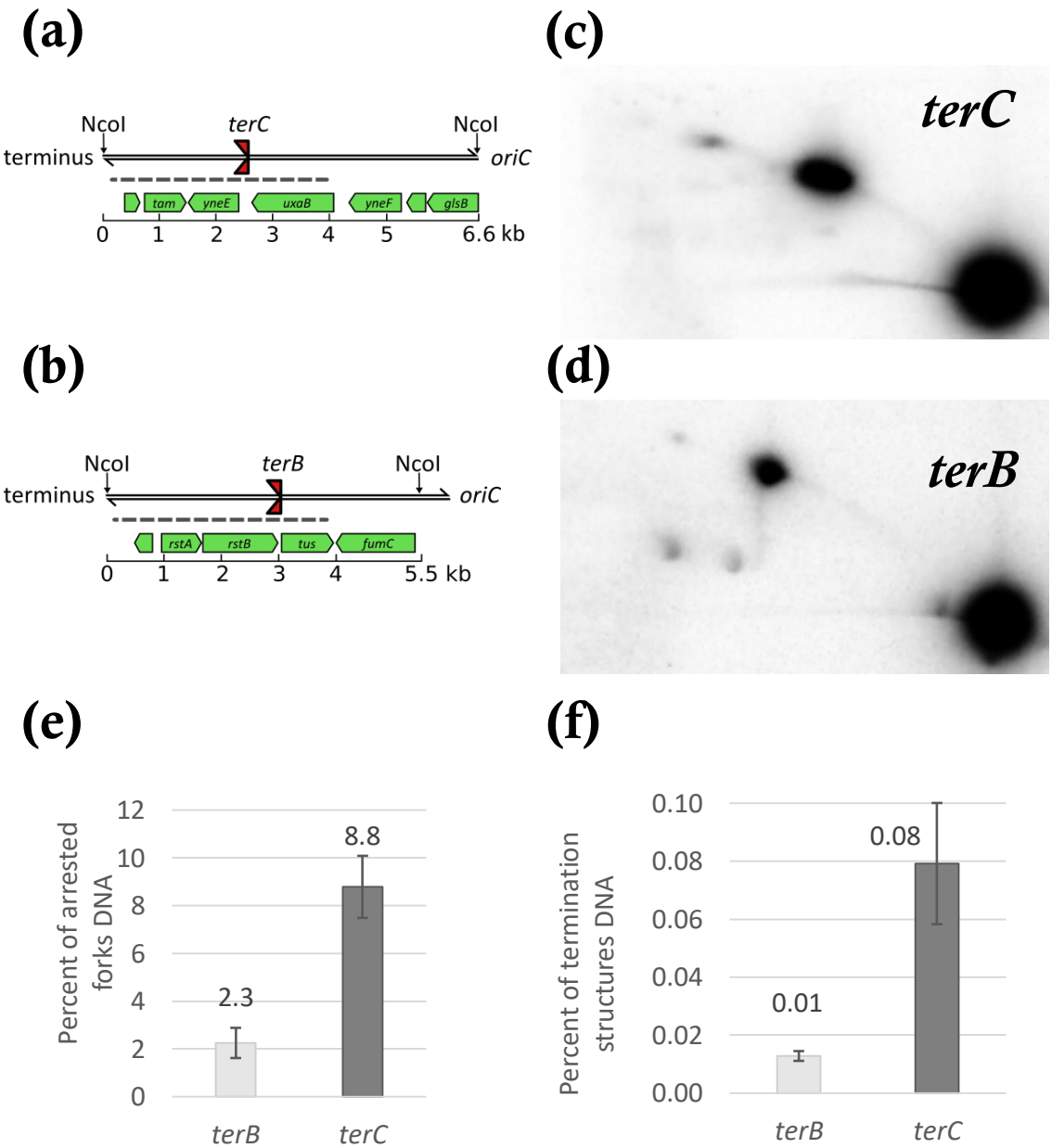

Figure 5.1

Arrested replication forks in *terC* and *terB* loci of the *E. coli* Δ*recG* strain DL6643. **(a,b)** Schematic representation of NcoI fragments of the *terC* (a) and *terB* (b) chromosomal loci (previously described in Figure 3.3 and Figure 3.5). **(c,d)** Southern blots of replication intermediates in the *terC* (c) and *terB* (d) loci visualised with terC_A-B and terB_A-B probes, respectively. **(e,f)** Quantification of the percentage of arrested forks (e) and termination structures (f) relative to the total DNA signal at each *ter* site. The quantification is done by calculating the ratio of the signal of arrested replication forks represented by Y and double Y-spots (e) or double Y-spots (f) to that of the total labelled DNA. The average of three repeats is shown. Error bars represent the standard deviation of the distribution.

The four-times difference in the arrest activity of *terC* and *terB* imply that only about a fifth of replication forks were able to progress through the *terC* site and reach the non-permissive side of the following *terB* site, compared to approximantely one-third in wild-type situation.

Faint double Y-spikes emanating from the arrest spots on the Y-arc and double Y-spots indicate the presence of converging forks close to fusion in the left replichore in Δ*uvrD* cells. Quantification of termination structures was done as described in paragraph 4.2 and results are shown in Figure 4.1f. The signal of double Y-shaped intermediates was the strongest at the *terC* site, implying that fork fusion events occur predominantly near the middle point of the chromosome. However, in a small proportion of molecules, fork fusion was detected at the *terB* site as well.

5.2.3 Replication arrest efficiency does not depend on the *ter* sequence and *ter* position in Δ*uvrD* cells.

It has been shown that the strength of the barrier formed by *terC* and *terB* sequence is different, where the Tus/*terC* barrier functions as a weaker and more permeable replication terminator (see Replication fork arrest at ter sites in the terminus region3 and 3.14). To test whether *ter* sequence is important for the replication fork arrest efficiency in Δ*uvrD* cells, several strains that carried mutations in the sequences of *terC* and *terB* sites were made *uvrD*$^-$. pDL2391 was used to introduce Δ*uvrD* mutation into DL6505 (*terC*-›*terB*), DL6602 (Δ*terC*), and DL6507 (Δ*terC terB*-›*terC*) via the PMGR method as described in 2.2.1.5. The resulting strains were named DL6685, DL6686, and DL6688, respectively.

(a)

wt terminus (DL6643)

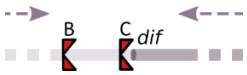

Δ*uvrD*

Quantification of arrested forks in the Δ*uvrD*

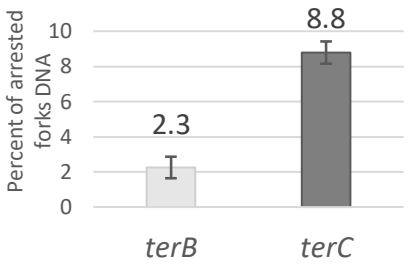

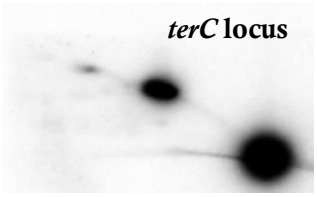

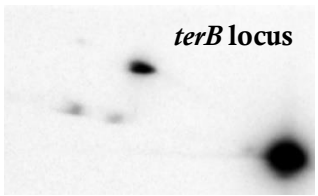

(b)

terC->B (DL6685)

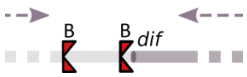

Quantification of arrested forks in the Δ*uvrD terC→terB*

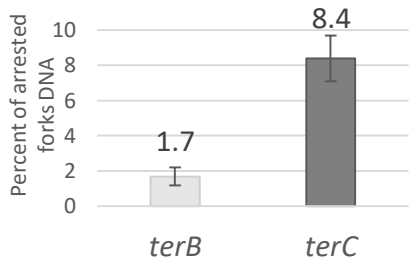

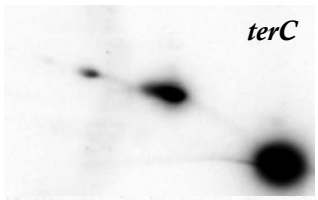

(c)

Δ*terC* (DL6686)

Quantification of arrested forks in the Δ*uvrD* Δ*terC*

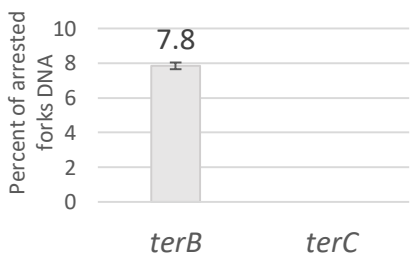

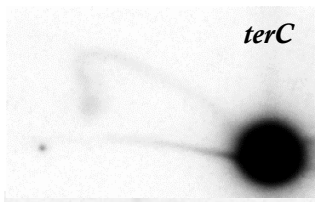

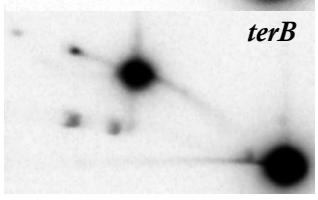

(d)

Δ*terC terB->C* (DL6688)

Quantification of arrested forks in the Δ*uvrD* Δ*terC terB→terC*

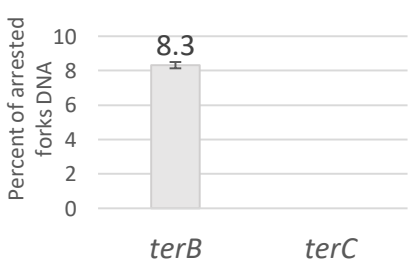

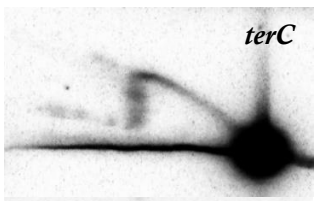

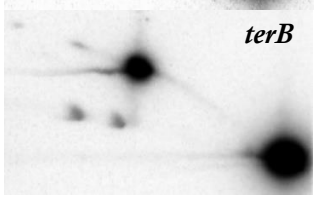

Figure 5.2

Quantification of arrested replication forks in *terC* and *terB* loci of *E. coli* DL6643 (Δ*uvrD*), DL6685 (Δ*uvrD terC→terB*), 6678 (Δ*uvrD* Δ*terC*) and DL6557 (Δ*uvrD* Δ*terC terB→terC*) strains.

(a-d) Schematic representation of the terminus region of each strain is shown on the left (described as in Figure 3.7). 2-D gels of *terC* and *terB* loci are shown on the right. Quantification of arrested replication forks was done as described in in Figure 3.7 and resulting charts for each strain are presented in the middle.

The successful deletion of the *uvrD* gene was confirmed by the UV sensitivity assay and by the electrophoresis analysis of the chromosomal DNA amplified by PCR using UvrD.F1 and UvrD.R2 primers.

Visualised *terC* and *terB* loci and arrested fork signal quantification are shown in Figure 5.2. Normalisation was done as described in 3.3.4. Arrested replication forks represented by Y-spots were detected in *ter* loci of all strains, except where the *terC* sequence was deleted. In all cases, the position of the Y-spot was consistent with the position of the *ter* site within each fragment. A high degree of fork arrest was detected at the first *ter* site in all strains. Converging replication fork intermediates were present at *ter* sites forming Y-spot and faint double Y-spike signal near the inflexion point of Y-arcs. Quantification of the level of fork arrest revealed that approximately 8.3% of the total DNA was concentrated at Y-spots of the first *ter* sites clockwise-moving replication forks encounter. Although average values fluctuated between 7.8% and 8.8%, the difference was not statistically significant as the probability (P) that, values of the Y-spot signal at *terC* for Δ*uvrD* and Δ*uvrD terC→terB* and at *terB* for Δ*uvrD* Δ*terC* and Δ*uvrD* Δ*terC terB→terC* strains are different is $P>0.4$ (Student's paired t-test, with a two-tailed distribution; P values were within the 0.4-1 range for all tests; two values are considered different if $P<0.05$). Therefore, no difference was observed in the arrest efficiency of the clockwise replication at the first *terC* or *terB* sequence in the left replichore. Although small,

the difference in the arrested fork signal in the *terB* locus in Δ*uvrD* and Δ*uvrD terC→terB* strains suggest that fewer replication forks bypassed Tus/*terB* in the *terC* locus of the Δ*uvrD terC→ terB* strain. These observations suggest that the presence of UvrD facilitates replication fork bypass of *terC*, but not *terB* sequence.

5.3 UvrD facilitates replication fork bypass of the Tus/*terC* barrier

5.3.1 Introduction

It has been demonstrated that the majority of replication forks bypass the Tus/*terC* barrier in the *terC* locus under the condition of the terminus over-replication in the absence of RecG (Azeroglu *et al.*, 2016; paragraph 4.2.2). If the UvrD helicase facilitates the replication fork progress through the *terC* locus, then in the Δ*recG* Δ*uvrD* double mutant replication is expected to arrest more frequently at the Tus/*terC* barrier. The Δ*recG* Δ*uvrD* double mutant strain is not viable, however the lethality can be rescued by introducing the third mutation, Δ*recO* (Fonville *et al.*, 2010). To determine whether the UvrD helicase is responsible for the replication fork bypass of Tus/*terC* in the Δ*recG* strain, replication intermediates in the *terC* and *terB* loci of the Δ*recG* Δ*uvrD* Δ*recO* triple mutant were visualised and quantified. First, Δ*recO* mutation was introduced into the DL6554 Δ*recG* and DL6643 Δ*uvrD* strain using pDL2710 (pTOF24_*recO*_KO) plasmid via the PMGR method as described in 2.2.1.5. The resulting Δ*recG* Δ*recO* and Δ*uvrD* Δ*recO* strains were named DL6644 and DL6645, respectively. Then, Δ*recG* mutation was introduced into the Δ*uvrD* Δ*recO* DL6645 strain using pDL2429 (pTOF24_*recG*_KO) plasmid via PMGR. The resulting Δ*recG* Δ*uvrD* Δ*recO* triple mutant strain was named DL6646. Successful deletion of *uvrD*, *recO* and *recG* was confirmed by UV sensitivity assay and by electrophoresis analysis of the chromosomal DNA amplified by PCR

using UvrD.F1 and UvrD.R2, recO-KO-F1 and recO-KO-R2, and recG - F1 and recG - R2b primer pairs, respectively. The growth rate profiles of the Δ*recG* Δ*uvrD* Δ*recO* triple mutant and control strains were determined by the growth rate assay in LB broth (described in 2.2.1.6) and presented in Figure 5.3. The average of three repeats is shown. Error bars represent the standard deviation of the distribution.

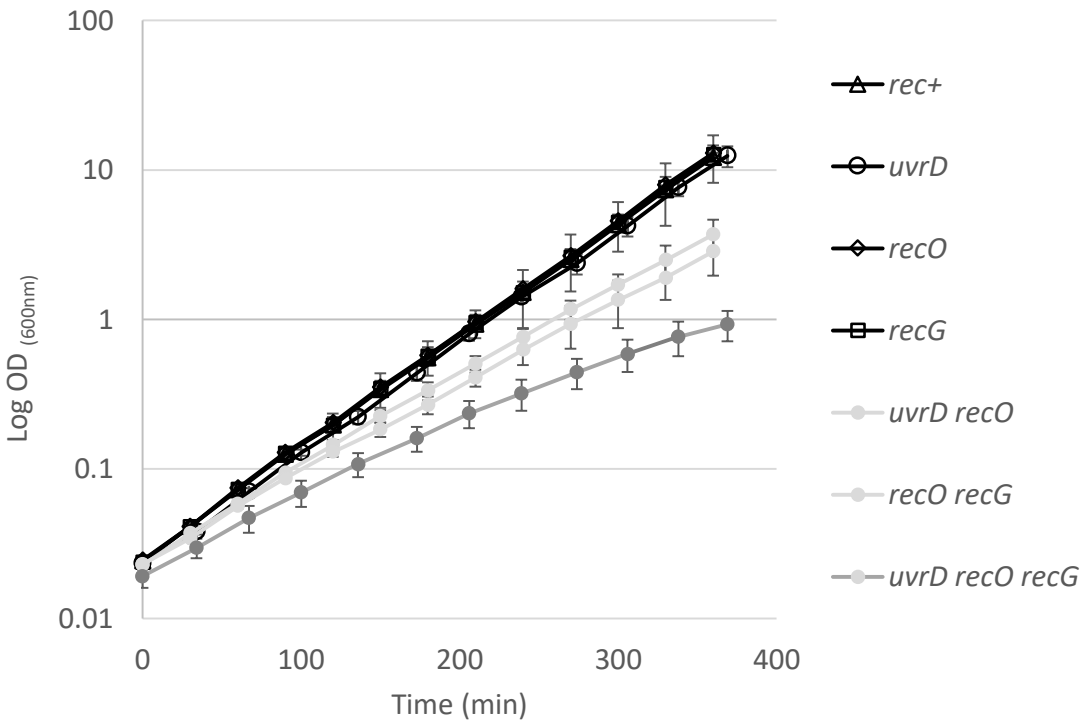

Figure 5.3

Growth of the *E. coli* Δ*recG* Δ*uvrD* Δ*recO* triple mutant strain DL6646 and control strains DL6504 (wild type), DL6643 (Δ*uvrD*), DL6604 (Δ*recO*), DL6554 (Δ*recG*), DL6645 (Δ*recO* Δ*uvrD*) and DL6644 (Δ*recO* Δ*recG*). All cultures were maintained in exponential growth phase by being diluted regularly in fresh LB-broth, in order to maintain the OD_{600nm} below 0.3. The average of three repeats is shown. Error bars represent standard deviation of the distribution.

2-D GE experiments were performed as described in paragraph 2.2.2.7. Resulting fragments were separated using 2-D GE, and the 6.6 kb region containing *terC* and the 5.5 kb region containing *terB* were visualised by Southern blotting using the terC_A-B and terB_A-B probe, respectively.

5.3.2 Terminus over-replication in the Δ *uvrD* Δ *recG* Δ *recO* strain is restricted at *terC*.

Results and quantified data are shown in Figure 5.4. Normalisation was done as described in 3.3.4. Arrested replication forks were present in both *ter* loci, and the position of the corresponding Y-spot was consistent with the expected position on the Y-arc. Converging replication fork intermediates were clearly visible in the *terC* locus as a single double Y-spike and a faint double Y-spot. Quantification of the signal of Y-spots revealed that clockwise-moving replication forks were arrested predominantly at the first *ter* sequence, *terC*. As can be seen in Figure 5.4-e, more than half of the total DNA in the *terC* locus corresponded to the arrested at Tus/*terC* replication forks. Approximately five times weaker signal of the arrested forks in the *terB* locus indicates that a relatively small fraction of replication forks were able to progress through *terC* in the absence of the UvrD helicase. In contrast, in the *uvrD*$^{+}$ *recG*$^{-}$ cells, the strongest arrested fork signal was detected at the secondary *ter* site, *terB* (compare with Figure 4.1). These data suggests, that in the absence of UvrD, *terC* can now terminate majority of replication originating in terminus in the absence of RecG.

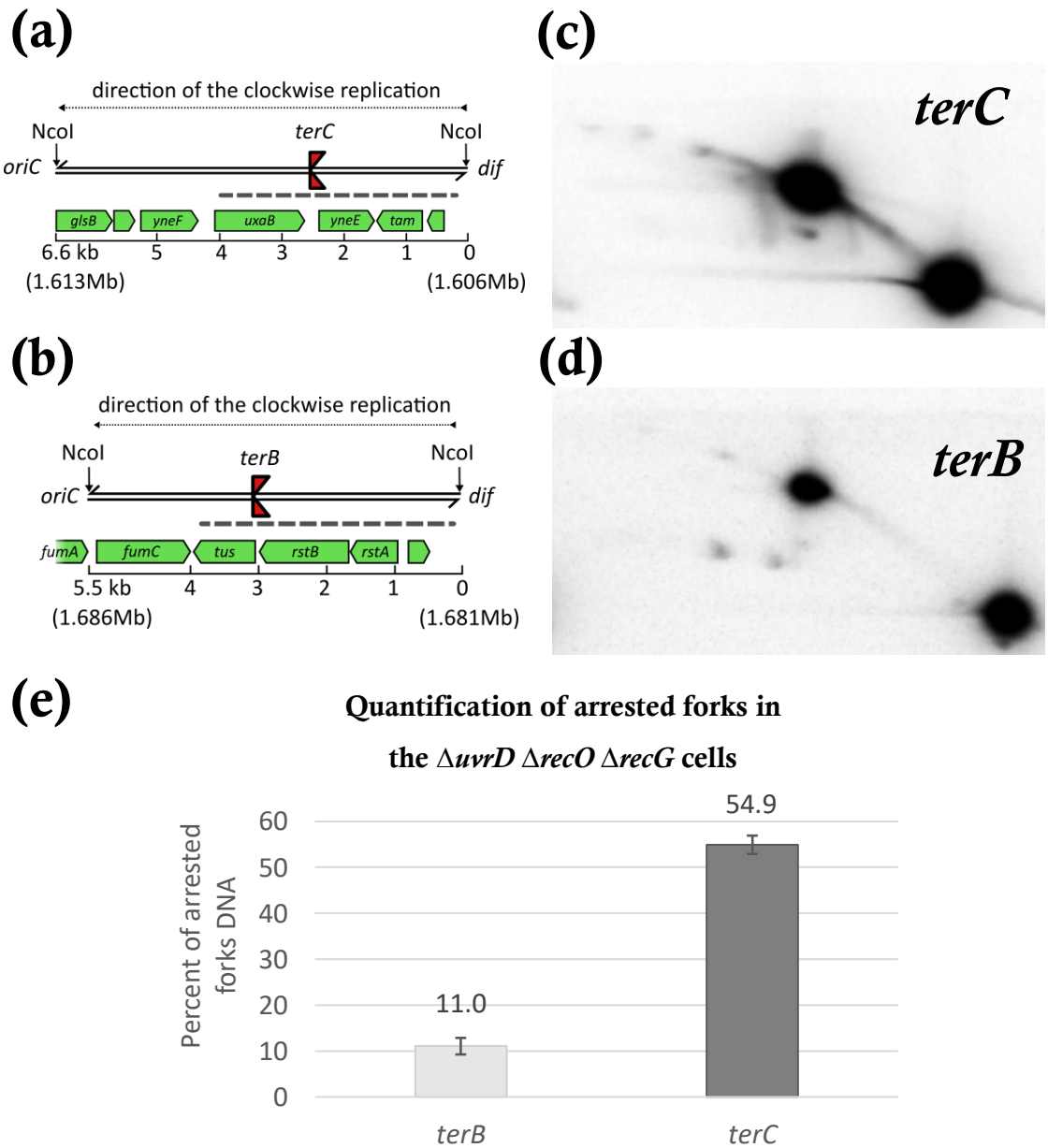

Figure 5.4

Arrested replication forks in *terC* and *terB* loci of the *E. coli* Δ*recG* Δ*uvrD* Δ*recO* triple mutant strain DL6646. **(a,b)** Schematic representation of NcoI fragments of the *terC* (a) and *terB* (b) chromosomal loci (previously described in Figure 3.3 and Figure 3.5). **(c,d)** Southern blots of replication intermediates in the *terC* (c) and *terB* (d) loci visualised with terC_A-B and terB A-B probes, respectively. **(e)** Quantification of the percentage of arrested forks. Quantification of arrested replication forks was done as described in in Figure 3.7 and resulting charts for each strain are presented in the middle.

5.3.3 Distribution of arrested replication forks in the terminus region in Δ*uvrD* cells

In order to test whether UvrD facilitates replication fork bypass of Tus/*terC* under normal conditions in the presence of RecG, the distribution of arrested forks across four *ter* sites in the terminus was determined. For that replication fork intermediates in *terB, terC, terA* and *terD* loci in the chromosome of the Δ*uvrD* DL6643 strain were visualised and quantified using 2-D GE method.

The 2-D GE experiment was performed as described in paragraph 2.2.2.7. DNA samples containing four *ter* loci were extracted from a single culture of cells as described in paragraph 4.3.1. Resulting chromosomal fragments were separated using 2-D GE. The 6.6 kb NcoI fragment containing *terC* and the 5.5 kb NcoI fragment containing *terB* were visualised by Southern blotting using terC_A-B and terB_A-B probes, respectively (Figure 5.5-a, b). The 3.7 kb NsiI fragment containing *terA* and the 6 kb NsiI fragment containing *terD* were visualised using terA_XmnI_ps1-p and terD_long probes, respectively (Figure 5.5-c, d).

Visualised fragments containing *terB*, *terC*, *terA*, or *terD* of the Δ*uvrD* strain DL6643 are presented in Figure 5.5. Normalisation was done as described in 3.3.4. As expected, arrested replication forks formed large Y-spots in all four *ter* loci. Fork fusion intermediates were detected at the innermost *ter* sites, *terC* and *terA*. A faint double Y-spot can also be seen at the subsidiary *ter* site on the right replichore, *terD.* Quantification of arrested replication forks in each *ter* loci is shown in Figure 5.6-a. The degree of fork pausing at the Tus/*terC* and Tus/*terB* correlated with the results obtained earlier in paragraph 5.2.2.

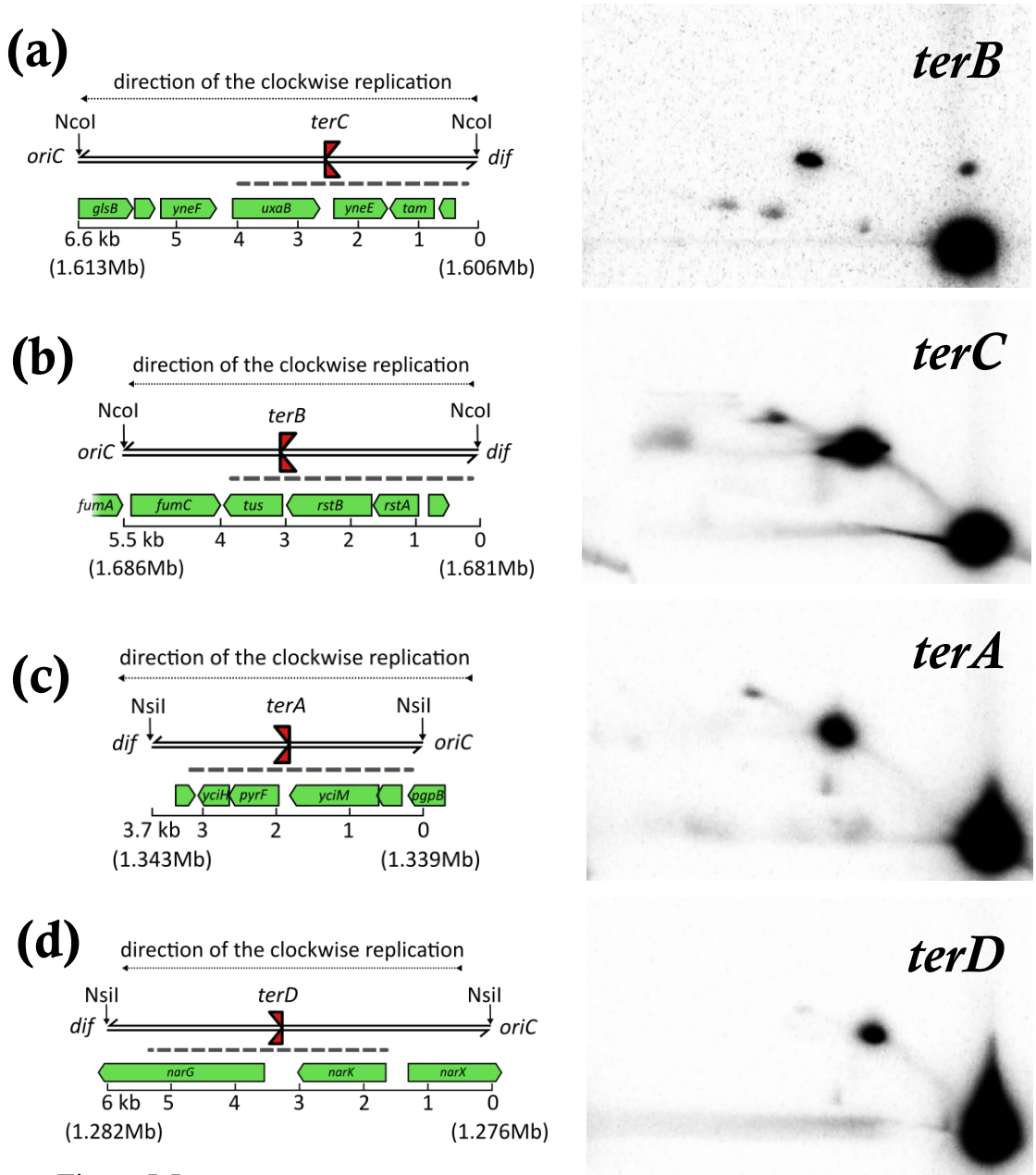

Figure 5.5

Replication fork intermediates in the terminus of the Δ*uvrD* strain DL6643. **(a-d)** Schematic representation of the NcoI fragment containing the *terB* (a), *terC* (b) site (left panels). Southern blots of replication intermediates in the *terB* (a) and *terC* (b) loci visualised with terC_A-B and terB A-B probes, respectively (right panels). Schematic representation of the NsiI fragment containing the *terA* (c), *terD* (d) site (left panels). Southern blots of replication intermediates in the *terA* (c) and *terD* (d) loci visualised with terC_A-B and terB_A-B probes, respectively (right panels).

As expected, arrested replication forks accumulated predominantly at the nearest to the middle point of the chromosome *ter* site, *terC*. In contrast, the signal strength of arrested forks at *ter* sites in the right replichore was notably weaker. This correlates with the distance between the middle point of the chromosome and *terA* and *terD* counter clockwise-moving replication forks must travel before encountering the non-permissive side of Tus/*terA*. To evaluate the distribution of replication forks across four *ter* sites, the obtained values of replication fork arrest signals were normalised by calculating the contribution of each arrest site in the total sum of all four *ter* sites in the terminus in percentage. The results are presented in Figure 5.6-b. The distribution of the signal of arrested replication forks in the terminus of the Δ*uvrD* strain is best compared to that of that the wild type strain DL6504. Data revealed limited fork bypass of the innermost Tus/*ter* barriers in each replichore. In the left replichore, the difference between arrested fork signals at *terC* and *terB* increased from approximately 2-fold in the wild-type to 5-fold in the *uvrD* mutant, whereas in the right replichore the increase was even more substantial, from 4-fold to almost 10-fold difference between *terA* and *terD*. These data suggests that deletion of *uvrD* is causing large increase in amount of paused replication forks at all four *ter* sites. This could be explained by the greater desynchronization of the *oriC*-originated replication in the absence of the accessory helicase UvrD.

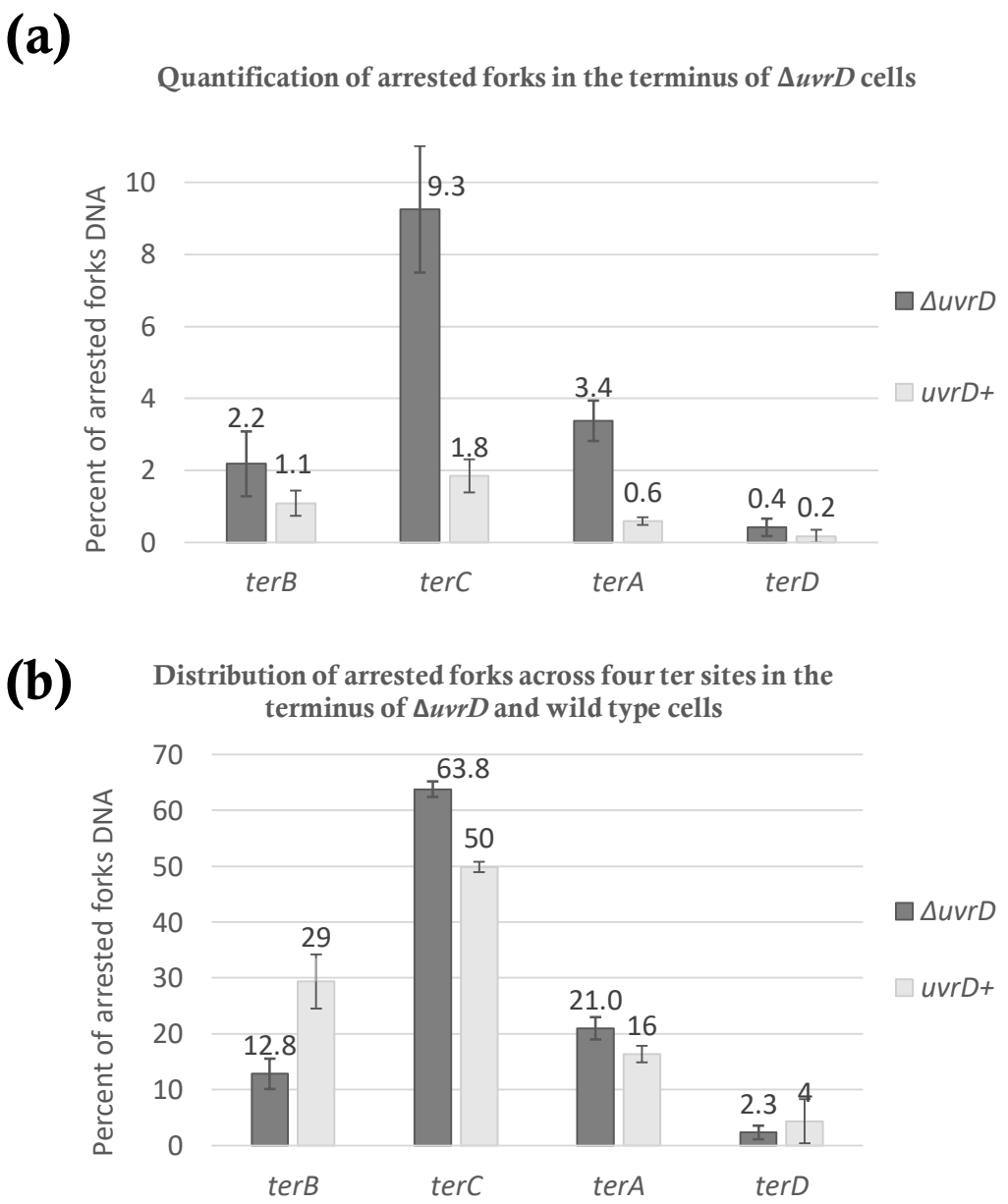

Figure 5.6

Quantification of arrested replication forks in the terminus of the Δ*uvrD* DL6643 and *uvrD*$^+$ DL6504 strains. **(a)** Percent of arrested forks relative to the total DNA signal at each *ter* site of the Δ*uvrD* DL6643 strain. The calculation is done as described in Figure 4.5. **(b)** Distribution of arrested forks in the terminus. For the *uvrD*$^+$ DL6504 strain data from Figure 4.4 was used. The calculation is done as described in Figure 4.1. The average of three repeats is shown. Error bars represent the standard deviation of the distribution.

5.4 Interaction of UvrD with the Tus/*terC* barrier

5.4.1 Introduction

Previous studies, in the Michel laboratory, revealed that the UvrD helicase could promote the bypass of a synthetically introduced Tus/*terB* replication fork barrier in the middle of both replichores, but only as a consequence of RecA- and RecBCD-mediated homologous recombination (Bidnenko, Lestini and Michel, 2006). The proposed model implies that in order for UrvD to access the DNA strand at the ectopic Tus/*terB* barrier, the RecA-dependent homologous recombination reaction has to occur at the arrested fork. If this model is correct for the endogenous Tus/*ter* barriers, then *recA* gene deletion should inactivate the homologous recombination pathway, and the frequency of replication fork bypass should decrease. To test whether UvrD requires homologous recombination to facilitate fork bypass in the terminus, replication fork intermediates in the terminus of Δ*recA* and Δ*recA* Δ*uvrD* strains were visualised and analysed. First, *recA* mutation was introduced into the wild type strain DL6504 and the Δ*uvrD* strain DL6643 strain using pDL2711 (pTOF24_*recA*_KO) plasmid via the PMGR method as described in 2.2.1.5. The resulting strains were named DL6931, DL6933, respectively. The successful deletion of the *recA* gene was confirmed by the UV sensitivity assay and by the electrophoresis analysis of the chromosomal DNA amplified by PCR using RecA-KO-F1 and RecA-KO-R2 primers. Then, the 2-D GE experiment was performed as described in paragraph 2.2.2.7. DNA samples containing four *ter* loci were extracted from a single culture of cells as described in paragraph 4.3.1. Resulting chromosomal fragments were separated using 2-D GE and visualised by Southern blotting using corresponding probes for each *ter*.

5.4.2 RecA protein is not required for UvrD to act at the *terC* site in the terminus

Quantification of arrested replication forks in each *ter* loci of Δ*recA* and Δ*recA* Δ*uvrD* strains is shown in Figure 5.7a. Normalisation was done as described in 3.3.4. In the absence of RecA, the strength of the replication arrest signal was strikingly different from what has been observed for other strains in this work. In the left replichore the arrest efficiency of *terC* and *terB* sites were nearly identical, with slightly higher signal in the *terB* locus. The signal intensity of the Y-spot at the *terA* was similar to that at *terC* and *terB*, whereas at *terD* it was markedly weaker. In contrast, in the Δ*recA* Δ*uvrD* strain, the degree of fork arrest was the greatest at the innermost *ter* sites in each replichore. Interestingly, the signal intensity of the Y-spot at *terC* of the Δ*recA* Δ*uvrD* strain was weaker than in *recA*$^+$ Δ*uvrD*, but the opposite is true for the signal intensity at *terA,* suggesting that a greater proportion of counter clockwise-moving replication forks reach the more distal *ter* site before the opposite fork arrives in the terminus in the *recA*$^+$ Δ*uvrD* mutant.

Absolute values of Y-spot signals were normalised by calculating the contribution of each arrest site in the total sum of all four *ter* sites in the terminus in percentage. Normalised distribution of arrested fork signal across four *ter* sites is shown in Figure 5.7b. In Δ*recA* Δ*uvrD* cells the signal intensity at *ter* sites in the left replichore was drastically different and was 10-fold greater at the *terC* than *terB* compared to nearly same in Δ*recA* alone. Similarly, the signal intensity of arrested forks in the right replichore revealed a notable shift from the 3-fold difference between *terA* and *terD* in Δ*recA* cells to the 10-fold fold difference in the Δ*recA* Δ*uvrD* cells.

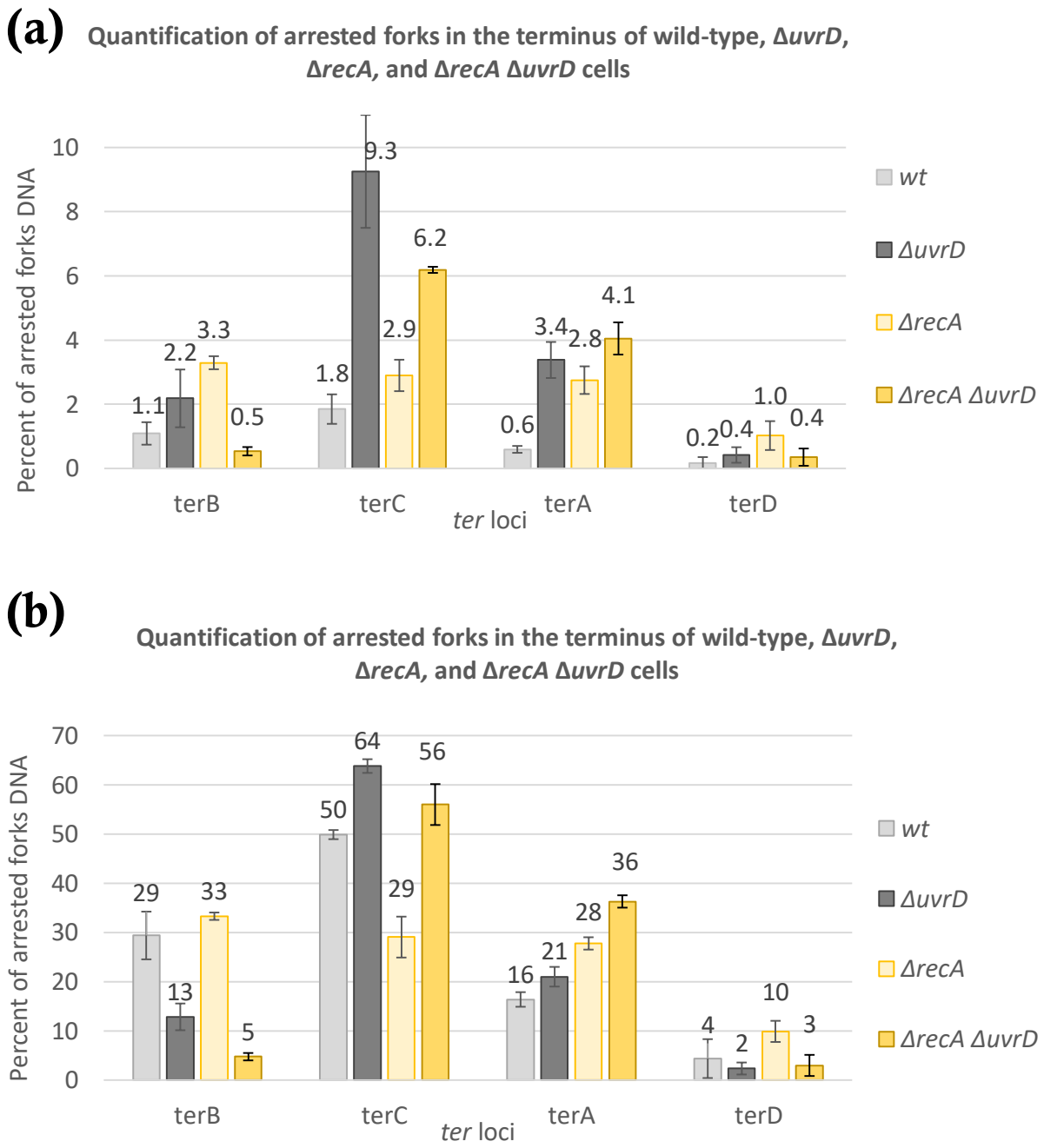

Figure 5.7

Quantification of arrested replication forks in the terminus of Δ*recA* and Δ*recA* Δ*uvrD* strains. **(a)** Percent of arrested forks relative to the total DNA signal at each *ter* site. The calculation is done as described in Figure 4.1. **(b)** Distribution of arrested forks across the terminus. Normalisation is done as described in Figure 4.5. The average of three repeats is shown. Error bars represent the standard deviation of the distribution.

The data presented here reveal frequent replication fork bypass of Tus/*terC* and less frequent, but substantial, at Tus/*terA* in the *recA*$^{-}$ cells. Furthermore, in the absence of RecA the proportion of replication forks arrested at the secondary *ter* site is higher than that observed in *recA*$^{+}$ cells (Figure 5.6-b), indicating that RecA is not required for UvrD mediated bypass of *terC* and *terA*.

5.4.3 Limited access of the UvrD helicase to the barrier formed by the *terB* sequence.

In the study of the replication fork bypass of ectopic *ter* sites, the *terB* sequence was used to determine the pathway the UvrD helicase utilises to elicit the block (Bidnenko, Lestini and Michel, 2006). In previous paragraphs, it was demonstrated that the *terC* sequence in the *terC* locus establishes an equally efficient Tus/*ter* barrier as the *terB* sequence in the absence of UvrD (paragraph 5.2.3). However, the amount of arrested replication forks at the following *ter* site was lower if the first sequence was *terB*. The latter observation suggests that UvrD interacts differently with barriers formed by *terC* and *terB*. If UvrD cannot access the Tus/*terB* barrier as easily as Tus/*terC*, then no appreciable difference in the distribution of arrested replication fork signal should be detected between *uvrD*$^{+}$ *terC→terB* (Figure 3.8b) and Δ*uvrD terC→terB* (Figure 5.2b). To test if the UvrD helicase can facilitate the replication fork bypass of the Tus/*terB* in the terminus, replication fork intermediates in the terminus region of *uvrD*$^{+}$ *terC→terB* DL6505 and Δ*uvrD terC→terB* DL6685 strains were visualised and analysed. DNA samples containing four *ter* loci were extracted from a single culture of cells as described in paragraph 4.3.1. Resulting chromosomal fragments were separated using 2-D GE and visualised by Southern blotting using corresponding probes for each *ter* locus. Quantification of arrested replication forks in *ter* loci of *uvrD*$^{+}$ *terC→terB* and Δ*uvrD terC→terB* strains is shown in Figure 5.8-a.

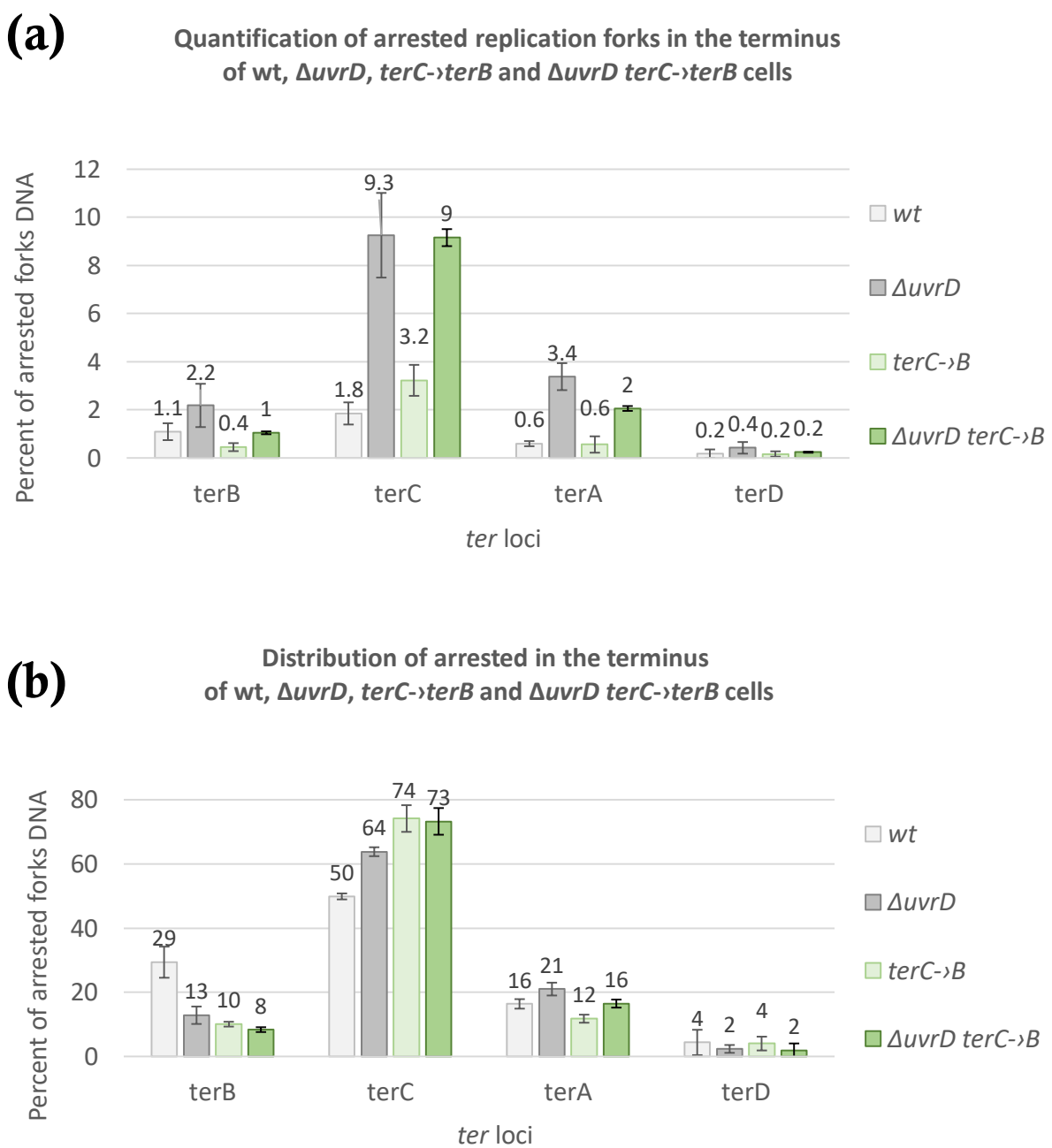

Figure 5.8

Quantification of arrested replication forks in the terminus of *uvrD*$^{+}$ *terC-›terB* and Δ*uvrD terC-›terB* strains. For the *uvrD*$^{+}$ and Δ*uvrD* strains data from Figure 4.4 and Figure 5.6 was used, respectively. **(a)** Percent of arrested forks relative to the total DNA signal at each *ter* site. The calculation is done as described in Figure 4.1. **(b)** Distribution of arrested forks across the terminus. Normalisation is done as described in Figure 4.5. The average of three repeats is shown. Error bars represent the standard deviation of the distribution.

Y-spot signal intensity at *terC* and *terB* loci of both strains was as previously reported in paragraphs 3.4.3 and 5.2.3 (compare Figure 3.8 and Figure 5.2b with Figure 5.8a). In the absence of UvrD, the strength of the replication arrest signal was almost three times greater at *terA*, *terB* and *terC* sites than in the *uvrD*$^{+}$ strain. Arrested replication forks were localised predominantly in the left replichore consistent with the proximity of *terC* and *terB* to the chromosomal midpoint where *oriC*-initiated replication forks are expected to meet. Absolute values of Y-spot signals were normalised by calculating the contribution of each arrest site in the total sum of all four *ter* sites in the terminus in percentage. Normalised distribution of the arrested fork signal revealed that the presence of UvrD in the *uvrD*$^{+}$ *terC-›terB* strain does not siginificantly change the proportion of termination at the first and second *ter* in the left replichore Figure 5.8-b. This strongly correlates with the observed decrease of the signal strength at *terB* in Δ*uvrD* and Δ*recA* strains when compared with that in *uvrD*$^{+}$ and Δ*recA uvrD*$^{+}$ strains (see Figure 5.7b). Interestingly, the similar, albeit weaker, effect was observed in the right replichore at *terA* and *terD* site, suggesting that the UvrD helicase has more limited access to the Tus/*terA* barrier.

5.4.4 Role of the 7th nucleotide and flanking regions of *ter* in the replication fork bypass of Tus/*terC*.

The observed difference in the interaction between the UvrD helicase and Tus/*terB* and Tus/*terC* barriers demonstrates that the *ter* sequence is critical for the frequency of UvrD-mediated replication fork bypass. 23 nt *ter* sequence consists of the 14 nt consensus sequence and two variable flanking regions (Figure 5.9). DNA sequence alignment of four *ter* sites of the terminus region reveals key differences between the *terC* and *terB* sequence in all three regions. Three nucleotides in the 2nd, 3rd and 4th positions in the non-permissive flanking

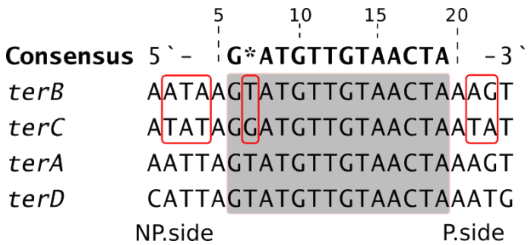

Figure 5.9

DNA sequence alignment of *ter* sites in the terminus region of the *E. coli* chromosome. The consensus sequence of all *ter* sites identified in the *E. coli* K-12 DL1777 chromosome is shown in bold. Nucleotides of the conserved motif are inside the grey rectangle. Nucleotide position within *ter* sequences is shown above. Regions that are different between *terC* and *terB* are marked with red rectangles. NP.side and P.side indicate non-permissive and permissive side of *ter* sequences.

region, one nucleotide at position 7, within the conserved region, and two nucleotides at position 21-22, in the permissive flanking region, are different. In order to determine whether any of the identified differences in the sequence contribute to the observed variability in the UvrD-dependent replication fork bypass, mutants in the *ter* sequence of the *terC* locus of the wild type and Δ*uvrD* strains were constructed.

First, pTOF24 plasmids carrying the desired *terC* locus mutation were constructed as described in paragraph 2.2.1.5 using the appropriate primer pairs to generate *terC*[G7T] (7th nucleotide of *terC* was replaced with that of *terB*), *terC*›*terB*[T7G] (vice versa, i.e. 7th nucleotide of *terB* was replaced with that of *terC*), *terC*[NP.fl-B] (non-permissive flanking region of *terC* was replaced with that of *terB*), *terC*[P.fl-B] (permissive flanking region of *terC* was replaced with that of *terB*), *terC*›*terB*[NP.fl-C] (non-permissive flanking region of *terB* was replaced with that of *terC*), *terC*›*terB*[P.fl-C] (permissive flanking region of *terB* was replaced with that of *terC*) inserts (Figure 5.10). Then, the resulting plasmids were used to transform the wild type

DL6504 and Δ*uvrD* DL6643 strain and introduce the desired *ter* mutation using the PMGR method (2.2.1.5). Successful introduction of *ter* mutations in the *terC* locus was confirmed by gel electrophoresis migration analysis of chromosomal DNA generated by PCR using yneEter - F1 and uxaBter - R2 primers.

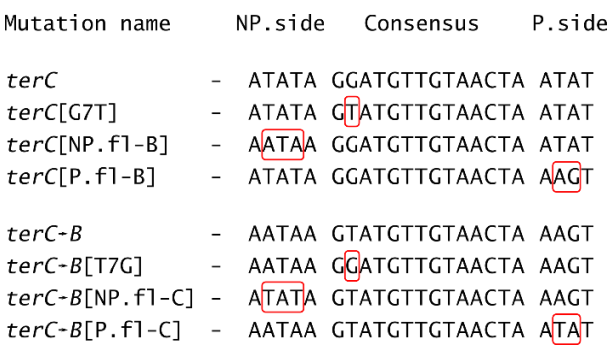

Figure 5.10

DNA sequence alignment of *terC* mutations in the *terC* locus of the *E. coli* chromosome. Non-permissive (NP.) and permissive (P.) sides and consensus region with a single spacing between. Mutated nucleotides are marked with red rectangles.

To determine the effect introduced mutations have on the replication fork bypass in the *terC* locus, replication fork intermediates in the terminus region of constructed strains were visualised and analysed. DNA samples containing four *ter* loci were extracted from a single culture of cells as described in paragraph 4.3.1. Resulting chromosomal fragments were separated using 2-D GE and visualised by Southern blotting using corresponding probes for each *ter* locus.

First, the effect of the 7th nucleotide in the conserved region of *ter* on the UvrD-dependent replication fork bypass of Tus/*terC* and Tus/*terB* in the *terC* locus was determined. If the 7th nucleotide is important for the interaction between UvrD and Tus/*ter*, the mutation in the 7th nucleotide of *terC* should result in the weaker arrested fork signal in the secondary *ter* locus, *terB*. The opposite is expected in the strain in which the 7th nucleotide of the *terB*

sequence in the *terC* locus was changed. Quantification of arrested replication forks in *ter* loci of wild type DL6504 and *terC*[G7T] DL7935 strains is shown in Figure 5.11. Normalisation was done as described in 3.3.4. The strength of the arrested fork signal detected in the left replichore in the *terC*[G7T] DL7935 strain was comparable to that in the wild-type strain. Weaker signal at the Tus/*terC* was not significantly different from that of the wild-type. (Student's paired t-test, with a two-tailed distribution; P value was 0.4; two values are considered different if $P<0.05$). Similarly, no difference in the signal strength of Y-spots at *terC* and *terB* of *terC-›terB* DL6505 and *terC-›terB*[T7G] DL7936 strains was observed (Figure 5.12). Obtained data clearly indicate that the 7th nucleotide in the conserved region of *ter* is not important for the UvrD-dependent replication fork bypass of Tus/*ter* in the *terC* locus.

(a)

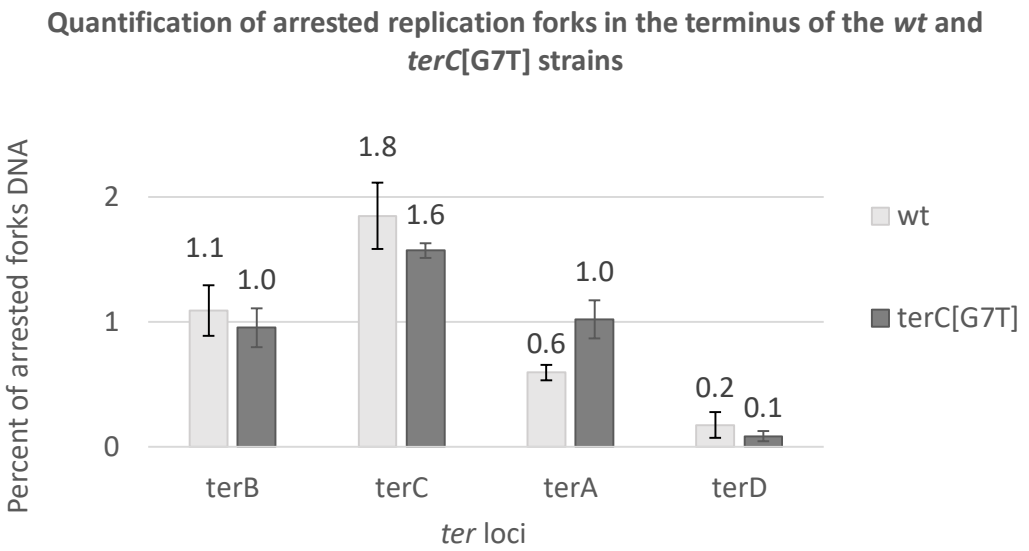

(b)

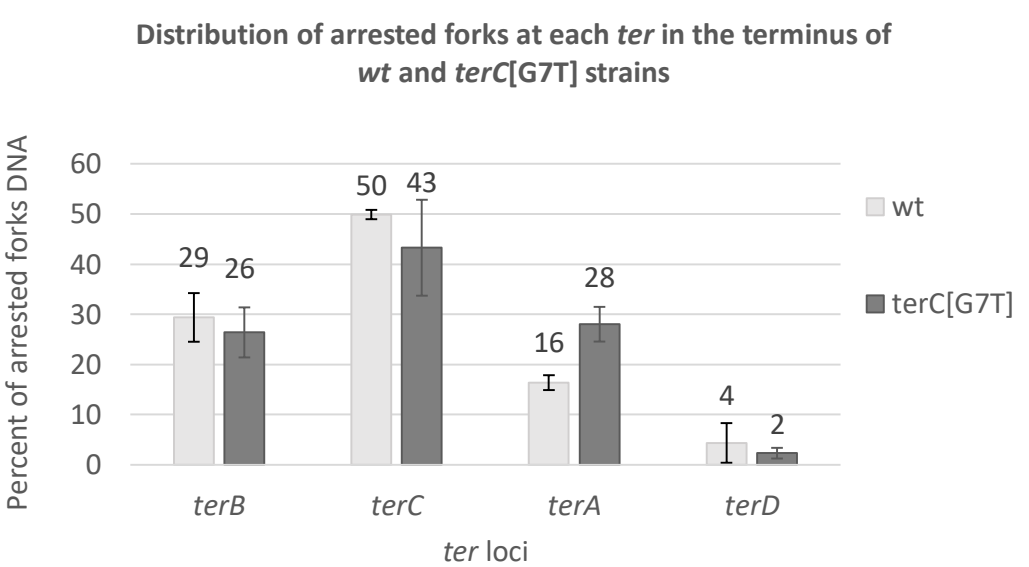

Figure 5.11

Quantification of arrested replication forks in the terminus of wild-type DL6504 and *terC*[G7T] DL7935 strains. **(a)** Percent of arrested forks relative to the total DNA signal at each *ter* site. The calculation is done as described in Figure 4.1. **(b)** Distribution of arrested forks across the terminus. Normalisation is done as described in Figure 4.5. The average of three repeats is shown. Error bars represent the standard deviation of the distribution.

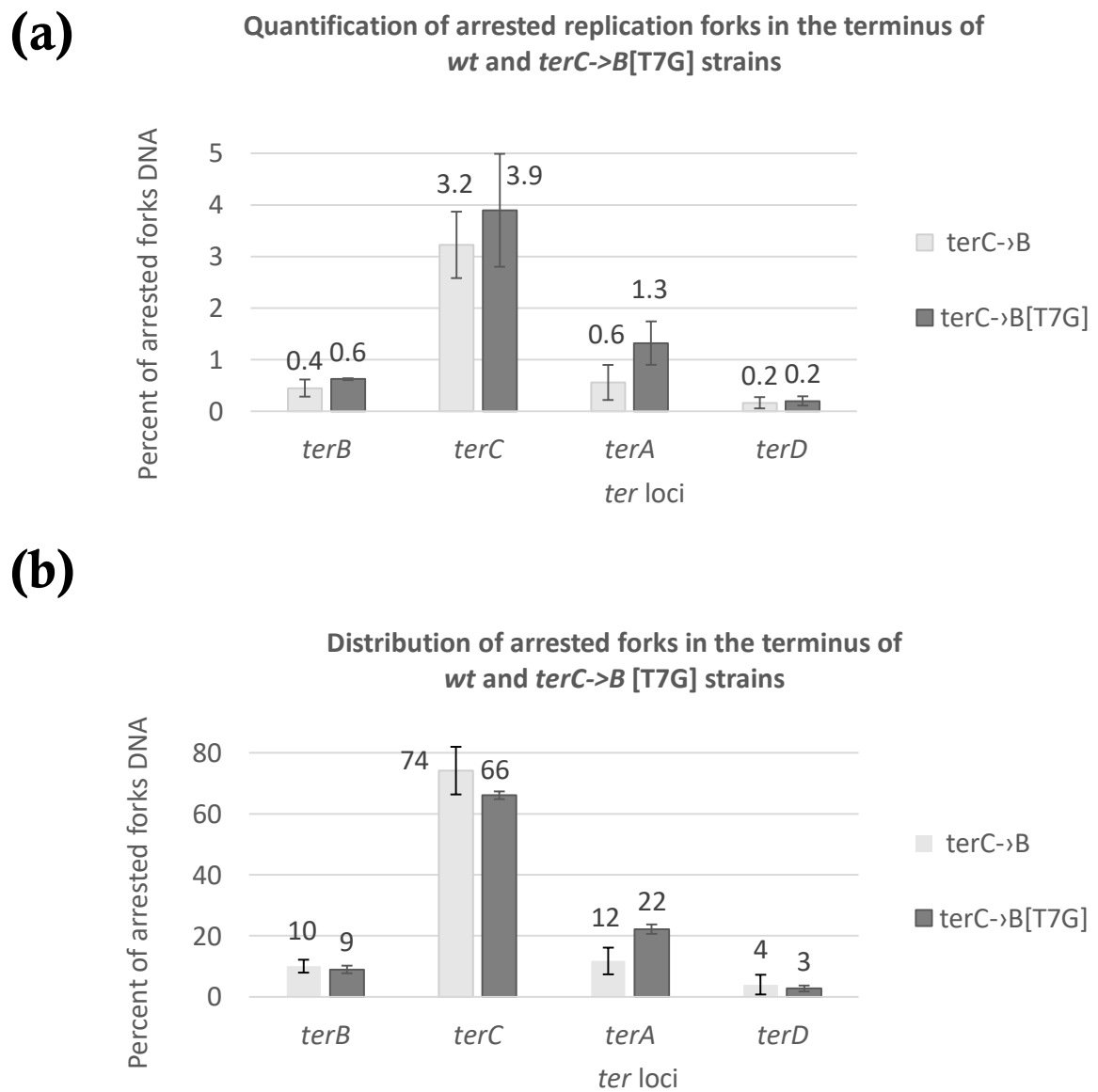

Figure 5.12

Quantification of arrested replication forks in the terminus of *terC->terB* DL6505 and *terC->terB*[T7G] DL7936 strains. **(a)** Percent of arrested forks relative to the total DNA signal at each *ter* site. The calculation is done as described in Figure 4.1. **(b)** Distribution of arrested forks across the terminus. Normalisation is done as described in Figure 4.5. The average of three repeats is shown. Error bars represent the standard deviation of the distribution.

To determine whether flanking regions of *ter* are important for the UvrD-dependent replication fork bypass of Tus/*ter* in the *terC* locus, quantification of arrested replication forks in *ter* loci of *terC*[P.fl-B], *terC*[NP.fl-B], Δ*uvrD terC*[P.fl-B] and Δ*uvrD terC*[NP.fl-B] was performed and presented in Figure 5.13-a. Normalisation was done as described in 3.3.4. The signal strength Y-spots in the *terC* locus was similar to the wild type strain in $uvrD^{+}$ strains. In the absence of UvrD, the signal was expectedly high at *terC*, as was shown for the Δ*uvrD* DL6643 strain in 5.2.2. This demonstrates that flanking regions do not affect the efficiency of replication arrest of the Tus/*terC* barrier in the *terC* locus.

Absolute values of Y-spot signals were normalised by calculating the contribution of each arrest site in the total sum of all four *ter* sites in the terminus in percentage and the resulting values are shown in Figure 5.13-b. Normalised distribution of the arrested fork signal revealed a dramatic change in the signal strength difference between *terC* and *terB* of the *terC*[NP.fl-B] strain. The distribution of arrested replication forks in the left replichore of the *terC*[P.fl-B] strain was identical to that of the wild strain. Conversely, the distribution of arrested forks in the *terC*[NP.fl-B] strain was similar to that of Δ*uvrD* strains. Expectedly, in both Δ*uvrD* strains, 10-fold difference between the arrested fork signal strength at *terC* and *terB* was observed that correlated with the distribution of arrested forks in the terminus shown earlier for Δ*uvrD* mutation (paragraph 5.3.3).

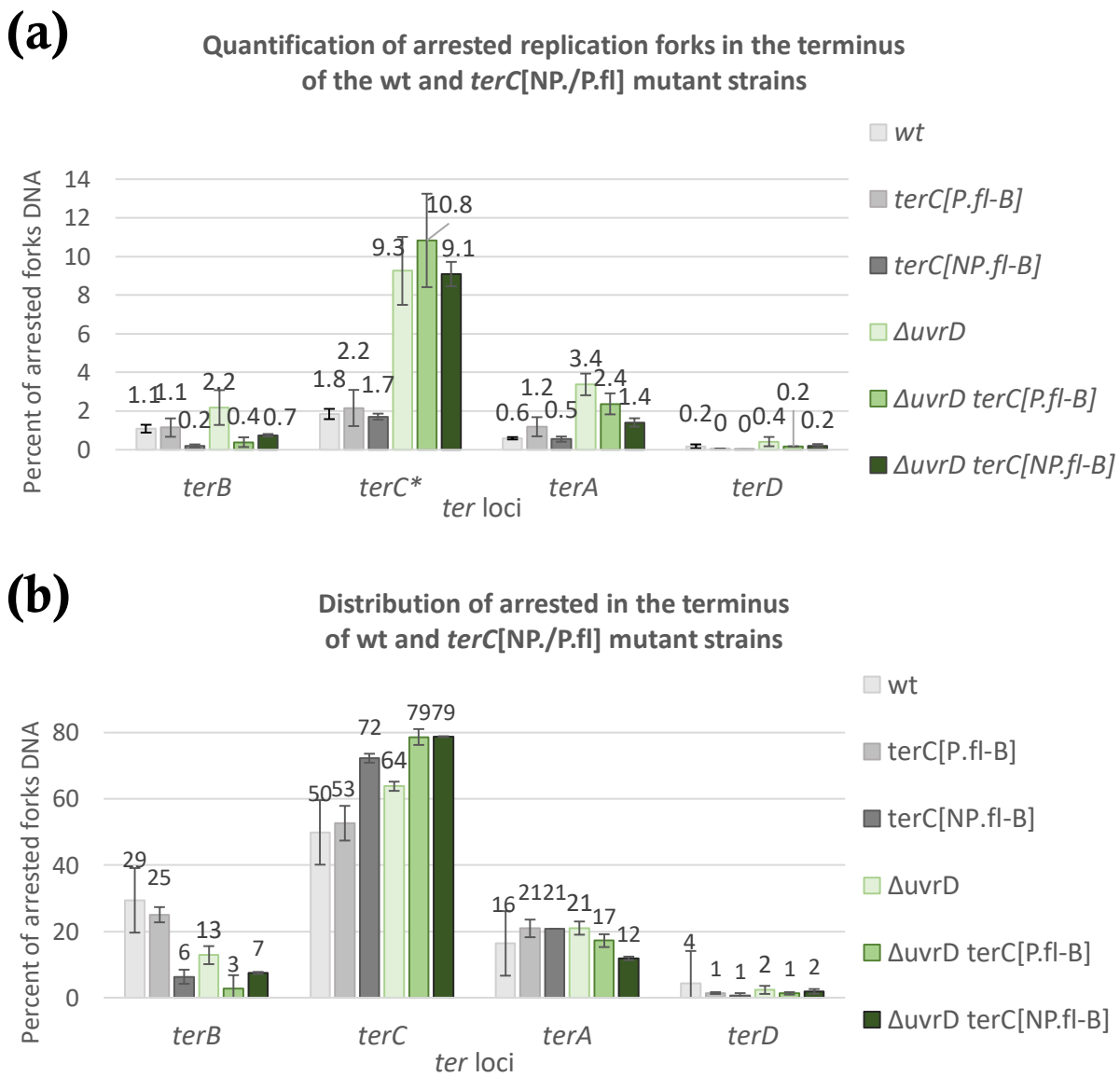

Figure 5.13

Quantification of arrested replication forks in the terminus of *terC*[P.fl-B], *terC*[NP.fl-B], Δ*uvrD* *terC*[P.fl-B] and Δ*uvrD* *terC*[NP.fl-B] strains. **(a)** Percent of arrested forks relative to the total DNA signal at each *ter* site. The calculation is done as described in Figure 4.1. For the Δ*uvrD* DL6643 strain data from Figure 5.6 was used. **(b)** Distribution of arrested forks across the terminus. Normalisation is done as described in Figure 4.5. The average of three repeats is shown. Error bars represent the standard deviation of the distribution.

In addition, to test whether similar mutations in flanking regions of the *terB* sequence are important for the UvrD-dependent replication fork bypass of Tus/*terC-›B* in the *terC* locus, quantification of arrested replication forks in *ter* loci of *terC-›terB*[P.fl-C], *terC-›terB*[NP.fl-C], Δ*uvrD terC-›terB*[P.fl-C] and Δ*uvrD terC-›terB*[NP.fl-C] strains was performed and presented in Figure 5.14-a. Normalisation was done as described in 3.3.4. The efficiencies of replication fork arrest at *ter* sites were as observed earlier for *uvrD*$^{+}$ and Δ*uvrD* strains, except for the *terC-›terB*[NP.fl-C] that had dramatically weaker Y-spot signals at *terC* and *terA* sites in a Δ*uvrD*$^{+}$ background. Absolute values of Y-spot signals were normalised as explained in the previous paragraph, and the resulting values are shown in Figure 5.14-b. Normalised distribution of the arrested fork signal revealed a dramatic change in the signal strength difference between *terC* and *terB* of the *terC-›terB*[NP.fl-C] strain. This correlates with a similar dramatic change observed when the non-permissive flanking region was changed in the *terC*[NP.fl-B] strain. Taken together, presented data demonstrate the critical role of the non-permissive flanking region in mediating the UvrD-dependent replication fork bypass of the Tus/*ter* barrier in the *terC* locus.

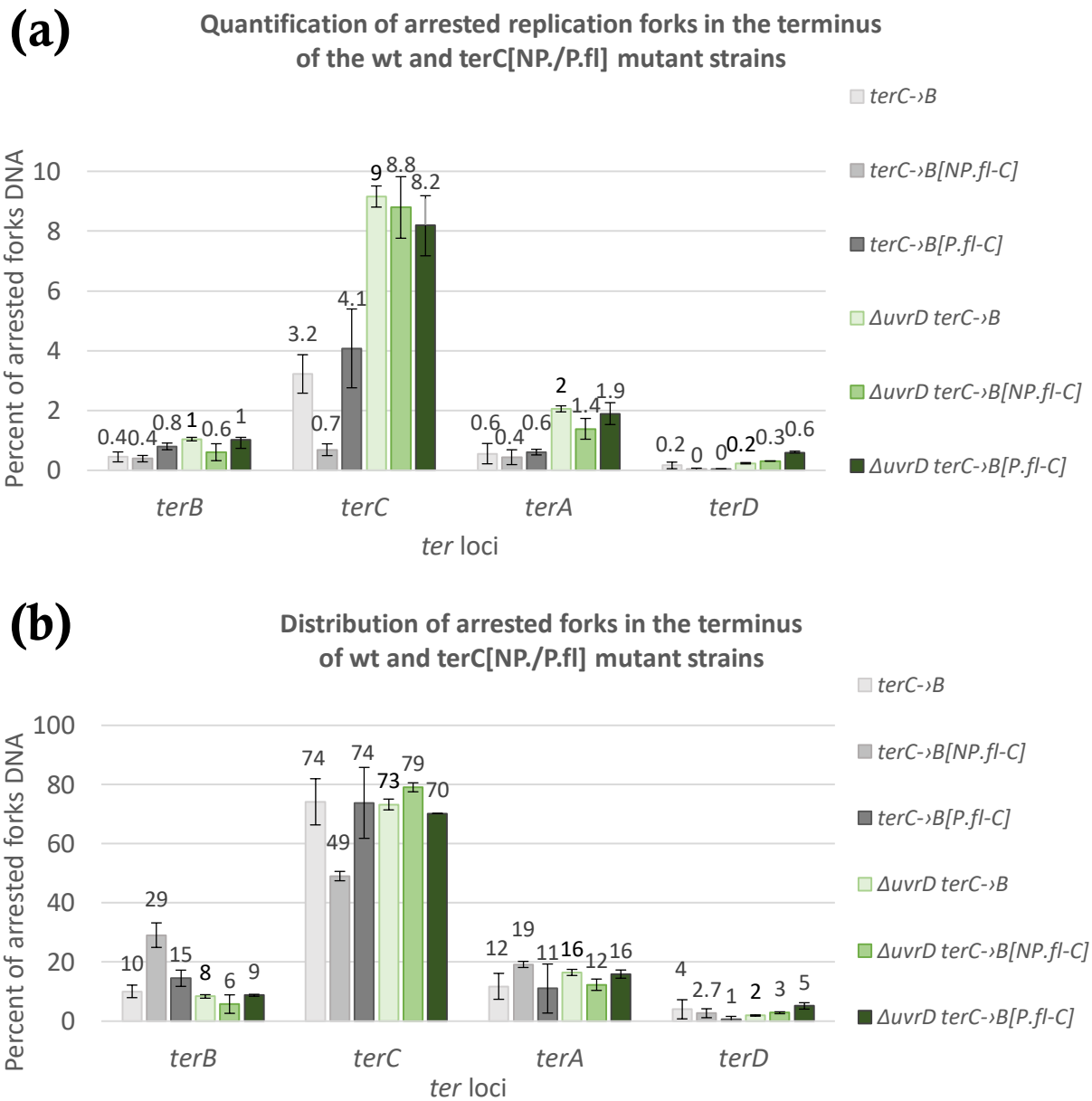

Figure 5.14

Quantification of arrested replication forks in the terminus of *terC-›terB*[P.fl-C], *terC-›terB*[NP.fl-C], Δ*uvrD terC-›terB*[P.fl-C] and Δ*uvrD terC-›terB*[NP.fl-C] strains. **(a)** Percent of arrested forks relative to the total DNA signal at each *ter* site. The calculation is done as described in Figure 4.1. For the Δ*uvrD terC-›terB* DL6685 strain data from Figure 5.6 was used. **(b)** Distribution of arrested forks across the terminus. Normalisation is done as described in Figure 4.5. The average of three repeats is shown. Error bars represent the standard deviation of the distribution.

5.5 Discussion

In this chapter, 2-D GE method was used to study the replication fork bypass of the Tus/*ter* barrier in the *terC* locus and the role of the UvrD helicase in mediating this process. It was previously shown that the terminus over-replication associated with the absence of RecG is not limited by the *terC* site, but is terminated predominantly at the second *ter* site, *terB*, in the left replichore (Rudolph *et al.*, 2013; Wendel, Courcelle and Courcelle, 2014). Based on the study of the replication fork bypass of an ectopic Tus/*terB* barrier that indicated that UvrD can elicit bypass of the barrier ahead of the fork (Bidnenko, Ehrlich and Michel, 2002), it was hypothesized that in the absence of RecG and UvrD the majority of clockwise-moving replication forks in the terminus should be arrested in the *terC* locus. In the work presented here, the signal strength of the Y-spot in *terC* and *terB* loci in Δ*uvrD* Δ*recO* Δ*recG* cells indicated that replication was arrested predominantly at the first *ter* site, *terC*, instead of *terB* when compared with that in Δ*recG* cells. The majority of replication forks in the terminus in the absence of RecG were shown to be of non-*oriC* origin and generated as a result of backwards-initiated DNA synthesis at *ter* sites (Azeroglu *et al.*, 2016) and pathological events associated with the head-on collision of replisomes (Rudolph *et al.*, 2013; Wendel, Courcelle and Courcelle, 2014). The dramatic shift in the frequency of the non-*oriC* replication fork bypass of Tus/*terC* in Δ*uvrD* Δ*recO* Δ*recG* cells suggests that UvrD can frequently access repair-initiated forks or be permanently associated with them to facilitate replication across DNA-bound proteins.

Under normal conditions, a greater proportion of arrested forks at *ter* sites in the terminus of the Δ*uvrD* strain was detected in comparison with the wild type strain. The signal strength was approximately five times greater at two innermost *ter* sites, *terC* and *terA*, and

only two times greater at secondary sites, *terB* and *terD*. This could be explained by the presence of non-*oriC* initiated replication forks. Alternatively, discoordination of *oriC*-originated replication forks can also cause elevated accumulation of arrested forks at *ter* sites, as fewer replisomes would fuse before reaching a Tus/*ter* barrier. Marker frequency analysis (MFA) of the terminus region of Δ*uvrD* cells showed no noticeable level of over-replication when compared to *uvrD*$^{+}$ cells (Hasan, personal communication), suggesting no noticable change in the number of non-*oriC* replication forks in the terminus. Furthermore, the presence of non-*oriC* replication forks in the terminus was shown to skew the distribution of the fork arrest signal between the left and right replichore towards the 50:50 ratio as was shown for the Δ*recG* strain. However, this was not the case in Δ*uvrD* strains, for which the distribution of arrested forks in the terminus was determined and had approximately 80% of forks arrested at *terC* and *terB* sites in the left replichore and the remaining 20% of forks arrested at *terA* and *terD*. The 80:20 ratio is characteristic of the bidirectional replication from *oriC* as was shown for the wild type strain. These findings suggest that the observed increase of the fraction of arrested forks in the terminus is caused predominantly by *oriC*-originated replication forks that failed to fuse before reaching a Tus/*ter* barrier.

In chapters 3 and 4 it has been demonstrated that in the wild-type and Δ*recG* strains the degree of fork arrest at Tus/*ter* depends on the *ter* sequence, with the *terB* sequence arresting greater proportion of forks than *terC*. Therefore, it was expected that in Δ*uvrD* cells the arrested fork signal at the *terB* sequence in the *terC* locus would be stronger than that at *terC* in the *terC* locus. Surprisingly, no notable difference in the degree of fork arresting activity was observed in the Δ*uvrD* strains between *terC* and *terB* sequences in the *terC* locus (Figure 5.2a and b). Also, placing the first *ter* site clockwise-moving replication forks encounter from the non-

permissive side 74 kb further away from the middle point of the chromosome did not change the level of fork arresting activity of *terC* and *terB* sequences appreciably (Figure 5.2c and d). Therefore, in the absence of UvrD, Tus/*terC* and Tus/*terB* barriers arrest a similar proportion of replication forks relative to the total amount of DNA in the locus. These data suggest that the UvrD helicase is the key player that determines the observed difference in the replication arresting activity of *ter* sequences and it has a varying degree of access to replication forks at Tus/*ter* barriers in the terminus.

It has been demonstrated that UvrD can access replication forks arrested at an ectopic Tus/*terB* barrier and facilitate the block bypass, but only as a consequence of RecA-mediated homologous recombination initiated upon the arrival of replisomes of the second round of replication to the blocked fork (Bidnenko, Lestini and Michel, 2006). Consequently, DnaB run-off occurs at one of the two re-established forks as they approach Tus/*terB*, allowing UvrD to access DNA ahead of the polymerase. Therefore, if homologous recombination is required for the UvrD helicase to help bypass of arrested replication forks in the terminus, then in the absence of RecA, replication arrest should take place primarily at the innermost *ter* site in each replichore. Analysis of the distribution of arrested forks in the terminus of the Δ*recA* strain revealed that a considerable percentage of replisomes reaches secondary *ter* sites, *terB* and *terD*. Therefore, it can be concluded that RecA-mediated homologous recombination is not required in order for UvrD to facilitate replication fork bypass of innermost *ter* sites and the helicase may utilise a different pathway or directly access arrested forks at endogenous Tus/*ter* barriers. Interestingly, the ratio of arrested fork signal between two replichores in the Δ*recA* strain was similar to that in Δ*recG*, as only about 60% of the total arrested fork signal was localised in the left replichore, and the remaining 40% was distributed between *ter* sites

in the right replichore. This is unexpected, as, unlike Δ*recG*, Δ*recA* mutation is not associated with the DNA over-replication in the terminus (Midgley-Smith *et al.*, 2018), suggesting that the distribution of arrested forks is skewed less towards the left replichore in recombination deficient cells.

It has been demonstrated that in the left replichore the degree of fork pausing at the secondary *ter* site, *terB*, decreases when the first *ter* sequence, *terC*, is replaced with *terB* in both Δ*uvrD* and *uvrD*$^{+}$ strains (Figure 3.8b and Figure 5.2b). This observation implied that UvrD interacts differently with Tus/*terC* and Tus/*terB* barriers. The distribution of arrested replication forks in the terminus of *uvrD*$^{+}$, *uvrD*$^{+}$ *terC*→*terB* and Δ*uvrD terC*→*terB* strains (Figure 5.8) demonstrated that the replication fork bypass frequency of the Tus/*terB* in the *terC* locus is identical in presence or absence of UvrD and is notably lower than that of Tus/*terC*. These data confirmed that the fork bypass of the Tus/*terB* in the *terC* locus is mediated by the UvrD helicase differently from Tus/*terC* in the *terC* locus.

Comparison of the *terC* and *terB* sequence revealed differences in the permissive and non-permissive flanking regions and a single nucleotide difference in the conserved region at the 7th position. In the *terB* sequence, the 7th nucleotide's pyrimidine base was shown to have a stacking interaction with the phenyl ring of F140 residue and play a role in the formation and maintenance of the locked state of the Tus/*ter* complex (Berghuis *et al.*, 2015). In contrast, *terC* has a purine base in the 7th position that could be less efficient in establishing the stacking interaction with F140 of the Tus protein. Surprisingly, changing the 7th nucleotide of the *terC* sequence to that of the *terB* sequence and vice versa did not confer a different frequency of replication progress through Tus/*ter* in the *terC* locus, suggesting that the 7th nucleotide is not important for the UvrD-mediated Tus/*terC* replication fork bypass. Neither non-permissive

nor permissive regions of *ter* interact with Tus, as shown in the crystal structure studies of the Tus/*terB* complex (Mulcair *et al.*, 2006). Unexpectedly, analysis of the distribution of arrested forks in the terminus in *terC*[NP.fl-B] and *terC*→*terB*[NP.fl-C] strains revealed that the non-permissive flanking region is important for the UvrD-mediated fork bypass. When the flanking region (5`-ATATA-3`) of the *terC* sequence in the *terC* locus was replaced with that of the *terB* (5`-AATAA-3`), the distribution of arrested fork signal in the *terC*[NP.fl-B] strain was identical to that of the *terC*→*terB* strain, whereas the opposite effect was observed in the *terC*→*terB*[NP.fl-C] strain that was shown to be identical to the wild type strain (compare Figure 5.13 and Figure 5.14). A potential explanation of the observed effect of these nucleotide substitutions is that stacking interactions between repeating A bases in the flanking region of the *terB* sequence prevent efficient loading of UvrD ahead of the arrested replication fork. UvrD requires eight nucleotide-long DNA fragment on the leading strand to bind and translocate along the DNA ahead of the fork (Tomko *et al.*, 2010), whereas stalled replication forks were shown to stop three nucleotides away from the blocking protein (Xu and Dixon, 2018). Consequently, the five nucleotide-long flanking region of *ter* sequences together with three nucleotides before the stalled fork provide a sufficiently large DNA region for the UvrD to bind. Recent studies of the thermal stability of the DNA double helix provided experimental evidence for the importance of Van der Waals forces that mediate stacking interactions between bases for the DNA duplex rigidity and showed that greater force is required to unpair DNA strands with repeating nucleotides (Krueger, Protozanova and Frank-Kamenetskii, 2006; Yakovchuk, Protozanova and Frank-Kamenetskii, 2006; Zhang *et al.*, 2015).

6 GENERAL DISCUSSION

Two-dimensional gel electrophoresis technique is a powerful tool that allows the structural characteristics of replication intermediates corresponding to specific DNA loci to be differentiated and visualised. The quantitative analysis of the observed data provides a unique opportunity to study replication related processes in detail. The aim of this thesis was to utilise this powerful method to investigate Tus-*ter* mediated termination of DNA replication and the role of the UvrD helicase in this process.

In the *E. coli* chromosome, in total 14 *ter* sites (*terA-L*, *terY* and *terZ*) have been identified using bioinformatic analysis and these are located predominantly in the left and right macrodomains and the terminus. The arrangement of *ter* sites possessed a certain degree of symmetry that has been puzzling researchers ever since their discovery. The significance of having the replication fork trap spread across more than half of the chromosome is still poorly understood.

In 2009 Duggin and Bell investigated the presence of arrested replication forks at all *ter* sites in *E. coli* cells grown in minimal media (Duggin and Bell, 2009). They detected paused replication forks at seven out of fourteen *ter* sites, four of which were localised in the terminus region, *terA-D*, while the remaining three were in the neighbouring left and right chromosome macrodomains. They concluded, that replication forks generally meet at the innermost *ter* sites, *terC* and *terA*, and less frequently at the *terB*, and the biological role of the remaining *ter* was yet to be determined. In this work arrested replication forks intermediates at *terA-D* sites of the terminus region were characterised in detail and precise quantification of these structures was performed in cells grown in rich media.

Visualised replication intermediates at *ter* sites in the terminus showed the presence of arrested replication forks not only at the innermost *ter* sites, *terC* and *terA*, but at secondary *ter* sites, *terB* and *terD* in both replichores. Clockwise-moving replication forks formed Y-spots at *ter* sites in the left replichore, whereas counter clockwise-moving forks were arrested in the right replichore. This correlates with the replication fork trap hypothesis and arrested forks at terminus *ter* sites demonstrated by Duggin and Bell in 2009. The data in this thesis also confirm that Tus/*ter* complexes in the terminus pose a permeable rather than an absolute block to replisome progression under normal conditions. It is conceivable that *ter* sites may not always be occupied by Tus during replication. The overlap of *terB* and *tus* promoter sequences indicates that *tus* is transcribed after counter clockwise-moving replication fork removes Tus from the *terB* sequence (Natarajan, Kelley and Bastia, 1991; Roecklein, Pelletier and Kuempel, 1991; Neylon *et al.*, 2005). Zhou and colleagues demonstrated that the transcript level of *tus* did not change significantly during the cell cycle in synchronised cells, although the level could be too low to detect the change (Zhou *et al.*, 1997). However, the endogenous Tus concentration was shown to be between 20 and 100 nM (Natarajan *et al.*, 1993), which is 100 to 500 times higher than the K_d of Tus/*terA-D* complexes at 150 mM KCl (Moreau and Schaeffer, 2012). In that study the half-life of the Tus/*ter* barriers at *terA-D* sequences was estimated to be much longer than a single cell cycle. Therefore, these *ter* sites are likely to be bound by Tus throughout the entirety of the cell replication period.

Quantification of the signal formed by arrested replication forks at *ter* sites in the terminus indicated that under normal conditions most of clockwise-moving replisomes are trapped at the *terC* site. The pause signal at the *terB* site was twice weaker, whereas the pause signal at *terA* and *terD* together was almost three times weaker. Expectedly, the distribution

of replication forks between two replichores was uneven, with 80% of all arrested forks in the terminus detected in the left replichore and the remaining 20% in the right replichore. In order to reach *terA*, replication forks have to replicate 250 kb past the chromosome midpoint, which is equal to 5.5% of the total length of the chromosome, whereas *terC* and *terB* are only 4.2 and 78 kb away, respectively. Consequently, counter clockwise-moving replisomes are much more likely to fuse with the oppositely directed ones before reaching *terA* and *terD*. The obtained distribution of arrested replication forks correlates well with the location where *oriC*-initiated replisomes are expected to meet, suggesting that in fast-growing cells bidirectional replication can become discoordinated, but only in a small fraction of cells.

Extensive studies of Tus/*ter* complex thermodynamic and kinetic properties demonstrated substantial differences in the K_d and half-life of Tus/*terB* and Tus/*terC* complexes (Mulcair *et al.*, 2006; Moreau and Schaeffer, 2012) which correlated with the replication arrest activities of these sites in plasmid replication arrest experiments (Coskun-Ari and Hill, 1997; Duggin and Bell, 2009). In this study, I quantified replication fork arrest signal in strains with mutated *ter* sequences in *terC* and *terB* loci. The results obtained confirm that the Tus/*terB* complex has a greater replication arrest activity than Tus/*terC* when arranged to be the first Tus/*ter* barrier clockwise-moving replication forks encounter. The signal strength at the following Tus/*ter* barrier in the *terB* locus correlated with the strength of the *ter* sequence in the *terC* locus, suggesting different rates of the replication fork bypass of Tus/*terC* and Tus/*terB*. Therefore, the terminator site sequence determines not only the arresting activity of Tus/*ter* but also the frequency of Tus/*ter* bypass. Noteworthy, relocating the first *ter* site clockwise-moving forks encounter from the *terC* locus to the *terB* locus did not change the signal strength of the arrested forks, indicating that the proximity to the

chromosome midpoint does not influence the arresting activity of *terC* and *terB* sequences appreciably.

The observed permeability of the Tus/*terC* barrier in the terminus can be attributed to the action of accessory helicases in *E. coli* cells, as their primary function is to clear the path from physical obstacles ahead of replisomes. In experiments with ectopic *terB* sites introduced in the middle of each replichore in the orientation that blocks *oriC*-initiated replication, Bidnenko and colleagues demonstrated that cells require RecA and SOS-inducible helicase UvrD for viability (Bidnenko, Lestini and Michel, 2006). Furthermore, RecA-ChIP experiments conducted in our laboratory showed the presence of a strong chi-dependent RecA signal near the *terC* locus in the Δ*uvrD* Δ*recG* strain (also carrying an unknown mutation that suppressed Δ*uvrD* Δ*recG* lethality), whereas in the *uvrD*$^+$ Δ*recG* strain the signal at that position was very weak (Azeroglu et al., personal communication). This indicates the appearance of Tus/*ter*-dependent double-strand breaks, generated by replication forks arrested at Tus/*terC* in the absence of UvrD. 2-D GE experiments presented in this work demonstrated frequent replication fork bypass of the *terC* and *terB* sequence in the *terC* locus in the *uvrD*$^+$ Δ*recG* and *terC*›*terB uvrD*$^+$ Δ*recG* strains (Figure 4.6). The signal strength of arrested forks at *terA-D* sites of Δ*recG* strains was 5-25 times higher than in *recG*$^+$ strains which suggests the presence of additional replication forks in the terminus. These observations correlate with the increased number of sequence reads generated by non-*oriC* replication forks between *terA* and *terB*, but not between *terA* and *terC* (Rudolph *et al.*, 2013; Wendel, Courcelle and Courcelle, 2014; Azeroglu *et al.*, 2016). The efficiency of Tus/*ter* arresting activity in Δ*recG* strains further reinforces the hypothesis that Tus-*ter* system may have evolved specifically to arrest non-*oriC* initiated replication and prevent deleterious head-to-head replication-transcription collisions

and re-replication of the chromosome (Wendel *et al.*, 2017; Brochu *et al.*, 2018; Midgley-Smith *et al.*, 2018; Midgley-Smith, Dimude and Rudolph, 2019).

Deletion of *uvrD* gene in the Δ*recG* background renders cells inviable unless a suppressor mutation is introduced (Fonville *et al.*, 2010). To determine the role of UvrD in the fork bypass of the Tus/*terC* barrier in the absence of RecG, the Δ*recO* mutation was introduced to suppress Δ*uvrD* Δ*recG* lethality, and the resulting strain was used to quantify arrested replication intermediates in the *terC* and *terB* loci. The data obtained revealed that the UvrD helicase is indeed responsible for the observed replication fork bypass of the Tus/*terC* barrier in Δ*recG* strains. Interestingly, in *uvrD*$^{+}$ *recG*$^{+}$ cells 37%. of all forks arrested in the left replichore were detected in the *terB* locus, whereas in *uvrD*$^{+}$ Δ*recG* 67% were detected in the *terB* locus. The constitutively induced SOS response in Δ*recG* cells (Lloyd and Buckman, 1991; Asai and Kogoma, 1994; Ishioka, Iwasaki and Shinagawa, 1997) provides at least 2.5-fold increased rate of *uvrD* gene expression (George, Brosh and Matson, 1994; Courcelle *et al.*, 2001). Therefore, elevated number of UvrD molecules in Δ*recG* cells would make the helicase more readily available for assisting replication fork progress through Tus/*ter* barriers, explaining the observed discrepancy in the replication fork bypass frequency of the Tus/*terC* barrier between Δ*recG* and *recG*$^{+}$ strains.

The difference between *terC* and *terB* sequences in the degree of arresting activity initially observed in the wild-type and Δ*recG* strains was analysed in the Δ*uvrD* strains. Surprisingly, in the absence of UvrD, no notable difference in the fork arresting activity was observed between these sequences in the *terC* locus. These data suggest that the replication arrest efficiency of *ter* sites is largely dependent on the presence of the UvrD helicase and its ability to access blocked replisomes in the terminus. While it was shown that UvrD can unwind the

parental duplex of forked DNA substrates *in vitro* (Cadman, Matson and McGlynn, 2006; Atkinson *et al.*, 2009), in *E. coli* cells UvrD was unable to access replication forks arrested at ectopic Tus/*terB* barriers, unless RecA- and RecBCD-dependent homologous recombination was initiated at stalled forks (Bidnenko, Lestini and Michel, 2006). Consequently, UvrD appears to require a certain replication fork structure to bind the leading strand and unwind DNA ahead of the fork.

The ability of UvrD to facilitate replication fork progress through Tus/*ter* barriers in the terminus was tested in Δ*recA* and Δ*recA* Δ*uvrD* strains. Approximately half of arrested forks in the left replichore were detected in the *terB* locus of Δ*recA* cells, suggesting a relatively high frequency of the Tus/*terC* bypass in recombination deficient cells. In contrast, in the Δ*recA* Δ*uvrD* strain less than 10% of forks arrested in the left replichore were detected in the *terB* locus. It remains to be investigated how UvrD facilitates Tus/*ter* replication fork bypass in the terminus in the absence of RecA-mediated homologous recombination. It has been recently reported that Rep helicase monomers interact directly with DnaB monomers during DNA replication, suggesting that Rep monomers could be loaded by DnaB onto the leading strand ahead of the fork to clear the path whenever replisomes slows down before a DNA-bound protein (Guy *et al.*, 2009; Gupta *et al.*, 2013; Syeda *et al.*, 2019). UvrD and Rep share the directionality of DNA duplex unwinding and are likely to compete for the substrate at the replication fork (Veaute *et al.*, 2005; Tomko *et al.*, 2010; Yang, 2010; Brüning, Howard and McGlynn, 2014). However, no interaction between the replisome and UvrD has been reported, whereas Rep is recruited to the replisome by DnaB. Therefore, it is likely that UvrD is permitted to access replication forks only when DnaB is no longer present.

Interestingly, UvrD acts in concert with Pol III for rolling-circle replication of Gram-positive plasmids (Bruand and Ehrlich, 2000). Furthermore, UvrD was also copurified with the Pol III complex (Lahue, Au and Modrich, 1989), suggesting some degree of interaction between the helicase and replisome. It should be noted, that UvrD must be either in the oligomeric form or assisted by another protein, such as MutL, to be able to unwind DNA duplex (Ali, Maluf and Lohman, 1999; Maluf, Fischer and Lohman, 2003; Petrova *et al.*, 2015; Ordabayev *et al.*, 2018, 2019). It is tempting to speculate that UvrD is actively recruited to arrested replication forks in the absence of DnaB by the remaining components of the replication complex and is further assisted in initiating its dsDNA unwinding activity.

Finally, because UvrD was shown to mediate the replication bypass of Tus/*ter* and interact differently with *terC* and *terB*, mutational analysis of *terB* and *terC* nucleotide sequences was conducted to identify key differences that are critical for the interaction with UvrD. A single nucleotide substitution in the 7th position of the conserved region was shown to be present only in *terC* among *ter* sites in the terminus. However, despite its apparent significance in the formation of the locked state of the Tus/*ter* complex (Coskun-Ari and Hill, 1997; Berghuis *et al.*, 2015), no difference was revealed in the arrested fork distribution in the terminus when it was replaced with the 7th nucleotide of *terB*. Surprisingly, the non-permissive flanking region of *ter* was shown to be critical for the interaction of UvrD with Tus/*ter*. Five nucleotides of this region were not present in Tus crystal structures (Kamada *et al.*, 1996; Mulcair *et al.*, 2006), and except for the 5th nucleotide conserved across *terA-D*, thermodynamic and kinetic data revealed that nucleotides 1-4 provide no notable contribution to the Tus/*ter* barrier formation (Moreau and Schaeffer, 2013). A potential explanation of the observed difference between the non-permissive flanking region of *terC* (5`-ATATA-3`) and

that of *terB* (5`-AATAA-3`) is that stacking interactions in the *terB* flanking region increase the energy required to unwind the duplex due to the repeating A bases (Krueger, Protozanova and Frank-Kamenetskii, 2006; Zhang *et al.*, 2015). Alternatively, this may indicate yet undiscovered role of the first four nucleotides of *ter* in the Tus/*ter* complex biophysical properties *in vivo*.

Taken together, the results presented in this work suggest a distinct role of the UvrD helicase in the alleviation of replication fork stalling at the naturally occurring Tus/*terC* barrier in the chromosomal terminus. Replisome arrest at Tus/*ter* barriers can have deleterious effects on the genome stability if not resolved in time (Horiuchi and Fujimura, 1995; Bierne *et al.*, 1997; Azeroglu *et al.*, 2016). It is conceivable that the first Tus/*ter* barrier a replication fork encounters when escaping the terminus has been fine-tuned through evolution to exhibit partial arrest to help cells avoid potentially lethal consequences of prolonged fork stalling. This would also explain why there is more than one terminator site on each replichore in the terminus.

7 REFERENCES

Aguilera, A. and Gómez-González, B. (2008) 'Genome instability: a mechanistic view of its causes and consequences', *Nature Reviews Genetics*. Springer Science and Business Media LLC, 9(3), pp. 204–217. doi: 10.1038/nrg2268.

Ali, J. A. and Lohman, T. M. (1997) 'Kinetic Measurement of the Step Size of DNA Unwinding by Escherichia coli UvrD Helicase', *Science*. American Association for the Advancement of Science (AAAS), 275(5298), pp. 377–380. doi: 10.1126/science.275.5298.377.

Ali, J. A., Maluf, N. K. and Lohman, T. M. (1999) 'An oligomeric form of E. coli UvrD is required for optimal helicase activity 1 1Edited by D. E. Draper', *Journal of Molecular Biology*. Elsevier BV, 293(4), pp. 815–834. doi: 10.1006/jmbi.1999.3185.

Anderson, S. G. *et al.* (2007) 'A Function for the ψ Subunit in Loading theEscherichia coliDNA Polymerase Sliding Clamp', *Journal of Biological Chemistry*. American Society for Biochemistry & Molecular Biology (ASBMB), 282(10), pp. 7035–7045. doi: 10.1074/jbc.m610136200.

Arthur, H. M. and Lloyd, R. G. (1980) 'Hyper-recombination in uvrD mutants of Escherichia coli K-12', *MGG Molecular & General Genetics*. Springer Nature, 180(1), pp. 185–191. doi: 10.1007/bf00267368.

Asai, T. and Kogoma, T. (1994) 'Roles of ruvA, ruvC and recG gene functions in normal and DNA damage- inducible replication of the Escherichia coli chromosome', *Genetics*.

Atkinson, J. *et al.* (2009) 'Stimulation of UvrD helicase by UvrAB', *Journal of Biological Chemistry*, 284(14), pp. 9612–9623. doi: 10.1074/jbc.M808030200.

Atkinson, J., Gupta, M. K. and McGlynn, P. (2010) 'Interaction of Rep and DnaB on DNA', *Nucleic Acids Research*. Oxford University Press (OUP), 39(4), pp. 1351–1359. doi: 10.1093/nar/gkq975.

Atkinson, J. and McGlynn, P. (2009) 'Replication fork reversal and the maintenance of genome stability', *Nucleic Acids Research*. Oxford University Press (OUP), 37(11), pp. 3475–3492. doi: 10.1093/nar/gkp244.

Aussel, L. *et al.* (2002) 'FtsK Is a DNA Motor Protein that Activates Chromosome Dimer Resolution by Switching the Catalytic State of the XerC and XerD Recombinases', *Cell*, 108(2), pp. 195–205. doi: 10.1016/S0092-8674(02)00624-4.

Azeroglu, B. *et al.* (2016) 'RecG Directs DNA Synthesis during Double-Strand Break Repair', *PLOS Genetics*. Edited by J. Courcelle, 12(2), p. e1005799. doi: 10.1371/journal.pgen.1005799.

Azeroglu, B. and Leach, D. R. F. (2017) 'RecG controls DNA amplification at double-strand

breaks and arrested replication forks', *FEBS Letters*. Wiley, 591(8), pp. 1101–1113. doi: 10.1002/1873-3468.12583.

Baharoglu, Z. *et al.* (2006) 'RuvAB is essential for replication forks reversal in certain replication mutants', *EMBO Journal*. doi: 10.1038/sj.emboj.7600941.

Bárcena, M. *et al.* (2001) 'The DnaB·DnaC complex: A structure based on dimers assembled around an occluded channel', *EMBO Journal*. doi: 10.1093/emboj/20.6.1462.

Bates, D. *et al.* (2005) 'TheEscherichia colibaby cell column: a novel cell synchronization method provides new insight into the bacterial cell cycle', *Molecular Microbiology*. Wiley, 57(2), pp. 380–391. doi: 10.1111/j.1365-2958.2005.04693.x.

Beattie, T. R. and Reyes-Lamothe, R. (2015) 'A Replisome's journey through the bacterial chromosome', *Frontiers in Microbiology*, 6(JUN), pp. 1–12. doi: 10.3389/fmicb.2015.00562.

Bell, J. C. and Kowalczykowski, S. C. (2016) 'Mechanics and Single-Molecule Interrogation of DNA Recombination', *Annual Review of Biochemistry*, 85(1), pp. 193–226. doi: 10.1146/annurev-biochem-060614-034352.

Bell, L. and Byers, B. (1983) 'Separation of branched from linear DNA by two-dimensional gel electrophoresis', *Analytical Biochemistry*, 130(2), pp. 527–535. doi: 10.1016/0003-2697(83)90628-0.

Benkovic, S. J., Valentine, A. M. and Salinas, F. (2001) 'Replisome-Mediated DNA Replication', *Annual Review of Biochemistry*. Annual Reviews, 70(1), pp. 181–208. doi: 10.1146/annurev.biochem.70.1.181.

Berghuis, B. A. *et al.* (2015) 'Strand separation establishes a sustained lock at the Tus–Ter replication fork barrier', *Nature Chemical Biology*. Nature Publishing Group, 11(8), pp. 579–585. doi: 10.1038/nchembio.1857.

Bhattacharyya, B. *et al.* (2014) 'Structural mechanisms of PriA-mediated DNA replication restart', *Proceedings of the National Academy of Sciences*, 111(4), pp. 1373–1378. doi: 10.1073/pnas.1318001111.

Bidnenko, V., Ehrlich, S. D. and Michel, B. (2002) 'Replication fork collapse at replication terminator sequences', *EMBO Journal*. Wiley, 21(14), pp. 3898–3907. doi: 10.1093/emboj/cdf369.

Bidnenko, V., Lestini, R. and Michel, B. (2006) 'The Escherichia coli UvrD helicase is essential for Tus removal during recombination-dependent replication restart from Ter sites', *Molecular Microbiology*, 62(2), pp. 382–396. doi: 10.1111/j.1365-2958.2006.05382.x.

Bierne, H. *et al.* (1997) ' uvrD mutations enhance tandem repeat deletion in the Escherichia coli chromosome via SOS induction of the RecF recombination pathway ', *Molecular Microbiology*. doi: 10.1046/j.1365-2958.1997.6011973.x.

Bierne, H., Ehrlich, S. D. and Michel, B. (1991) 'The replication termination signal terB of the

Escherichia coli chromosome is a deletion hot spot.', *The EMBO Journal*. doi: 10.1002/j.1460-2075.1991.tb07814.x.

Bierne, H., Ehrlich, S. D. and Michel, B. (1997) 'Deletions at stalled replication forks occur by two different pathways', *EMBO Journal*. doi: 10.1093/emboj/16.11.3332.

Bigot, S. *et al.* (2005) 'KOPS: DNA motifs that control E. coli chromosome segregation by orienting the FtsK translocase', *The EMBO Journal*. Wiley, 24(21), pp. 3770–3780. doi: 10.1038/sj.emboj.7600835.

Blattner, F. R. (1997) 'The Complete Genome Sequence of Escherichia coli K-12', *Science*. American Association for the Advancement of Science (AAAS), 277(5331), pp. 1453–1462. doi: 10.1126/science.277.5331.1453.

Bonné, L. *et al.* (2009) 'Asymmetric DNA requirements in Xer recombination activation by FtsK', *Nucleic Acids Research*, 37(7), pp. 2371–2380. doi: 10.1093/nar/gkp104.

Boubakri, H. *et al.* (2010) 'The helicases DinG, Rep and UvrD cooperate to promote replication across transcription units in vivo', *EMBO Journal*. Wiley, 29(1), pp. 145–157. doi: 10.1038/emboj.2009.308.

Branzei, D. and Foiani, M. (2007) 'Interplay of replication checkpoints and repair proteins at stalled replication forks', *DNA Repair*, 6(7). doi: 10.1016/j.dnarep.2007.02.018.

Breier, A. M., Weier, H.-U. G. and Cozzarelli, N. R. (2005) 'Independence of replisomes in Escherichia coli chromosomal replication', *Proceedings of the National Academy of Sciences*. Proceedings of the National Academy of Sciences, 102(11), pp. 3942–3947. doi: 10.1073/pnas.0500812102.

Brewer, B. J. (1988) 'When polymerases collide: Replication and the transcriptional organization of the E. coli chromosome', *Cell*, 53(5), pp. 679–686. doi: 10.1016/0092-8674(88)90086-4.

Brewer, B. J. and Fangman, W. L. (1987) 'The localization of replication origins on ARS plasmids in S. cerevisiae', *Cell*, 51(3), pp. 463–471. doi: 10.1016/0092-8674(87)90642-8.

Brochu, J. *et al.* (2018) 'Topoisomerases I and III inhibit R-loop formation to prevent unregulated replication in the chromosomal Ter region of Escherichia coli', *PLoS Genetics*, 14(9), pp. 1–25. doi: 10.1371/journal.pgen.1007668.

Bruand, C. and Ehrlich, S. D. (2000) 'UvrD-dependent replication of rolling-circle plasmids in Escherichia coli', *Molecular Microbiology*. Wiley, 35(1), pp. 204–210. doi: 10.1046/j.1365-2958.2000.01700.x.

Brüning, J.-G., Howard, J. L. and McGlynn, P. (2014) 'Accessory Replicative Helicases and the Replication of Protein-Bound DNA', *Journal of Molecular Biology*. Elsevier B.V., 426(24), pp. 3917–3928. doi: 10.1016/j.jmb.2014.10.001.

Burnouf, D. Y. *et al.* (2004) 'Structural and Biochemical Analysis of Sliding Clamp/Ligand Interactions Suggest a Competition Between Replicative and Translesion DNA Polymerases', *Journal of Molecular Biology*. Elsevier BV, 335(5), pp. 1187–1197. doi: 10.1016/j.jmb.2003.11.049.

Cadman, C. J., Matson, S. W. and McGlynn, P. (2006) 'Unwinding of Forked DNA Structures by UvrD', *Journal of Molecular Biology*, 362(1), pp. 18–25. doi: 10.1016/j.jmb.2006.06.032.

Casper, A. M. *et al.* (2002) 'ATR regulates fragile site stability', *Cell*. doi: 10.1016/S0092-8674(02)01113-3.

Castillo, D. E. *et al.* (2016) 'The role of MatP, ZapA and ZapB in chromosomal organization and dynamics in Escherichia coli', *Nucleic Acids Research*, 44(3), pp. 1216–1226. doi: 10.1093/nar/gkv1484.

Colloms, S. D. *et al.* (1990) 'Recombination of ColE1 cer requires the Escherichia coli xerC gene product, a member of the lambda intergrase family of site-specific recombinases', *Journal of Bacteriology*, 172(12). doi: 10.1128/jb.172.12.6973-6980.1990.

Colloms, S. D. *et al.* (1996) 'Xer-mediated site-specific recombination in vitro.', *The EMBO Journal*, 15(5). doi: 10.1002/j.1460-2075.1996.tb00456.x.

Coskun-Ari, F. F. *et al.* (1994) 'Biophysical characteristics of Tus, the replication arrest protein of Escherichia coli.', *The Journal of biological chemistry*, 269(6), pp. 4027–34. Available at: http://www.ncbi.nlm.nih.gov/pubmed/8307958.

Coskun-Ari, F. F. and Hill, T. M. (1997) 'Sequence-specific interactions in the Tus-Ter complex and the effect of base pair substitutions on arrest of DNA replication in Escherichia coli', *Journal of Biological Chemistry*, 272(42), pp. 26448–26456. doi: 10.1074/jbc.272.42.26448.

Courcelle, J. *et al.* (2001) 'Comparative gene expression profiles following UV exposure in wild-type and SOS-deficient Escherichia coli.', *Genetics*, 158(1), pp. 41–64. Available at: http://www.ncbi.nlm.nih.gov/pubmed/11333217.

Courcelle, J. *et al.* (2003) 'DNA damage-induced replication fork regression and processing in Escherichia coli', *Science*, 299(5609), pp. 1064–1067. doi: 10.1126/science.1081328.

Cunningham, L., Gruer, M. J. and Guest, J. R. (1997) 'Transcriptional regulation of the aconitase genes (acnA and acnB) of Escherichia coli', *Microbiology*, 143(12), pp. 3795–3805. doi: 10.1099/00221287-143-12-3795.

Dalhus, B. *et al.* (2009) 'DNA base repair – recognition and initiation of catalysis', *FEMS Microbiology Reviews*, 33(6), pp. 1044–1078. doi: 10.1111/j.1574-6976.2009.00188.x.

Deegan, T. D. *et al.* (2019) 'Pif1-Family Helicases Support Fork Convergence during DNA Replication Termination in Eukaryotes', *Molecular Cell*, 74(2), pp. 231-244.e9. doi: 10.1016/j.molcel.2019.01.040.

Dennis, P. P. *et al.* (2009) 'Varying Rate of RNA Chain Elongation during rrn Transcription in Escherichia coli', *Journal of Bacteriology*. American Society for Microbiology, 191(11), pp. 3740–3746. doi: 10.1128/jb.00128-09.

Dimude, J. *et al.* (2016) 'Replication Termination: Containing Fork Fusion-Mediated Pathologies in Escherichia coli', *Genes*. MDPI AG, 7(8), p. 40. doi: 10.3390/genes7080040.

Dimude, J. U. *et al.* (2015) 'The Consequences of Replicating in the Wrong Orientation: Bacterial Chromosome Duplication without an Active Replication Origin', *mBio*. American Society for Microbiology, 6(6), pp. 1–13. doi: 10.1128/mbio.01294-15.

Dodson, M. L., Lloyd, R. S. and Schrock, R. D. (1993) 'Evidence for an Imino Intermediate in the T4 Endonuclease V Reaction', *Biochemistry*, 32(32). doi: 10.1021/bi00083a032.

Dohrmann, P. R. *et al.* (2016) 'The DNA polymerase III holoenzyme contains-and is not a trimeric polymerase', *Nucleic Acids Research*, 44(3), pp. 1285–1297. doi: 10.1093/nar/gkv1510.

Donachie, W. D. (1993) 'The Cell Cycle of Escherichia Coli', *Annual Review of Microbiology*. Annual Reviews, 47(1), pp. 199–230. doi: 10.1146/annurev.mi.47.100193.001215.

Duggin, I. G. *et al.* (2008) 'The replication fork trap and termination of chromosome replication', *Molecular Microbiology*, 70(6), pp. 1323–1333. doi: 10.1111/j.1365-2958.2008.06500.x.

Duggin, I. G. and Bell, S. D. (2009) 'Termination structures in the Escherichia coli chromosome replication fork trap.', *Journal of molecular biology*. Elsevier Ltd, 387(3), pp. 532–9. doi: 10.1016/j.jmb.2009.02.027.

Elshenawy, M. M. *et al.* (2015) 'Replisome speed determines the efficiency of the Tus-Ter replication termination barrier', *Nature*, 525(7569), pp. 394–398. doi: 10.1038/nature14866.

Engelman, J. A. *et al.* (2007) 'MET amplification leads to gefitinib resistance in lung cancer by activating ERBB3 signaling', *Science*. doi: 10.1126/science.1141478.

Esnault, E. *et al.* (2007) 'Chromosome Structuring Limits Genome Plasticity in Escherichia coli', *PLoS Genetics*. Public Library of Science (PLoS), 3(12), p. e226. doi: 10.1371/journal.pgen.0030226.

Espéli, O. *et al.* (2012) 'A MatP-divisome interaction coordinates chromosome segregation with cell division in E. coli', *The EMBO Journal*, 31(14), pp. 3198–3211. doi: 10.1038/emboj.2012.128.

Eykelenboom, J. K. *et al.* (2008) 'SbcCD Causes a Double-Strand Break at a DNA Palindrome in the Escherichia coli Chromosome', *Molecular Cell*, 29(5), pp. 644–651. doi: 10.1016/j.molcel.2007.12.020.

Fang, L., Davey, M. J. and O'Donnell, M. (1999) 'Replisome Assembly at oriC, the Replication Origin of E. coli, Reveals an Explanation for Initiation Sites outside an Origin', *Molecular Cell*. Elsevier BV, 4(4), pp. 541–553. doi: 10.1016/s1097-2765(00)80205-1.

Ferullo, D. J. *et al.* (2009) 'Cell cycle synchronization of Escherichia coli using the stringent response, with fluorescence labeling assays for DNA content and replication', *Methods*. Elsevier BV, 48(1), pp. 8–13. doi: 10.1016/j.ymeth.2009.02.010.

Fischer, C. J., Maluf, N. K. and Lohman, T. M. (2004) 'Mechanism of ATP-dependent Translocation of E.coli UvrD Monomers Along Single-stranded DNA', *Journal of Molecular Biology*. Elsevier BV, 344(5), pp. 1287–1309. doi: 10.1016/j.jmb.2004.10.005.

Florés, M.-J. J., Sanchez, N. and Michel, B. (2005) 'A fork-clearing role for UvrD', *Molecular Microbiology*. Wiley, 57(6), pp. 1664–1675. doi: 10.1111/j.1365-2958.2005.04753.x.

Flores, M. M.-J. *et al.* (2001) 'Rescue of arrested replication forks by homologous recombination', *Proceedings of the National Academy of Sciences*, 98(15), pp. 8181–8188. doi: 10.1073/pnas.111008798.

Fonville, N. C. *et al.* (2010) 'RecQ-dependent death-by-recombination in cells lacking RecG and UvrD', *DNA Repair*. Elsevier B.V., 9(4), pp. 403–413. doi: 10.1016/j.dnarep.2009.12.019.

Frick, D. N. and Richardson, C. C. (2001) 'DNA Primases', *Annual Review of Biochemistry*. Annual Reviews, 70(1), pp. 39–80. doi: 10.1146/annurev.biochem.70.1.39.

Fuchs, R. P. and Fujii, S. (2013) 'Translesion DNA synthesis and mutagenesis in prokaryotes.', *Cold Spring Harbor perspectives in biology*, 5(12), p. a012682. doi: 10.1101/cshperspect.a012682.

Fujimitsu, K., Senriuchi, T. and Katayama, T. (2009) 'Specific genomic sequences of E. coli promote replicational initiation by directly reactivating ADP-DnaA', *Genes & Development*. Cold Spring Harbor Laboratory, 23(10), pp. 1221–1233. doi: 10.1101/gad.1775809.

Gabbai, C. B. and Marians, K. J. (2010) 'Recruitment to stalled replication forks of the PriA DNA helicase and replisome-loading activities is essential for survival', *DNA Repair*. Elsevier BV, 9(3), pp. 202–209. doi: 10.1016/j.dnarep.2009.12.009.

George, J. W., Brosh, R. M. and Matson, S. W. (1994) 'A Dominant Negative Allele of the Escherichia coli uvrD Gene Encoding DNA Helicase II', *Journal of Molecular Biology*. Elsevier BV, 235(2), pp. 424–435. doi: 10.1006/jmbi.1994.1003.

Georgescu, R. E., Kurth, I. and O'Donnell, M. E. (2011) 'Single-molecule studies reveal the function of a third polymerase in the replisome', *Nature Structural & Molecular Biology*. Springer Science and Business Media LLC, 19(1), pp. 113–116. doi: 10.1038/nsmb.2179.

Georgescu, R. E., Yao, N. Y. and O'Donnell, M. (2010) 'Single-molecule analysis of the Escherichia coli replisome and use of clamps to bypass replication barriers', *FEBS Letters*. Federation of European Biochemical Societies, 584(12), pp. 2596–2605. doi: 10.1016/j.febslet.2010.04.003.

Graham, J. E. *et al.* (2009) 'FtsK translocation on DNA stops at XerCD-dif', *Nucleic Acids Research*, 38(1), pp. 72–81. doi: 10.1093/nar/gkp843.

Graham, J. E., Marians, K. J. and Kowalczykowski, S. C. (2017) 'Independent and Stochastic Action of DNA Polymerases in the Replisome', *Cell*. Elsevier, 169(7), pp. 1201-1213.e17. doi: 10.1016/j.cell.2017.05.041.

Gupta, M. K. *et al.* (2013) 'Protein-DNA complexes are the primary sources of replication fork pausing in Escherichia coli', *Proceedings of the National Academy of Sciences*, 110(18), pp. 7252–7257. doi: 10.1073/pnas.1303890110.

Gupta, S., Yeeles, J. T. P. and Marians, K. J. (2014) 'Regression of Replication Forks Stalled by Leading-strand Template Damage', *Journal of Biological Chemistry*. American Society for Biochemistry & Molecular Biology (ASBMB), 289(41), pp. 28376–28387. doi: 10.1074/jbc.m114.587881.

Guy, C. P. *et al.* (2009) 'Rep Provides a Second Motor at the Replisome to Promote Duplication of Protein-Bound DNA', *Molecular Cell*. Elsevier Ltd, 36(4), pp. 654–666. doi: 10.1016/j.molcel.2009.11.009.

Han, E. S. (2006) 'RecJ exonuclease: substrates, products and interaction with SSB', *Nucleic Acids Research*. Oxford University Press (OUP), 34(4), pp. 1084–1091. doi: 10.1093/nar/gkj503.

Hansen, F. G. and Atlung, T. (2018) 'The DnaA Tale', *Frontiers in Microbiology*. Frontiers Media SA, 9. doi: 10.3389/fmicb.2018.00319.

Harashima, H., Dissmeyer, N. and Schnittger, A. (2013) 'Cell cycle control across the eukaryotic kingdom', *Trends in Cell Biology*. Elsevier Ltd, 23(7), pp. 345–356. doi: 10.1016/j.tcb.2013.03.002.

Heller, R. C. and Marians, K. J. (2005) 'Unwinding of the nascent lagging strand by Rep and PriA enables the direct restart of stalled replication forks', *Journal of Biological Chemistry*, 280(40). doi: 10.1074/jbc.M507224200.

Heller, R. C. and Marians, K. J. (2006a) 'Replication fork reactivation downstream of a blocked nascent leading strand', *Nature*, 439(7076), pp. 557–562. doi: 10.1038/nature04329.

Heller, R. C. and Marians, K. J. (2006b) 'Replisome assembly and the direct restart of stalled replication forks', *Nature Reviews Molecular Cell Biology*. Springer Nature, 7(12), pp. 932–943. doi: 10.1038/nrm2058.

Helmrich, A. *et al.* (2013) 'Transcription-replication encounters, consequences and genomic instability', *Nature Structural & Molecular Biology*. Springer Science and Business Media LLC, 20(4), pp. 412–418. doi: 10.1038/nsmb.2543.

Hiasa, H. and Marians, K. J. (1994) 'Tus prevents overreplication of oriC plasmid DNA', *Journal of Biological Chemistry*, 269(43), pp. 26959–26968. doi: 10.1074/jbc.M104411200.

Hidaka, M., Akiyama, M. and Horiuchi, T. (1988) 'A consensus sequence of three DNA

replication terminus sites on the E. coli chromosome is highly homologous to the terR sites of the R6K plasmid', *Cell*, 55(3), pp. 467–475. doi: 10.1016/0092-8674(88)90033-5.

Hill, T. M. *et al.* (1989) 'tus, the trans-acting gene required for termination of DNA replication in Escherichia coli, encodes a DNA-binding protein.', *Proceedings of the National Academy of Sciences*. Proceedings of the National Academy of Sciences, 86(5), pp. 1593–1597. doi: 10.1073/pnas.86.5.1593.

Hizume, K. and Araki, H. (2019) 'Replication fork pausing at protein barriers on chromosomes', *FEBS Letters*, pp. 1–10. doi: 10.1002/1873-3468.13481.

Horiuchi, T. and Fujimura, Y. (1995) 'Recombinational rescue of the stalled DNA replication fork: A model based on analysis of an Escherichia coli strain with a chromosome region difficult to replicate', *Journal of Bacteriology*.

El Houry Mignan, S. *et al.* (2011) 'Characterization of the χψ subcomplex of Pseudomonas aeruginosa DNA polymerase III', *BMC Molecular Biology*. Springer Nature, 12(1), p. 43. doi: 10.1186/1471-2199-12-43.

Husain, I. *et al.* (1985) 'Effect of DNA polymerase I and DNA helicase II on the turnover rate of UvrABC excision nuclease.', *Proceedings of the National Academy of Sciences*. Proceedings of the National Academy of Sciences, 82(20), pp. 6774–6778. doi: 10.1073/pnas.82.20.6774.

Ishioka, K., Iwasaki, H. and Shinagawa, H. (1997) 'Roles of the recG gene product of Escherichia coli in recombination repair: Effects of the ΔrecG mutation on cell division and chromosome partition', *Genes and Genetic Systems*, 72(2), pp. 91–99. doi: 10.1266/ggs.72.91.

Ivanova, D. *et al.* (2015) 'Shaping the landscape of the Escherichia coli chromosome: Replication-transcription encounters in cells with an ectopic replication origin', *Nucleic Acids Research*, 43(16), pp. 7865–7877. doi: 10.1093/nar/gkv704.

Iyer, L. M. *et al.* (2004) 'Evolutionary history and higher order classification of AAA+ ATPases', *Journal of Structural Biology*. Elsevier BV, 146(1–2), pp. 11–31. doi: 10.1016/j.jsb.2003.10.010.

Iyer, R. R. *et al.* (2006) 'DNA Mismatch Repair: Functions and Mechanisms', *Chemical Reviews*. American Chemical Society (ACS), 106(2), pp. 302–323. doi: 10.1021/cr0404794.

Jiricny, J. (2013) 'Postreplicative Mismatch Repair', *Cold Spring Harbor Perspectives in Biology*, 5(4). doi: 10.1101/cshperspect.a012633.

Johnson, D. S. *et al.* (2007) 'Single-Molecule Studies Reveal Dynamics of DNA Unwinding by the Ring-Shaped T7 Helicase', *Cell*. Elsevier BV, 129(7), pp. 1299–1309. doi: 10.1016/j.cell.2007.04.038.

Jones, J. M. and Nakai, H. (2001) 'Escherichia coli PriA helicase: Fork binding orients the

helicase to unwind the lagging strand side of arrested replication forks', *Journal of Molecular Biology*, 312(5). doi: 10.1006/jmbi.2001.4930.

Joshi, M. C. *et al.* (2013) 'Regulation of Sister Chromosome Cohesion by the Replication Fork Tracking Protein SeqA', *PLoS Genetics*, 9(8). doi: 10.1371/journal.pgen.1003673.

Kamada, K. *et al.* (1996) 'Structure of a replication-terminator protein complexed with DNA', *Nature*, 383(6601), pp. 598–603. doi: 10.1038/383598a0.

Keyamura, K. *et al.* (2007) 'The interaction of DiaA and DnaA regulates the replication cycle in E. coli by directly promoting ATP DnaA-specific initiation complexes', *Genes & Development*. Cold Spring Harbor Laboratory, 21(16), pp. 2083–2099. doi: 10.1101/gad.1561207.

Khan, S. R. and Kuzminov, A. (2012) 'Replication forks stalled at ultraviolet lesions are rescued via RecA and RuvABC protein-catalyzed disintegration in Escherichia coli', *Journal of Biological Chemistry*. doi: 10.1074/jbc.M111.322990.

Kim, S. *et al.* (1996) 'Coupling of a Replicative Polymerase and Helicase: A τ–DnaB Interaction Mediates Rapid Replication Fork Movement', *Cell*. Elsevier BV, 84(4), pp. 643–650. doi: 10.1016/s0092-8674(00)81039-9.

Kim, S. R. *et al.* (2001) 'Roles of chromosomal and episomal dinB genes encoding DNA pol IV in targeted and untargeted mutagenesis in Escherichia coli', *Molecular Genetics and Genomics*, 266(2), pp. 207–215. doi: 10.1007/s004380100541.

Kisker, C. *et al.* (2013) 'Prokaryotic Nucleotide Excision Repair', *Cold Spring Harbor Perspectives in Biology*. Cold Spring Harbor Laboratory, 5(3), pp. a012591–a012591. doi: 10.1101/cshperspect.a012591.

Kleckner, N. *et al.* (2014) 'The bacterial nucleoid: nature, dynamics and sister segregation.', *Current opinion in microbiology*. Elsevier Ltd, 22, pp. 127–37. doi: 10.1016/j.mib.2014.10.001.

Kogoma, T. (1997) 'Stable DNA replication: interplay between DNA replication, homologous recombination, and transcription.', *Microbiology and molecular biology reviews : MMBR*.

Konieczny, I. (2003) 'Strategies for helicase recruitment and loading in bacteria', *EMBO reports*. Wiley, 4(1), pp. 37–41. doi: 10.1038/sj.embor.embor703.

Krabbe, M. *et al.* (1997) 'Inactivation of the replication-termination system affects the replication mode and causes unstable maintenance of plasmid R1', *Molecular Microbiology*. Wiley, 24(4), pp. 723–735. doi: 10.1046/j.1365-2958.1997.3791747.x.

Krasich, R. *et al.* (2015) 'Functions that protect Escherichia coli from DNA-protein crosslinks', *DNA Repair*. Elsevier B.V., 28, pp. 48–59. doi: 10.1016/j.dnarep.2015.01.016.

Krueger, A., Protozanova, E. and Frank-Kamenetskii, M. D. (2006) 'Sequence-dependent basepair opening in DNA double helix', *Biophysical Journal*. Elsevier, 90(9), pp. 3091–3099. doi:

10.1529/biophysj.105.078774.

Kurth, I. and O'Donnell, M. (2009) 'Replisome Dynamics during Chromosome Duplication', *EcoSal Plus*. American Society for Microbiology, 3(2). doi: 10.1128/ecosalplus.4.4.2.

Kuznetsov, S. V *et al.* (2006) 'Microsecond Dynamics of Protein–DNA Interactions: Direct Observation of the Wrapping/Unwrapping Kinetics of Single-stranded DNA around the E.coli SSB Tetramer', *Journal of Molecular Biology*. Elsevier BV, 359(1), pp. 55–65. doi: 10.1016/j.jmb.2006.02.070.

Lahue, R. S., Au, K. G. and Modrich, P. (1989) 'DNA mismatch correction in a defined system', *Science*. doi: 10.1126/science.2665076.

Lambert, S. *et al.* (2005) 'Gross Chromosomal Rearrangements and Elevated Recombination at an Inducible Site-Specific Replication Fork Barrier', *Cell*. Elsevier BV, 121(5), pp. 689–702. doi: 10.1016/j.cell.2005.03.022.

Larsen, N. B. *et al.* (2014) 'The Escherichia coli Tus–Ter replication fork barrier causes site-specific DNA replication perturbation in yeast', *Nature Communications*. Springer Science and Business Media LLC, 5(1). doi: 10.1038/ncomms4574.

LeBowitz, J. H. and McMacken, R. (1986) 'The Escherichia coli dnaB replication protein is a DNA helicase', *Journal of Biological Chemistry*, 261(10), pp. 4738–4748.

Lee, J. Y. *et al.* (2014) 'Single-Molecule Imaging of FtsK Translocation Reveals Mechanistic Features of Protein-Protein Collisions on DNA', *Molecular Cell*. Elsevier Inc., 54(5), pp. 832–843. doi: 10.1016/j.molcel.2014.03.033.

Lee, K. S. *et al.* (2013) 'Direct imaging of single UvrD helicase dynamics on long single-stranded DNA', *Nature Communications*. Nature Publishing Group, 4(1), p. 1878. doi: 10.1038/ncomms2882.

Lee, P. S. and Lee, K. H. (2003) 'Escherichia coli - A Model System That Benefits from and Contributes to the Evolution of Proteomics', *Biotechnology and Bioengineering*. doi: 10.1002/bit.10848.

Leonard, A. C. and Grimwade, J. E. (2004) 'Building a bacterial orisome: emergence of new regulatory features for replication origin unwinding', *Molecular Microbiology*. Wiley, 55(4), pp. 978–985. doi: 10.1111/j.1365-2958.2004.04467.x.

Lesterlin, C. *et al.* (2012) 'Sister chromatid interactions in bacteria revealed by a site-specific recombination assay', *The EMBO Journal*, 31(16), pp. 3468–3479. doi: 10.1038/emboj.2012.194.

Lestini, R. and Michel, B. (2007) 'UvrD controls the access of recombination proteins to blocked replication forks', *EMBO Journal*, 26(16), pp. 3804–3814. doi: 10.1038/sj.emboj.7601804.

Lewis, J. S., Jergic, S. and Dixon, N. E. (2016) 'The E. coli DNA Replication Fork', in *Enzymes*. 1st edn. Elsevier Inc., pp. 31–88. doi: 10.1016/bs.enz.2016.04.001.

Lia, G., Michel, B. and Allemand, J.-F. (2011) 'Polymerase Exchange During Okazaki

Fragment Synthesis Observed in Living Cells', *Science*. American Association for the Advancement of Science (AAAS), 335(6066), pp. 328–331. doi: 10.1126/science.1210400.

Lloyd, R. G. and Buckman, C. (1991) 'Genetic analysis of the recG locus of Escherichia coli K-12 and of its role in recombination and DNA repair.', *Journal of Bacteriology*. American Society for Microbiology, 173(3), pp. 1004–1011. doi: 10.1128/jb.173.3.1004-1011.1991.

Lohman, T. M., Tomko, E. J. and Wu, C. G. (2008) 'Non-hexameric DNA helicases and translocases: mechanisms and regulation', *Nature Reviews Molecular Cell Biology*. Springer Science and Business Media LLC, 9(5), pp. 391–401. doi: 10.1038/nrm2394.

López Castel, A., Cleary, J. D. and Pearson, C. E. (2010) 'Repeat instability as the basis for human diseases and as a potential target for therapy', *Nature Reviews Molecular Cell Biology*. Springer Science and Business Media LLC, 11(3), pp. 165–170. doi: 10.1038/nrm2854.

Lu, D. and Keck, J. L. (2008) 'Structural basis of Escherichia coli single-stranded DNA-binding protein stimulation of exonuclease I', *Proceedings of the National Academy of Sciences*. Proceedings of the National Academy of Sciences, 105(27), pp. 9169–9174. doi: 10.1073/pnas.0800741105.

Maduike, N. Z. *et al.* (2014) 'Replication of the Escherichia coli chromosome in RNase HI-deficient cells: Multiple initiation regions and fork dynamics', *Molecular Microbiology*, 91(1), pp. 39–56. doi: 10.1111/mmi.12440.

Maluf, N. K., Ali, J. A. and Lohman, T. M. (2003) 'Kinetic mechanism for formation of the active, dimeric UvrD helicase-DNA complex', *Journal of Biological Chemistry*. doi: 10.1074/jbc.M304223200.

Maluf, N. K., Fischer, C. J. and Lohman, T. M. (2003) 'A Dimer of Escherichia coli UvrD is the Active Form of the Helicase In Vitro', *Journal of Molecular Biology*. Elsevier BV, 325(5), pp. 913–935. doi: 10.1016/s0022-2836(02)01277-9.

Marians, K. J. *et al.* (1998) 'Role of the Core DNA Polymerase III Subunits at the Replication Fork', *Journal of Biological Chemistry*. American Society for Biochemistry & Molecular Biology (ASBMB), 273(4), pp. 2452–2457. doi: 10.1074/jbc.273.4.2452.

Marians, K. J. (2018) 'Lesion Bypass and the Reactivation of Stalled Replication Forks', *Annual Review of Biochemistry*, 87(1), pp. 217–238. doi: 10.1146/annurev-biochem-062917-011921.

Markovitz, A. (2005) 'A new in vivo termination function for DNA polymerase I of Escherichia coli K12', *Molecular Microbiology*, 55(6), pp. 1867–1882. doi: 10.1111/j.1365-2958.2005.04513.x.

Matson, S. W. (1991) 'DNA Helicases of Escherichia coli', *Progress in Nucleic Acid Research and Molecular Biology*. Elsevier, pp. 289–326. doi: 10.1016/s0079-6603(08)60845-4.

Matson, S. W. and Robertson, A. B. (2006) 'The UvrD helicase and its modulation by the mismatch repair protein MutL', *Nucleic Acids Research*. Oxford University Press (OUP), 34(15), pp.

4089–4097. doi: 10.1093/nar/gkl450.

McGarry, K. C. *et al.* (2004) 'Two discriminatory binding sites in the Escherichia coli replication origin are required for DNA strand opening by initiator DnaA-ATP', *Proceedings of the National Academy of Sciences*. Proceedings of the National Academy of Sciences, 101(9), pp. 2811–2816. doi: 10.1073/pnas.0400340101.

McGlynn, P. and Guy, C. P. (2008) 'Replication Forks Blocked by Protein–DNA Complexes Have Limited Stability In Vitro', *Journal of Molecular Biology*. Elsevier BV, 381(2), pp. 249–255. doi: 10.1016/j.jmb.2008.05.053.

McGlynn, P. and Lloyd, R. G. (2002) 'Recombinational repair and restart of damaged replication forks', *Nature Reviews Molecular Cell Biology*. Springer Nature, 3(11), pp. 859–870. doi: 10.1038/nrm951.

McHenry, C. S. (2003) 'Chromosomal replicases as asymmetric dimers: studies of subunit arrangement and functional consequences', *Molecular Microbiology*. Wiley, 49(5), pp. 1157–1165. doi: 10.1046/j.1365-2958.2003.03645.x.

McInerney, P. *et al.* (2007) 'Characterization of a Triple DNA Polymerase Replisome', *Molecular Cell*. Elsevier BV, 27(4), pp. 527–538. doi: 10.1016/j.molcel.2007.06.019.

McLean, M. J., Wolfe, K. H. and Devine, K. M. (1998) 'Base composition skews, replication orientation, and gene orientation in 12 prokaryote genomes', *Journal of Molecular Evolution*. doi: 10.1007/PL00006428.

Mercier, R. *et al.* (2008) 'The MatP/matS Site-Specific System Organizes the Terminus Region of the E. coli Chromosome into a Macrodomain', *Cell*, 135(3), pp. 475–485. doi: 10.1016/j.cell.2008.08.031.

Merrikh, H. *et al.* (2011) 'Co-directional replication–transcription conflicts lead to replication restart', *Nature*. Springer Science and Business Media LLC, 470(7335), pp. 554–557. doi: 10.1038/nature09758.

Merrikh, H. *et al.* (2012) 'Replication–transcription conflicts in bacteria', *Nature Reviews Microbiology*. Springer Science and Business Media LLC, 10(7), pp. 449–458. doi: 10.1038/nrmicro2800.

Messer, W. (2002) 'The bacterial replication initiator DnaA. DnaA andoriC, the bacterial mode to initiate DNA replication', *FEMS Microbiology Reviews*. Oxford University Press (OUP), 26(4), pp. 355–374. doi: 10.1111/j.1574-6976.2002.tb00620.x.

Mettrick, K. A. and Grainge, I. (2015) 'Stability of blocked replication forks in vivo', *Nucleic Acids Research*, 44(2), pp. 657–668. doi: 10.1093/nar/gkv1079.

Meyer, R. R. and Laine, P. S. (1990) 'The single-stranded DNA-binding protein of Escherichia

coli', *Microbiological Reviews*.

Michel, B., Ehrlich, S. D. and Uzest, M. (1997) 'DNA double-strand breaks caused by replication arrest', *The EMBO Journal*, 16(2), pp. 430–438. doi: 10.1093/emboj/16.2.430.

Michel, B. and Sandler, S. J. (2017) 'Replication Restart in Bacteria', *Journal of Bacteriology*. American Society for Microbiology, 199(13). doi: 10.1128/jb.00102-17.

Midgley-Smith, S. L. *et al.* (2018) 'Chromosomal over-replication in Escherichia coli recG cells is triggered by replication fork fusion and amplified if replichore symmetry is disturbed', *Nucleic Acids Research*. Oxford University Press, 46(15), pp. 7701–7715. doi: 10.1093/nar/gky566.

Midgley-Smith, S. L., Dimude, J. U. and Rudolph, C. J. (2019) 'A role for 3 exonucleases at the final stages of chromosome duplication in Escherichia coli', *Nucleic Acids Research*. Oxford University Press, 47(4), pp. 1847–1860. doi: 10.1093/nar/gky1253.

Miles, J. S. and Guest, J. R. (1984) 'Complete nuleotide sequence of the fumarase gene fumA , of Escherichia coli', *Nucleic Acids Research*, 12(8), pp. 3631–3642. doi: 10.1093/nar/12.8.3631.

Miller, D. T. *et al.* (2009) 'Bacterial origin recognition complexes direct assembly of higher-order DnaA oligomeric structures', *Proceedings of the National Academy of Sciences*. Proceedings of the National Academy of Sciences, 106(44), pp. 18479–18484. doi: 10.1073/pnas.0909472106.

Mirkin, E. V. and Mirkin, S. M. (2007) 'Replication Fork Stalling at Natural Impediments', *Microbiology and Molecular Biology Reviews*. American Society for Microbiology, 71(1), pp. 13–35. doi: 10.1128/mmbr.00030-06.

Mitkova, A. V, Khopde, S. M. and Biswas, S. B. (2003) 'Mechanism and Stoichiometry of Interaction of DnaG Primase with DnaB Helicase ofEscherichia coliin RNA Primer Synthesis', *Journal of Biological Chemistry*. American Society for Biochemistry & Molecular Biology (ASBMB), 278(52), pp. 52253–52261. doi: 10.1074/jbc.m308956200.

Moolenaar, G. F., Moorman, C. and Goosen, N. (2000) 'Role of the Escherichia coli nucleotide excision repair proteins in DNA replication', *Journal of Bacteriology*, 182(20), pp. 5706–5714. doi: 10.1128/JB.182.20.5706-5714.2000.

Moolman, M. C. *et al.* (2016) 'The progression of replication forks at natural replication barriers in live bacteria', *Nucleic Acids Research*. Oxford University Press (OUP), 44(13), pp. 6262–6273. doi: 10.1093/nar/gkw397.

Moreau, M. J. J. and Schaeffer, P. M. (2012) 'Differential Tus-Ter binding and lock formation: Implications for DNA replication termination in Escherichia coli', *Molecular BioSystems*, 8(10), pp. 2783–2791. doi: 10.1039/c2mb25281c.

Moreau, M. J. J. and Schaeffer, P. M. (2013) 'Dissecting the salt dependence of the Tus-Ter protein-DNA complexes by high-throughput differential scanning fluorimetry of a GFP-tagged Tus',

Molecular BioSystems, 9(12), pp. 3146–3154. doi: 10.1039/c3mb70426b.

Morel, P. *et al.* (1993) 'Antipairing and strand transferase activities ofE.colihelicase II (UvrD)', *Nucleic Acids Research*. Oxford University Press (OUP), 21(14), pp. 3205–3209. doi: 10.1093/nar/21.14.3205.

Mott, M. L. and Berger, J. M. (2007) 'DNA replication initiation: mechanisms and regulation in bacteria', *Nature Reviews Microbiology*. Springer Science and Business Media LLC, 5(5), pp. 343–354. doi: 10.1038/nrmicro1640.

Mulcair, M. D. *et al.* (2006) 'A Molecular Mousetrap Determines Polarity of Termination of DNA Replication in E. coli', *Cell*. Elsevier BV, 125(7), pp. 1309–1319. doi: 10.1016/j.cell.2006.04.040.

Nakano, T. *et al.* (2007) 'Nucleotide Excision Repair and Homologous Recombination Systems Commit Differentially to the Repair of DNA-Protein Crosslinks', *Molecular Cell*, 28(1), pp. 147–158. doi: 10.1016/j.molcel.2007.07.029.

Natarajan, S. *et al.* (1993) 'A 27 kd protein of E. coli promotes antitermination of replication in vitro at a sequence-specific replication terminus', *Cell*. doi: 10.1016/0092-8674(93)90055-U.

Natarajan, S., Kelley, W. L. and Bastia, D. (1991) 'Replication terminator protein of Escherichia coli is a transcriptional repressor of its own synthesis.', *Proceedings of the National Academy of Sciences*. Proceedings of the National Academy of Sciences, 88(9), pp. 3867–3871. doi: 10.1073/pnas.88.9.3867.

Neylon, C. *et al.* (2000) 'Interaction of theEscherichia coliReplication Terminator Protein (Tus) with DNA: A Model Derived from DNA-Binding Studies of Mutant Proteins by Surface Plasmon Resonance†', *Biochemistry*. American Chemical Society (ACS), 39(39), pp. 11989–11999. doi: 10.1021/bi001174w.

Neylon, C. *et al.* (2005) 'Replication termination in Escherichia coli: structure and antihelicase activity of the Tus-Ter complex.', *Microbiology and molecular biology reviews : MMBR*. American Society for Microbiology, 69(3), pp. 501–26. doi: 10.1128/MMBR.69.3.501-526.2005.

Nielsen, O. and Løbner-Olesen, A. (2008) 'Once in a lifetime: strategies for preventing re-replication in prokaryotic and eukaryotic cells', *EMBO reports*. Wiley, 9(2), pp. 151–156. doi: 10.1038/sj.embor.2008.2.

Nurse, P., Liu, J. and Marians, K. J. (1999) 'Two Modes of PriA Binding to DNA', *Journal of Biological Chemistry*. American Society for Biochemistry & Molecular Biology (ASBMB), 274(35), pp. 25026–25032. doi: 10.1074/jbc.274.35.25026.

Oeda, K., Horiuchi, T. and Sekiguchi, M. (1982) 'The uvrD gene of E. coli encodes a DNA-dependent ATPase', *Nature*. Springer Nature, 298(5869), pp. 98–100. doi: 10.1038/298098a0.

Ordabayev, Y. A. *et al.* (2018) 'Regulation of UvrD Helicase Activity by MutL', *Journal of Molecular Biology*. Elsevier Ltd, 430(21), pp. 4260–4274. doi: 10.1016/j.jmb.2018.08.022.

Ordabayev, Y. A. *et al.* (2019) 'UvrD helicase activation by MutL involves rotation of its 2B subdomain', *Proceedings of the National Academy of Sciences*, 116(33), pp. 16320–16325. doi: 10.1073/pnas.1905513116.

Ozaki, S. and Katayama, T. (2009) 'DnaA structure, function, and dynamics in the initiation at the chromosomal origin', *Plasmid*. Elsevier BV, 62(2), pp. 71–82. doi: 10.1016/j.plasmid.2009.06.003.

Pandey, M. *et al.* (2015) 'Two mechanisms coordinate replication termination by the Escherichia coli Tus-Ter complex', *Nucleic Acids Research*, 43(12), pp. 5924–5935. doi: 10.1093/nar/gkv527.

Park, S. J. and Gunsalus, R. P. (1995) 'Oxygen, iron, carbon, and superoxide control of the fumarase fumA and fumC genes of Escherichia coli: role of the arcA, fnr, and soxR gene products.', *Journal of bacteriology*, 177(21), pp. 6255–6262. doi: 10.1128/JB.177.21.6255-6262.1995.

Patel, S. S. and Picha, K. M. (2000) 'Structure and Function of Hexameric Helicases', *Annual Review of Biochemistry*. Annual Reviews, 69(1), pp. 651–697. doi: 10.1146/annurev.biochem.69.1.651.

Petrova, V. *et al.* (2015) 'Active displacement of RecA filaments by UvrD translocase activity', *Nucleic Acids Research*. Oxford University Press (OUP), 43(8), pp. 4133–4149. doi: 10.1093/nar/gkv186.

Pham, T. M. *et al.* (2013) 'A single-molecule approach to DNA replication in Escherichia coli cells demonstrated that DNA polymerase III is a major determinant of fork speed', *Molecular Microbiology*, 90(3), pp. 584–596. doi: 10.1111/mmi.12386.

De Piccoli, G. *et al.* (2012) 'Replisome Stability at Defective DNA Replication Forks Is Independent of S Phase Checkpoint Kinases', *Molecular Cell*, 45(5). doi: 10.1016/j.molcel.2012.01.007.

Pomerantz, R. T. and O'Donnell, M. (2007) 'Replisome mechanics: insights into a twin DNA polymerase machine', *Trends in Microbiology*. Elsevier BV, 15(4), pp. 156–164. doi: 10.1016/j.tim.2007.02.007.

Pomerantz, R. T. and O'Donnell, M. (2010) 'Direct Restart of a Replication Fork Stalled by a Head-On RNA Polymerase', *Science*. American Association for the Advancement of Science (AAAS), 327(5965), pp. 590–592. doi: 10.1126/science.1179595.

Possoz, C. *et al.* (2006) 'Tracking of controlled Escherichia coli replication fork stalling and restart at repressor-bound DNA in vivo', *EMBO Journal*, 25(11), pp. 2596–2604. doi: 10.1038/sj.emboj.7601155.

Radman, M. *et al.* (1995) 'Editing DNA replication and recombination by mismatch repair: from

bacterial genetics to mechanisms of predisposition to cancer in humans', *DNA Repair and Recombination*. Springer Netherlands, pp. 93–99. doi: 10.1007/978-94-011-0537-8_14.

Raghunathan, S. *et al.* (1997) 'Crystal structure of the homo-tetrameric DNA binding domain of Escherichia coli single-stranded DNA-binding protein determined by multiwavelength x-ray diffraction on the selenomethionyl protein at 2.9-A resolution', *Proceedings of the National Academy of Sciences*. Proceedings of the National Academy of Sciences, 94(13), pp. 6652–6657. doi: 10.1073/pnas.94.13.6652.

Raghunathan, S. *et al.* (2000) 'Structure of the DNA binding domain of E. coli SSB bound to ssDNA.', *Nature structural biology*. Springer Nature, 7(8), pp. 648–52. doi: 10.1038/77943.

Roecklein, B. A. and Kuempel, P. L. (1992) 'In vivo characterization of tus gene expression in Escherichia coli', *Molecular Microbiology*. Elsevier Ltd, 6(12), pp. 1655–1661. doi: 10.1111/j.1365-2958.1992.tb00890.x.

Roecklein, B., Pelletier, A. and Kuempel, P. (1991) 'The tus gene of Escherichia coli: autoregulation, analysis of flanking sequences and identification of a complementary system in Salmonella typhimurium', *Research in Microbiology*. Elsevier BV, 142(2–3), pp. 169–175. doi: 10.1016/0923-2508(91)90026-7.

Rudolph, C. J. *et al.* (2009) 'Pathological replication in cells lacking RecG DNA translocase', *Molecular Microbiology*. Wiley, 73(3), pp. 352–366. doi: 10.1111/j.1365-2958.2009.06773.x.

Rudolph, C. J. *et al.* (2010) 'Is RecG a general guardian of the bacterial genome?', *DNA Repair*. Elsevier BV, 9(3), pp. 210–223. doi: 10.1016/j.dnarep.2009.12.014.

Rudolph, C. J. *et al.* (2013) 'Avoiding chromosome pathology when replication forks collide', *Nature*, 500(7464), pp. 608–611. doi: 10.1038/nature12312.

Rudolph, C. J., Upton, A. L. and Lloyd, R. G. (2009) 'Replication fork collisions cause pathological chromosomal amplification in cells lacking RecG DNA translocase', *Molecular Microbiology*. Wiley, 74(4), pp. 940–955. doi: 10.1111/j.1365-2958.2009.06909.x.

Sandegren, L. and Andersson, D. I. (2009) 'Bacterial gene amplification: Implications for the evolution of antibiotic resistance', *Nature Reviews Microbiology*. doi: 10.1038/nrmicro2174.

Sandler, S. J. *et al.* (1999) 'dnaC mutations suppress defects in DNA replication- and recombination-associated functions in priB and priC double mutants in Escherichia coli K-12', *Molecular Microbiology*. Wiley, 34(1), pp. 91–101. doi: 10.1046/j.1365-2958.1999.01576.x.

El Sayyed, H. *et al.* (2016) 'Mapping Topoisomerase IV Binding and Activity Sites on the E. coli Genome', *PLOS Genetics*. Edited by P. H. Viollier, 12(5), p. e1006025. doi: 10.1371/journal.pgen.1006025.

Schaeffer, P., Headlam, M. and Dixon, N. (2005) 'Protein–Protein Interactions in the

Eubacterial Replisome', *IUBMB Life (International Union of Biochemistry and Molecular Biology: Life)*. Wiley, 57(1), pp. 5–12. doi: 10.1080/15216540500058956.

Schalbetter, S. A. *et al.* (2015) 'Fork rotation and DNA precatenation are restricted during DNA replication to prevent chromosomal instability', *Proceedings of the National Academy of Sciences of the United States of America*, 112(33), pp. E4565–E4570. doi: 10.1073/pnas.1505356112.

Seigneur, M. *et al.* (1998) 'RuvAB acts at arrested replication forks', *Cell*. doi: 10.1016/S0092-8674(00)81772-9.

Shen, Z. (2011) 'Genomic instability and cancer: an introduction', *Journal of Molecular Cell Biology*. Oxford University Press (OUP), 3(1), pp. 1–3. doi: 10.1093/jmcb/mjq057.

Shereda, R. D. *et al.* (2008) 'SSB as an Organizer/Mobilizer of Genome Maintenance Complexes', *Critical Reviews in Biochemistry and Molecular Biology*. Informa UK Limited, 43(5), pp. 289–318. doi: 10.1080/10409230802341296.

Shereda, R. D., Bernstein, D. A. and Keck, J. L. (2007) 'A central role for SSB in Escherichia coli RecQ DNA helicase function', *Journal of Biological Chemistry*, 282(26), pp. 19247–19258. doi: 10.1074/jbc.M608011200.

Singleton, M. R., Dillingham, M. S. and Wigley, D. B. (2007) 'Structure and Mechanism of Helicases and Nucleic Acid Translocases', *Annual Review of Biochemistry*. Annual Reviews, 76(1), pp. 23–50. doi: 10.1146/annurev.biochem.76.052305.115300.

Soubry, N., Wang, A. and Reyes-Lamothe, R. (2019) 'Replisome activity slowdown after exposure to ultraviolet light in Escherichia coli', *Proceedings of the National Academy of Sciences of the United States of America*, 116(24), pp. 11747–11753. doi: 10.1073/pnas.1819297116.

Stouf, M., Meile, J.-C. and Cornet, F. (2013) 'FtsK actively segregates sister chromosomes in Escherichia coli', *Proceedings of the National Academy of Sciences*, 110(27), pp. 11157–11162. doi: 10.1073/pnas.1304080110.

Suski, C. and Marians, K. J. (2008) 'Resolution of Converging Replication Forks by RecQ and Topoisomerase III', *Molecular Cell*, 30(6), pp. 779–789. doi: 10.1016/j.molcel.2008.04.020.

Sutherland, J. H. and Tse-Dinh, Y. C. (2010) 'Analysis of RuvABC and RecG involvement in the Escherichia coli response to the covalent topoisomerase-DNA complex', *Journal of Bacteriology*. doi: 10.1128/JB.00350-10.

Syeda, A. H. *et al.* (2019) 'Single-molecule live cell imaging of Rep reveals the dynamic interplay between an accessory replicative helicase and the replisome', *Nucleic Acids Research*, 47(12), pp. 6287–6298. doi: 10.1093/nar/gkz298.

Tanaka, T. and Masai, H. (2005) 'Stabilization of a Stalled Replication Fork by Concerted Actions of Two Helicases', *Journal of Biological Chemistry*. American Society for Biochemistry &

Molecular Biology (ASBMB), 281(6), pp. 3484–3493. doi: 10.1074/jbc.m510979200.

Tomasetti, C., Li, L. and Vogelstein, B. (2017) 'Stem cell divisions, somatic mutations, cancer etiology, and cancer prevention', *Science*. American Association for the Advancement of Science (AAAS), 355(6331), pp. 1330–1334. doi: 10.1126/science.aaf9011.

Tomko, E. J. *et al.* (2007) 'A Nonuniform Stepping Mechanism for E. coli UvrD Monomer Translocation along Single-Stranded DNA', *Molecular Cell*. Elsevier BV, 26(3), pp. 335–347. doi: 10.1016/j.molcel.2007.03.024.

Tomko, E. J. *et al.* (2010) '5'-Single-stranded/duplex DNA junctions are loading sites for E. coli UvrD translocase', *EMBO Journal*. Nature Publishing Group, 29(22), pp. 3826–3839. doi: 10.1038/emboj.2010.242.

Tomko, E. J., Fischer, C. J. and Lohman, T. M. (2012) 'Single-Stranded DNA Translocation of E. coli UvrD Monomer Is Tightly Coupled to ATP Hydrolysis', *Journal of Molecular Biology*. Elsevier BV, 418(1–2), pp. 32–46. doi: 10.1016/j.jmb.2012.02.013.

Touchon, M. and Rocha, E. P. C. (2016) 'Coevolution of the Organization and Structure of Prokaryotic Genomes', *Cold Spring Harbor Perspectives in Biology*, 8(1), p. a018168. doi: 10.1101/cshperspect.a018168.

Trautinger, B. W. *et al.* (2005) 'RNA Polymerase Modulators and DNA Repair Activities Resolve Conflicts between DNA Replication and Transcription', *Molecular Cell*. Elsevier BV, 19(2), pp. 247–258. doi: 10.1016/j.molcel.2005.06.004.

Vandecraen, J. *et al.* (2017) 'The impact of insertion sequences on bacterial genome plasticity and adaptability', *Critical Reviews in Microbiology*. doi: 10.1080/1040841X.2017.1303661.

Veaute, X. *et al.* (2005) 'UvrD helicase, unlike Rep helicase, dismantles RecA nucleoprotein filaments in Escherichia coli', *EMBO Journal*. Wiley, 24(1), pp. 180–189. doi: 10.1038/sj.emboj.7600485.

Wang, J. C. (1996) 'DNA Topoisomerases', *Annual Review of Biochemistry*. Annual Reviews, 65(1), pp. 635–692. doi: 10.1146/annurev.bi.65.070196.003223.

Weigel, C. *et al.* (1999) 'The N-terminus promotes oligomerization of the Escherichia coli initiator protein DnaA', *Molecular Microbiology*. Wiley, 34(1), pp. 53–66. doi: 10.1046/j.1365-2958.1999.01568.x.

Wendel, B. M. *et al.* (2017) 'SbcC-SbcD and ExoI process convergent forks to complete chromosome replication', *Proceedings of the National Academy of Sciences*. Proceedings of the National Academy of Sciences, 115(2), pp. 349–354. doi: 10.1073/pnas.1715960114.

Wendel, B. M., Courcelle, C. T. and Courcelle, J. (2014) 'Completion of DNA replication in Escherichia coli', *Proceedings of the National Academy of Sciences*, 111(46), pp. 16454–16459. doi:

10.1073/pnas.1415025111.

Windgassen, T. A. *et al.* (2017) 'Mechanisms of bacterial DNA replication restart', *Nucleic Acids Research*. Oxford University Press (OUP), 46(2), pp. 504–519. doi: 10.1093/nar/gkx1203.

Wing, R. A., Bailey, S. and Steitz, T. A. (2008) 'Insights into the Replisome from the Crystral Structure of the Ternary Complex of the Eubacterial DNA Polymerase III alpha-subunit'. Protein Data Bank, Rutgers University. doi: 10.2210/pdb3e0d/pdb.

Witte, G. (2003) 'DNA polymerase III subunit ties single-stranded DNA binding protein to the bacterial replication machinery', *Nucleic Acids Research*. Oxford University Press (OUP), 31(15), pp. 4434–4440. doi: 10.1093/nar/gkg498.

Xu, Z. Q. and Dixon, N. E. (2018) 'Bacterial replisomes', *Current Opinion in Structural Biology*. doi: 10.1016/j.sbi.2018.09.006.

Yakovchuk, P., Protozanova, E. and Frank-Kamenetskii, M. D. (2006) 'Base-stacking and base-pairing contributions into thermal stability of the DNA double helix', *Nucleic Acids Research*, 34(2), pp. 564–574. doi: 10.1093/nar/gkj454.

Yang, W. (2010) 'Lessons Learned from UvrD Helicase: Mechanism for Directional Movement', *Annual Review of Biophysics*, 39(1), pp. 367–385. doi: 10.1146/annurev.biophys.093008.131415.

Yao, N. Y. and O'Donnell, M. (2008) 'Replisome dynamics and use of DNA trombone loops to bypass replication blocks', *Molecular BioSystems*. Royal Society of Chemistry (RSC), 4(11), p. 1075. doi: 10.1039/b811097b.

Yeeles, J. T. P. and Marians, K. J. (2011) 'The Escherichia coli Replisome Is Inherently DNA Damage Tolerant', *Science*. American Association for the Advancement of Science (AAAS), 334(6053), pp. 235–238. doi: 10.1126/science.1209111.

Yokota, H., Chujo, Yuko Ayabe and Harada, Y. (2013) 'Single-Molecule Imaging of the Oligomer Formation of the Nonhexameric Escherichia coli UvrD Helicase', *Biophysical Journal*. Elsevier BV, 104(4), pp. 924–933. doi: 10.1016/j.bpj.2013.01.014.

Yokota, H., Chujo, Yuko Ayabe and Harada, Y. (2013) 'Single-molecule imaging of the oligomer formation of the nonhexameric escherichia coliUvrD helicase', *Biophysical Journal*. Biophysical Society, 104(4), pp. 924–933. doi: 10.1016/j.bpj.2013.01.014.

Yu, C. *et al.* (2016) 'SSB binds to the RecG and PriA helicasesin vivoin the absence of DNA', *Genes to Cells*. Wiley, 21(2), pp. 163–184. doi: 10.1111/gtc.12334.

Zechiedrich, E. L., Khodursky, A. B. and Cozzarelli, N. R. (1997) 'Topoisomerase IV, not gyrase, decatenates products of site-specific recombination in Escherichia coli', *Genes & Development*. Cold Spring Harbor Laboratory, 11(19), pp. 2580–2592. doi: 10.1101/gad.11.19.2580.

Zhang, T. B. *et al.* (2015) 'Determination of Base Binding Strength and Base Stacking Interaction of DNA Duplex Using Atomic Force Microscope', *Scientific Reports*, 5, pp. 1–7. doi: 10.1038/srep09143.

Zhivotovsky, B. and Kroemer, G. (2004) 'Apoptosis and genomic instability', *Nature Reviews Molecular Cell Biology*. Springer Nature, 5(9), pp. 752–762. doi: 10.1038/nrm1443.

Zhou, P. *et al.* (1997) 'Gene transcription and chromosome replication in Escherichia coli.', *Journal of Bacteriology*. American Society for Microbiology, 179(1), pp. 163–169. doi: 10.1128/jb.179.1.163-169.1997.